UNIVERSITY *of the*
WESTERN CAPE

Application of petrophysics and seismic in reservoir characterization. A case study on selected wells, in the Orange Basin, South Africa.

A Thesis in Applied Geology (Petroleum Geology Option)

BY

Nande Ingrid Mabona

Submitted in Fulfillment of the Requirements for the Degree of Magister Scientiae in the Department of Earth Sciences, University of the Western Cape, South Africa

Supervisor: Dr. Mimonitu Opuwari
Co- Supervisor: Prof. Jan Van Bever Donker

November 2012

Declaration

I declare “Application of petrophysics and seismic in reservoir characterization. A case study on selected wells, in the Orange Basin, South Africa” is my own work, that it has not been submitted before for any degree or examination in any other university, and that all the sources I have used or quoted have been indicated and acknowledged by means of complete references.

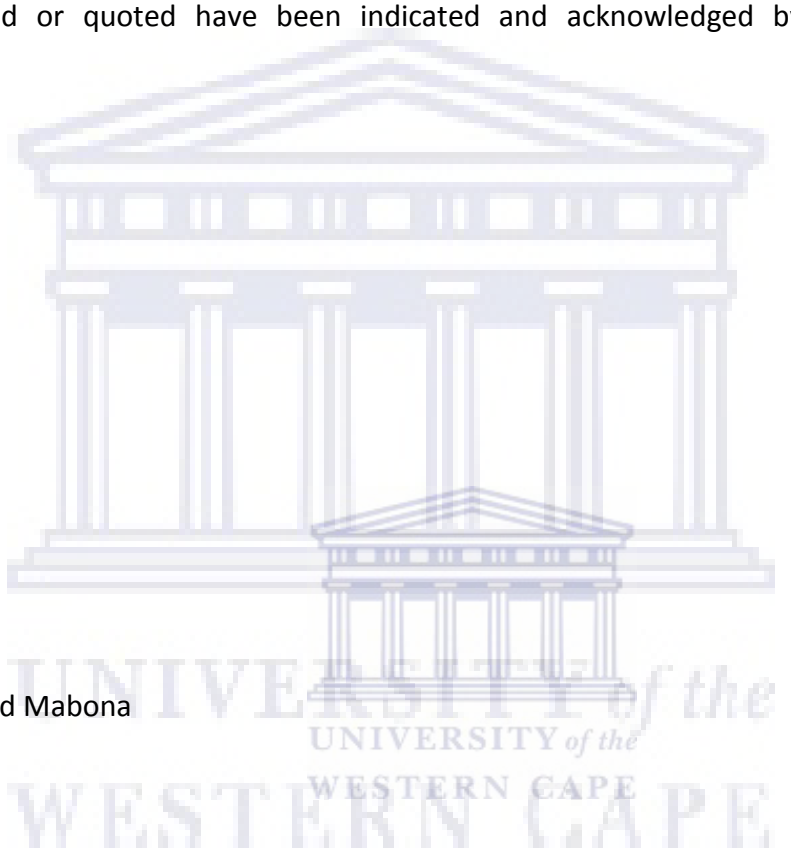

Nande Ingrid Mabona November 2012

Signature

Application of petrophysics and seismic in reservoir characterization. A case study on selected wells, in the Orange Basin, South Africa.

Nande Ingrid Mabona

Key Words

Orange Basin

Petrophysics

Seismic Interpretation

Wireline Logs

Geological modeling

Reservoir Characterization

Abstract

Application of petrophysics and seismic in reservoir characterization. A case study on selected wells, in the Orange Basin, South Africa.

The evaluation of petroleum reservoirs has shifted from single approach to an integrated approach. The integration, analysis and understanding of all available data from the well bore and creating property models is an exceptional way to characterize a reservoir.

Formulating, implementing, and demonstrating the applicability of the joint inversion of seismic and well-bore related observations, and the use of information about the relationship between porosity and permeability as the key parameters for identifying the rock types and reservoir characterization is a vital approach in this study. Correlating well and seismic data, potential reservoirs can be delineated and important horizons (markers) can be pointed out to better characterize the reservoir.

This thesis aims to evaluate the potential petroleum reservoirs of the Wells K-A1, K-A2, K-A3 and K-H1 of the Shungu Shungu field in the Orange Basin through the integration and comparison of results from core analysis, wireline logs and seismic and attempt to produce a good reservoir model and by additionally utilizing Petrophysics and seismic and trying to better understand why the area has dry wells.

Different rock types that comprise reservoir and non reservoirs are identified in the study and five Facie types are distinguished. Tight, fine grained sandstones with low porosity values ranging from 3% - 6% where dominant in the targeted sandstone layers. Porosity values ranging from 11% - 18% where identified in the massive sandstone lithologies which where hosted by Well's K-A2 and K-A3.

Low permeability values reaching 0.1mD exist throughout the study area. Areas with high porosity also

host high water saturation values ranging from 70 – 84%. An improvement in the porosity values at deeper zones (3700m -3725m) and is apparent.

Poroperm plots exhibit quartz cemented sandstones and density with neutron plot suggest that the sandstones in the area contain quarts and dolomite mineralization.

Well K-A3, consist of a cluster by quartzitic sandstone, meaning there is a large amount of sandstone present. There are apparent high porosity values around the sandstone. What is apparent from this plot is that there are many clusters that are scattered outside the chart. This could suggest some gas expulsions within this Well.

Sandstones within the 14B2t1 to 14At1 interval are less developed in the vicinity covered by well K-A2 than at the K-A1 well location. The main targeted sandstones belong to the lower cretaceous and lie just below 13At1.

The four wells drilled in this area are dry wells. The areas/blocks surrounding this area have shown to possess encouraging gas shows and a comparative study could reveal better answers.

At deeper zones of the well at an interval of 5350m -5750m, there are more developed sandstones with good porosity values. The volume of shale is low and so is the water saturation. The main target sandstones in the study area are the Lower Cretaceous sandstones which are at an interval 13At1. These sandstones are not well developed but from the property model of the target surface it can be seen that the porosity values are much more improved than the average values applied on all the zones on the 3D grid.

Acknowledgements

"My faith looks up to thee, Almighty God". The Almighty Father has granted me great favour with regards to the process of completion of this project. He has been my strength when I felt I did not have any strength. It is through HIS everlasting love that I have completed this project.

And yet again I can say that God has never failed me yet!!!

I would like to thank Dr. Opuwari and Prof Bever Donker for all the support, assistance and opportunities they offered me. Thank you for grooming me into becoming the professional I am today.

Thank you to the Petroleum Agency SA (PASA) for providing the data used in this project and their continued support. A great amount of appreciation is due to SPE for awarding me the SPE Star fellowship award. To the Inkaba ye Africa Foundation and the NRF; thank you for believing in my capabilities and for all the financial support.

To the Mandela Rhodes Foundation, thank you for helping establish the Nande BRAND and inspiring me to *A*spire to be …. All I can be.

To the Schlumberger team, it is a true fact that I am surrounded by people with exceptional minds and I thank you for everything you did for me and mostly for believing in me.

I would also like to thank my parents (Joel and Zoleka Mabona) for all the support and motivation.

And lastly, Zintle Mpayipheli and Amanda Amna Ncedane I dedicate this to you guys. THANK YOU!!!

Table of Contents

Declaration ..... **ii**

Key Words ..... **iii**

Abstract ..... **iv**

Acknowledgements ..... **vi**

List of Figures ..... **ix**

List of Tables ..... **xi**

List of Appendices ..... **xii**

CHAPTER ONE General Introduction **1**

1.1 Thesis Layout 1

1.2 Introduction 4

1.3 Scope of Work 8

1.4 Aims and Objectives 9

1.5 Location of Study Area 10

1.6 Well Summary 12

1.7 Geological background of the Orange Basin. 16

1.8 Previous Work on Orange Basin 17

CHAPTER 2: Geology of the Orange Basin **20**

2.1 Regional Geology 20

2.2 Depositional Environment 22

2.3 Regional Chronostratigraphy of Southern African offshore basins. 24

2.4 Stratigraphy 26

2.5 Tectonic Evolution 28

CHAPTER 3: Literature review **31**

3.1 Reservoir Characterization 32

3.2 Petrophysics 33

3.3 Wireline logs 34

3.3.1. Gamma Ray Logs 37

3.3.2 Neutron logs 38

3.3.3 Caliper Log 40

3.3.4 Spontaneous Potential Logs (SP) 43

3.3.5 Resistivity Log 44

3.3.6 Density Log 46
3.4 Seismic interpretation 48
3.6 Coring 49
CHAPTER 4: Methodological Approach 52
4.1 Materials 52
4.2 Methods 54
4.3 Data Loading 55
4.4 Data Quality 56
4.5 Core Description 57
4.6 Seismic data interpretation (General principle) 58
4.7 Petrophysical analysis procedure/steps 63
4.8 Wireline log interpretation 69
4.9 Methodological Approach 73
4.10 Deliverables 74
CHAPTER 5: Results and Interpretation 75
5.1 Core Analysis and interpretation 75
5.2 Poroperm Plots of Sampled zones 93
5.3 Petrophysical Analysis 99
5.3.1 Well Correlation and Stratigraphic Analysis 99
5.3.2 Log Correlation description 99
5.3.3 Wireline logs 104
5.3.4 Density Porosity Cross Plots 112
5.4 Seismic well Tie and Seismic Interpretation and surface Models 117
CHAPTER 6: Conclusions and Recommendations 128
6.1 Conclusions 128
6.2. Recommendations 130
References 131
Appendice 136

List of Figures

FIGURE 1.OUTLINE OF THE THESIS 3
FIGURE 2: MAP OF OFFSHORE ORANGE BASIN, SOUTH AFRICA INDICATING THE STUDY AREA WITH REFERENCE TO MAP SOUTH AFRICA SUPERIMPOSED WITH THE ORANGE BASIN ACREAGE MAP. SOURCE: MODIFIED FROM PETROLEUM AGENCY SA, 2003. 11
FIGURE 3: MAP SHOWING THE STUDY AREA (ORANGE STAR) ACROSS EXPLORATION BLOCKS IN THE ORANGE BASIN (PASA, 2003), AND THE KUDU AND IBHUBHESI GAS FIELDS. 13
FIGURE 4: WELL LOCATION MAP WITH WELL DESCRIPTION (GENERATED IN PETREL) 14
FIGURE 5: BOREHOLE LOCALITY MAP OF SELECTED WELLS IN THE ORANGE BASIN (MODIFIED FROM PASA, 2003). 15
FIGURE 6: SOUTH AFRICA CONTINENTAL MARGIN AND OCEANIC CRUST (MODIFIED AFTER BROAD, 2004) 16
FIGURE 7: STRUCTURAL ELEMENTS AND SEDIMENTARY BASINS OF SOUTH AFRICA (PASA BROCHURE, 2003) 21
FIGURE 8: MAP ILLUSTRATING THE LOCATIONS OF THE FLANK OF THE SOUTH WESTERN AGULHAS- COLUMBINE ARCH. ALSO ILLUSTRATED IS THE COURSE OF THE ORANGE RIVER, BEING THE MAJOR SEDIMENT SUPPLIER TO THE ORANGE BASIN. (MODIFIED FROM VAN DER SPUY, 2003) 22
FIGURE 9: SEDIMENTS DEPOSITED IN DELTAIC ENVIRONMENT (MCGOWEN & BLOCH, 1985). 23
FIGURE 10: EVOLUTION OF THE CAPE FOLD BELT. SOURCE: PETROLUEM AGENCY SA, 2003 25
FIGURE 11: SYNOPTIC BASIN EVOLUTIONARY MODEL FOR THE GRAVITY-DRIVEN SYSTEM OF THE ORANGE BASIN. A. LATE JURASSIC RIFTING (160–130 MA). B. HAUTERIVIAN–APTIAN (133–120 MA). C. MIDDLE APTIAN–CAMPANIAN (120–75 MA). D. CAMPANIAN–MAASTRICHTIAN (75–70 MA).E. BASE (DE VERA ET AL 2010) 28
FIGURE 12: CONTINENTAL RIFTING DURING LATE JURASSIC – LOWER VALANGINIAN (BROAD, 2004) 29
FIGURE 13: GRAPHICAL REPRESENTATION OF LOGS AND REFERENCE TO SUBSURFACE AND HYDROCARBONS. (AFTER VAN 35
FIGURE 14: WELL LOGGING OPERATIONS, AND SONDE IN THE FORMATIONS. AFTER STRACK 2002 36
FIGURE 15: GAMMA RAY SPECTRUM IN SPECTRAL CHANNELS. MODIFIED FROM SCHLUMBERGER 1972 37
FIGURE 16: TH/K CROSSPLOT AND MINERAL CLASSIFICATION. (SCHÖN, J.H, 1996) 38
FIGURE 17: A) NEUTRON EMITTED FROM NUCLEI. STRACK, 2002. B) NEUTRON LOGGING TOOL FROM SCHLUMBERGER NEXT BASIC LOGGING COURSE 39
FIGURE 18: TYPICAL CALIPER RESPONSE TO VARIOUS LITHOLOGIES. WESTERN ATLAS, 1992 41
FIGURE 19: SPONTANEOUS POTENTIAL LOGGING TOOL (RIDER, 1996) 44
FIGURE 20: RESISTIVITY SIGNATURE RESPONSE FROM 45
FIGURE 21: SEISMIC ACQUISITION AND REFLECTION ON A SEISMIC TRACE EXHIBITING LITHOLOGY CHANGES AND ANGULAR UNCONFORMITY AND. SOURCE: UNIVERSITY OF DERBY COURSE NOTES 48
FIGURE 22: WIRELINE CORING GRAPHICAL EXAMPLE (WWW.METU.EDU.TR) 50
FIGURE 23: GRAPHICAL AND PICTORIAL REPRESENATION OF SUMMARY LOG IN CORE BOX. MODIFIED FROM. PEP COURSE NOTES. SCHLUMBERGER (NEXT) 51
FIGURE 24: THE FLOW CHART OF THE RESEARCH METHODOLOGY 54
FIGURE 25: BASE MAP WITH SEISMIC LINES IN THE STUDY AREA, CONTROLLED BY 4 WELLS 57
FIGURE 26: WELL LOG RESPONSE CHARACTER (EMERY AND MYERS, 1996). 72
FIGURE 27: SUMMARY LOG SECTION OF WELL K-A2 CORE 2. SCALE 1:100 80
FIGURE 28: FULLY INTERPRETED LOG SECTION OF WELL K-A2 CORE 1 81
FIGURE 29: CORE POROSITY CHART FOR WELL K-A2 82
FIGURE 30: CORE PERMEABILITY CHART FOR WELL K-A2 82
FIGURE 31: SUMMARY LOG SECTION OF WELL K-A3 CORE 1 84
FIGURE 32: SUMMARY LOG SECTION OF WELL K-A3 CORE 2. 85
FIGURE 33: CORE POROSITY CHART FOR WELL K-A3 85
FIGURE 34: CORE PERMEABILITY CHART FOR WELL K-A3 86
FIGURE 35: SUMMARY LOG SECTION OF WELL K-H1 88
FIGURE 36: K- H1 LOG SUMMARY, DEPICTING WHAT WAS DESCRIBED IN THE CORE LOG. 89
FIGURE 37: CORE PERMEABILITY CHART FOR WELL K-H1 90

FIGURE 38: CORE POROSITY CHART, WELL K-H1 90
FIGURE 39: WATER AND OIL SATURATION OF CORE K-A2 91
FIGURE 40: WATER AND OIL SATURATION OF CORE K-A3 92
FIGURE 41: PERMEABILITY VS POROSITY CROSS PLOT DEPICTING LITHOLOGY TYPES. BASIC LOGGING COURSE NOTES. SCHLUMBERGER 94
FIGURE 42: LOG SECTION SHOWING CORE PLUG SAMPLED ZONE AND CALIBRATED CORE POROSITY IN WELL K-A2 95
FIGURE 43: POROPERM PLOT FOR A CORE PLUG IN WELL K-A2 A) CORE 1, AND B) CORE 2. 96
FIGURE 44: POROPERM PLOT FOR A CORE PLUG IN WELL K-A 3 97
FIGURE 45: LOG SECTION SHOWING CORE PLUG SAMPLED ZONE AND CALIBRATED CORE POROSITY IN WELL K-A3 98
FIGURE 46: WELL CORRELATED STRATIGRAPHIC SECTION OF K-A1 AND K-A2 100
FIGURE 47: CORRELATION OF STRATIGRAPHIC SECTION OF WELLS K-A1 , K-A2 AND K-A3 101
FIGURE 48: GENERALISED CHRONOSTRATIGRAPHY AND SEQUENCE STRATIGRAPHY OF ORANGE BASIN OFFSHORE 102
FIGURE 49: LOG TEMPLATE OF WELL K-A1 DEPICTING ZONES OF INTEREST AND PETROPHYSICAL PARAMENTERS 105
FIGURE 50: LOG TEMPLATE OF WELL K-A 2 DEPICTING ZONES OF INTEREST AND PETROPHYSICAL PARAMETERS. 107
FIGURE 51: K-A2 LOGS AT A DEEPER ZONE 108
FIGURE 52: LOG TEMPLATE OF WELL K-A 3 DEPICTING ZONES OF INTEREST AND PETROPHYSICAL PARAMENTERS 110
FIGURE 53: LOG TEMPLATE OF WELL K-H1 DEPICTING ZONES OF INTEREST 111
FIGURE 54: ENVIRONMENTAL CORRECTION CHART FOR NEUTRON POROSITY (NPHI) LOG TO COMPENSATED NEUTRON LOG (CNL). DENSITY CROSS PLOTS MODIFIED AFTER SCHLUMBERGER 1972. 112
FIGURE 55: CROSSPLOTS OF DENSITY (RHOB) AGAINST NEUTRON (NPHI) FOR MINERALOGICAL FOR MINERALOGICAL PREDICTION IN WELL K-A1. 113
FIGURE 56: CROSSPLOTS OF DENSITY (RHOB) AGAINST NEUTRON (NPHI) FOR MINERALOGICAL FOR MINERALOGICAL PREDICTION IN WELL K-A2. 114
FIGURE 57: CROSSPLOTS OF DENSITY (RHOB) AGAINST NEUTRON (NPHI) FOR MINERALOGICAL FOR MINERALOGICAL PREDICTION 115
FIGURE 58: CROSSPLOTS OF DENSITY (RHOB) AGAINST NEUTRON (NPHI) FOR MINERALOGICAL PREDICTION IN WELL K-H1. 115
FIGURE 59: SEISMIC AND WELL SECTION PRIOR TO APPLICATION OF SEISMIC WELL TIE 117
FIGURE 60: WELL CONTROLLED SEISMIC SECTIONS, SEISMIC WELL TIE APPLIED. 118
FIGURE 61: EXTRACTED WAVELET FROM THE SEISMIC TIE PROCESS. 119
FIGURE 62: SEISMIC WELL TIE WITH INTERPRETED HORIZONS WHICH MATCH. THE INTERVALS INTERPRETED ON THE SEISMIC HAVE A DIRECT MATCH TO THOSE THAT ARE VISIBLE ON THE WIRELINE LOGS. 120
FIGURE 63: ILLUSTRATION OF MODELED SEQUENCE SYSTEM TRACTS ON A SEISMIC SECTION. 121
FIGURE 64: FULLY INTERPRETED SEISMIC SECTION CONTROLLED BY WELL K-A1 AND K-A2. (INTERPRETED IN PETREL) 123
FIGURE 65: DEPTH MODEL OF SURFACES GENERATED WITH THE INTERPRETED HORIZONS AND A 3D DEPTH GRID WITH REFERENCE TO WELL POSITION. 124
FIGURE 66: GENERAL DISTRIBUTION OF AN UPSCALED NEUTRON LOG, WITH REFERENCE TO WELL POSITION 125
FIGURE 67: PROPERTY MODELED GRID USING THE GAUSSIAN RANDOM FUNCTION SIMULATION ALGORITHM (GRFS). 126
FIGURE 68: PROPERTY MODELED 13AT1 SURFACE USING THE GAUSSIAN RANDOM FUNCTION SIMULATION ALGORITHM. 127

List of Tables

TABLE 1:WELL LOCATION TABLE, CREATED IN PETREL.....12
TABLE 2: REPORTS USED FOR STUDY.....53
TABLE 3: TABLE OF DELIVERABLES AND SUMMARY OF METHODS APPLIED IN THE STUDY 55
TABLE 4: LOG SCALE.....56
TABLE 5:CRITERIA FOR ARCHIE RESERVOIR. WORTHINGTON ET AL 2011.....103

List of Appendices

Figure A1: Legend for the logs of Wells K-A2, KA-2, K-A3 and K-H1

Figure B1: Core parameters Table for K-A3 core 2

Figure B2: Core parameters table for K-A2 core 2

Figure B3: Legend of geophysical logs

Figure C1: Symbols Used in log interpretation

Figure D: i) Definition of A.P.I gravity. ii) Conversion factors used in the Oil Industry

CHAPTER ONE General Introduction

1.1 Thesis Layout

This thesis covers the examination of drilled cores, analysis, interpretation and discussion of potential reservoir zones of selected wells of the Orange Basin. It involves the application of techniques in an integrated manner to improve the understanding of the reservoir. The thesis write-up consists of two sections which together makeup six chapters. Figure 1 in the next page shows a simplified thesis layout.

Section1 provides a broad overview of the basic concepts in the thesis, which include the introduction, research rationale, regional and local geology of the study area and the methods employed for the work. This section reviews literature relating to reservoir characterization, Petrophysics and seismic techniques. The section is concluded by a discussion of the methodology and approaches adopted for this study including a synopsis of the software's used in the generation of the models and logs.

Section 1 covers Chapter one to four, as follows:

- Chapter one provides background information on the concepts that are discussed in the thesis. It argues the purpose and or relevance of the study. The aims, objectives and methodology of the study are covered in this chapter.
- Chapter two reviews the regional and local geology of the Orange Basin. This chapter further provides a synopsis of the lithology and general description of the wells.
- Chapter three discusses the literature review which gives clarity to the key concepts adopted in the study. Additionally, this section serves to provide the understanding of the research topic and outlines the theoretical and conceptual frameworks.

- Chapter four discusses the research approach applied and the workflow that is adopted for the study. It includes information on the data list provided and further discusses the well locations and selection process.

Section 2 consists of chapter's five and six where chapter five covers aspects on Petrophysical analysis and evaluation, well log correlation, core analysis and interpretation, seismic interpretation and model creation and provides discussions of the study's results. Chapter six provides the synopsis of the study including some recommendations.

- Chapter five is divided into three subsections, namely;
- The core description and analysis. These results will then be used in determining the reservoir quality of selected reservoir zones in the areas.
- Wireline Log Interpretation and Petrophysical Evaluation focuses on the Petrophysical evaluation, Petrophysical properties and their application in the study. This sub-section includes the results from the calibration of core data with log data, the creation of log facie and litho-facie distribution.
- Seismic well Tie and Seismic Interpretation and surface Models, involves the integration of seismic data with log data in order to provide greater accuracy in the characterization process.
- Chapter six covers the conclusion and recommendations of the study which are based on the observations made in the various phases of analysis.

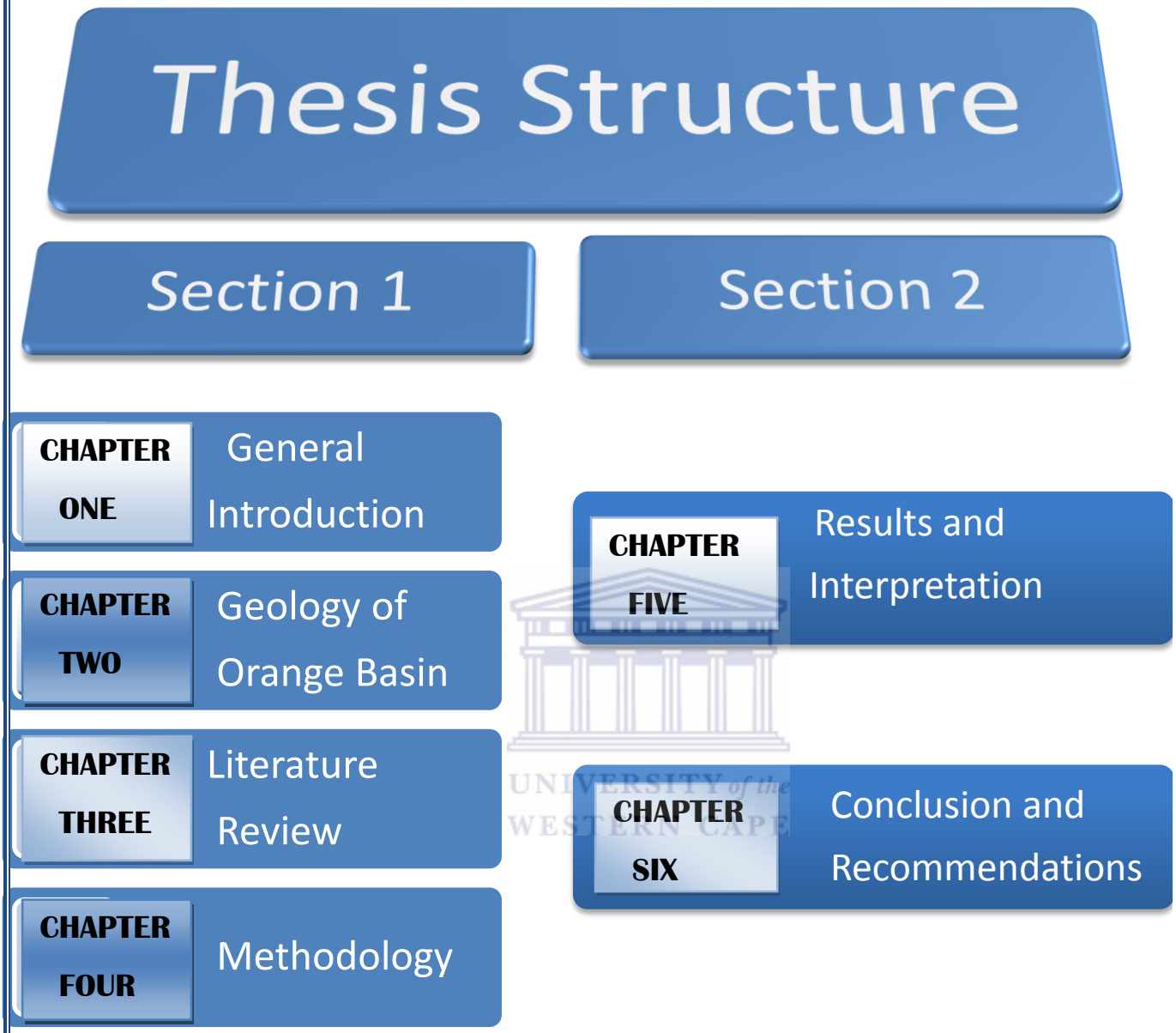

Figure 1.Outline of the thesis

1.2 Introduction

Petroleum reservoir characterization can be described as a process that includes studying, integrating, analyzing and understanding all available data and information about the well (Lombard and Akinlua, 2009). The integration of seismic interpretation with evaluation of petrophysical properties provides a comprehensive approach to reservoir characterization.

The evaluation of reservoirs has shifted from single approach to an integrated approach. The integrated approach has proved to be vital in petroleum geology because it has proved its significance in solving exploration and production problems (Ketzer,2002).

Nowadays, reservoirs are becoming more and more intricate or need significant investigations and studying; in many areas it is recognized that the "easy oil" is produced and the challenges are now involving added complex geology and or more difficult locations, for example, sub-salt or deep water etc.

This would propose a need to raise the standard for data analysis capability. Many data types are used in this study, and correlation between core properties and wireline logs to work out a depositional model and perform a seismic well tie form a valuable basis in the characterization of the reservoirs in the selected wells of this study.

Porosity, permeability and shale volume are a few of the fundamental properties that govern the quality of reservoir rocks. Understanding the reservoir characteristics is crucial and the obtained evaluated and other properties can effectively be used for well log calibration which can aid in the correlation of wire-line signatures (Lofts et al., 1994).

Certain parts of Africa are very rich in hydrocarbons, and South Africa promotes the exploration of oil and gas. Investigating potential reservoirs and plays often results in production opportunities which lead to the

development of a country. The Orange Basin has been a prospect area for hydrocarbon discovery for many years. The area is not widely studied and the results of previous research have not been made public, while some aspects of it have not yet been documented.

This thesis aims to evaluate the potential petroleum reservoirs in the Orange Basin by utilizing Petrophysics and seismic and trying to better understand why the area has dry wells.

The study focuses on designing and performing higher level analyses of these petroleum reservoirs through the assessment of petrophysical parameters, namely; percentage of porosity, permeability, water saturation and volume of shale. These parameters are deduced from well logs, core analysis, and well tests and are integrated with seismic data to assist in better comprehension of the heterogeneities of the petroleum reservoirs of the selected wells in the study.

The integration, analysis and understanding of all available data from the well bore and creation of property models is an exceptional way to characterize a reservoir.

This study shows the role of wireline petrophysical analysis as a tool in reservoir characterization and furthermore examines the use of seismic data, log analysis and means petrophysical reservoir parameters as a tool in successfully establishing reservoir architecture. Core and log data are the true representation of lithologies in the subsurface and no data is more accurate, and as it gives better results of what happens in the subsurface than other means. Hence an integration of these methods in the study will produce much more accurate results and greater understanding of the area.

The advancement of geological exploration involves the use of integrated methods of analysis and use of new technologies and techniques. Seismic data, in particular 3-D seismic data form a strong basis for reliable exploration in the petroleum industry. For instance seismic attributes are able to help predict both qualitative and quantitative reservoir properties and geometries if correctly used in reservoir characterization. Seismic

data and well data used in collaboration allows for greater scientific understanding and interpretation. Data from Gamma Ray, Neutron, Density, Sonic and Resistivity logs are utilized for petrophysical analysis to correlate layers in the reservoir characterization study. Porosity models,Vsh, facies models are used as structural models to aid in better comprehension of the area.

Although the development of passive margins has been extensively studied over a number of decades, the Orange Basin located on the south-west African continental margin is an area of high hydrocarbon potential that is under-explored. Using seismic attribute analysis, inversion of seismic traces and integration with log data, properties including porosity, lithology, pressure and saturation can be estimated.

Problem Statement: The Orange Basin has many dry wells and minor gas discoveries. In the aim of evaluating these reservoirs, the study will attempt to use an integrated approach in methods applied to try and better understand the area and provide answers or recommendations of where areas of better prospect could lie.

This study aims to use all data available to try and analyze the study area.

The study area has four wells drilled in it, these are dry wells. The areas/blocks surrounding this area have been drilled and the wells give encouraging gas shows. Areas like the Ibubesi gas field and some areas in the northern sector of the Orange Basin have proven potential for the discovery of large gas reserves. Previous workers like Jungslager (1999) and van der Spuy (2003) have carried out some studies on evaluation of the source rock potential of sediments from the Orange Basin in an attempt to broaden the analysis of the petroleum system. However, the extensive characterization of reservoirs in this area with use of seismic and petrophysics has not been done to any large extent.

The study area, the Orange Basin, is located offshore South Africa and is largely under-explored (de Vera, 2010). The basin hosts two gas fields, namely, the Ibhubesi and the Kudu gas fields, and possesses oil and gas

potential but in the past has not been given much attention (Figure 3). The area has only 34 wells drilled in the area (Van der Spuy, 2005).

The Orange Basin has recently been the topic of investigation because of the belief that it may hold economic quantities of hydrocarbons. Further studies and exploration of this area is vital to ascertain this belief. This will only be possible through the detailed research analysis of this area; and petrophysical analysis and seismic interpretation and modeling are excellent methods for the advancement of exploration in this area.

Oil and gas has been proven in neighbouring basins, and comparative study in future can result in more prospects being discovered within the study area.

The analysis of core data and petrophysical parameters will lead to detailed comprehension of the reservoir and improved reservoir characterization and possibly pick out potential hydrocarbon plays.

1.3 Scope of Work

The use of integrated approach to evaluate reservoir characteristics is becoming increasingly important in petroleum geology. “The shared earth model” – Petrel Logo best explains why when different disciples come together research becomes feasible and the scope of the study will be based on this “shared earth model’.

The scope of work will cover:-

- Editing of raw wireline log data
- Delineation of reservoir zones
- Investigating the petrophysical characteristics of selected wells of the Orange Basin
- Technically evaluate laboratory data from reports and downhole measurements for reservoir properties namely; Volume of shale, Porosity, water saturation and permeability.
- Understanding the structural configuration and the general stratigraphy of the study area.
- Classification of lithofacies
- Providing a plausible reservoir description of the study area.
- Advancing geological knowledge and understanding of the area.
- Determination of horizons from seismic data
- Correlation of core data and log data
- The aim is establish a seismic petrophysical framework of reservoir characteristics which could lead to further exploration in the Basin.

1.4 Aims and Objectives

The study aims to conduct an investigation and analysis of the petroleum reservoir zones of selected wells in the Orange Basin in an attempt to answer why the wells are dry and provide recommendations as to where hydrocarbon accumulations of economic quantities could be.

The objectives of the study include:-

- Construction of composite stratigraphic sections together with lithologic and sedimentological descriptions for each well.
- Comparison of the petrophysical characteristics of the wells
- Identification and characterization of potential reservoir zones,
- Evaluate the reservoir properties, using seismic petrophysical analysis as a good applicable technique in analysing reservoir characteristics.
- Create correlation and comparisons of cores and logs and provide a detailed petrophysical analysis to assist in hydrocarbon evaluation.
- Improvement on previous studies through the use of new techniques.
- Attempt to eliminate uncertainties in 2D seismic interpretation through the use of data integration and seismic well tie.

1.5 Location of Study Area

The Orange Basin is situated on the passive continental margin offshore South Africa and southern Namibia. (De Vera 2010) Figure 2 in page 11 represents the study area with an inset of the map of Africa and South Africa. It covers approximately 130 000 $km^{2,}$ which makes it South Africa's largest offshore basin. (Gerrard & Smith, 1982) It developed in a passive margin along the west coast of southern Africa which formed as a result of the middle to late Jurassic Continental rifting of the South Atlantic and resultant separation between the South American and African plates (Stewart et al, 2000).

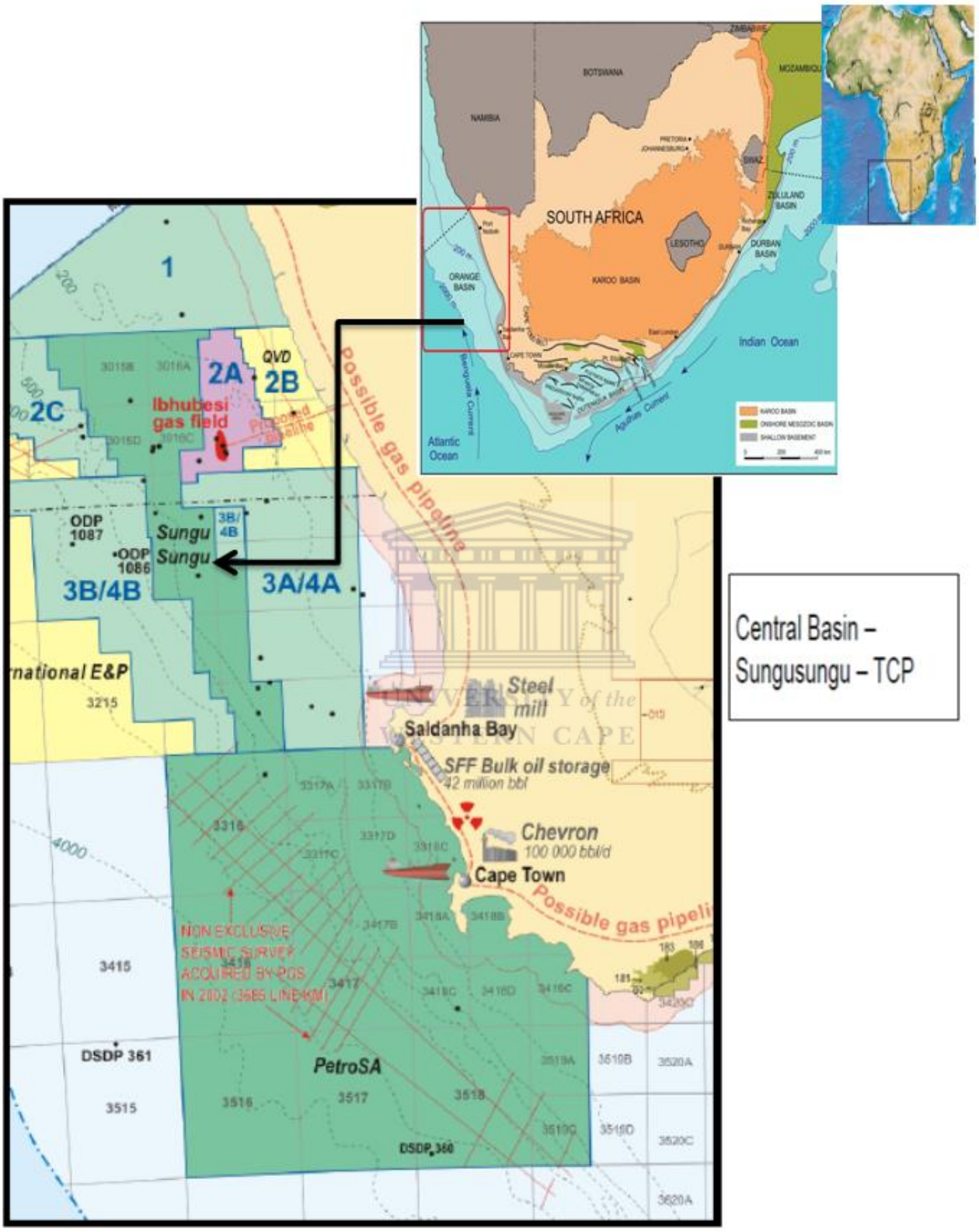

Figure 2: Map of offshore Orange Basin, South Africa indicating the study area with reference to map South Africa superimposed with the Orange Basin acreage map. Source: Modified from Petroleum agency SA, 2003.

The Orange Basin extends for approximately 500km between Cape Town and the South Africa-Namibia border: It has water depth that ranges between 250m at the continental shelf and 2500m in deepwater environment. The large areal extent of the Orange Basin, extending from the shelf to the ultra-deep marine, makes it a relatively under explored basin with only 37 wells drilled to date.

The area of study is situated in the Central Orange Basin (Sungu Sungu) and is bounded to the south by blocks 3B\4B of the South African offshore acreage within the Orange Basin (Figure 2). The study encompasses a reservoir characterization study that utilized 10 seismic lines and petrophysical data from 4 wells to evaluate the reservoir within the southern Orange Basin.

1.6 Well Summary

The Orange Basin has 37 wells drilled, with approximately one well drilled for every 4000 square kilometers (Campher et al., 2009). Table 1; below shows the wells that were used in this study and include their location and depths. The table was created in the Petrel 2011 Software. Figure 3, depicts the study area as an Orange star. The Kudu and Ibhubhesi gas fields are also represented in this figure.

Table 1: Showing the location coordinates of four wells: K-A1, K-A2, K-A3 and K-H1, of the study.

	Name	UWI	Surface X	Surface Y	Latitude	Longitude	KB	TD (TVDSS)	TD (MD)	Spud date
1	K-A1		597257.00	6591495.00	30°48'20.33"S	16°01'0.04"E	25.9	4794.1	4820.0	15/04/1979
2	K-H1		588108.00	6565912.00	31°02'13.83"S	15°55'23.75"E	25.0	4875.0	4900.0	03/11/1989
3	K-A2		596574.50	6588662.30	30°49'52.53"S	16°00'35.32"E	25.9	5804.1	5830.0	09/10/1979
4	K-A3		601817.00	6592040.00	30°48'1.25"S	16°03'51.43"E	25.9	4274.1	4300.0	01/01/1981

The well descriptions and location are depicted as points in Figure 4 and provide a greater scale than the locality map shown in figure 5 which was originally from PASA. These figures's assist in understanding how and where the wells are located in reference to the other well known fields and blocks, for example the Ibhubhesi gas field.

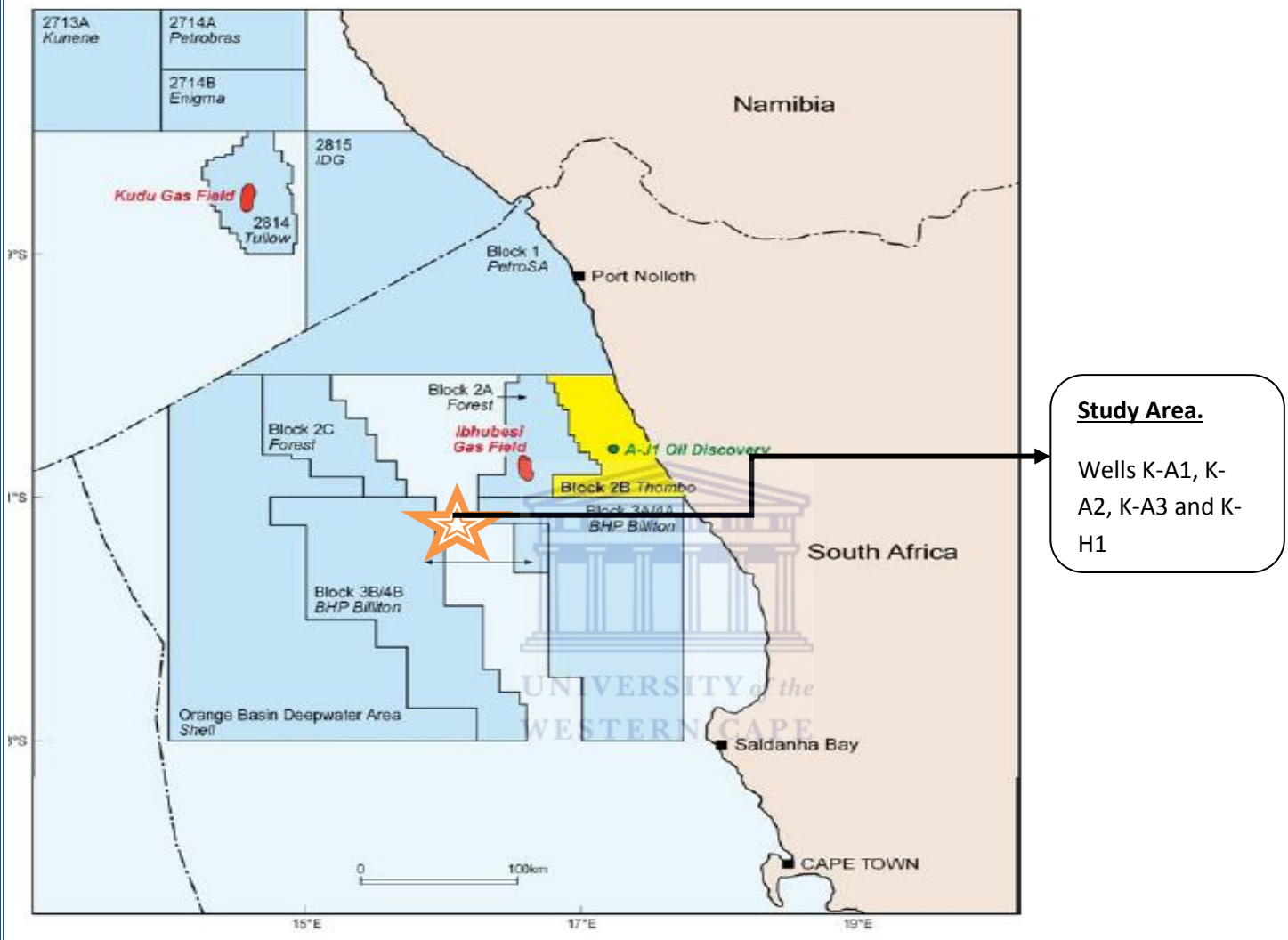

Figure 3: Map showing the study area (Orange star) across exploration blocks in the Orange Basin (PASA, 2003), and the Kudu and ibhubhesi gas fields.

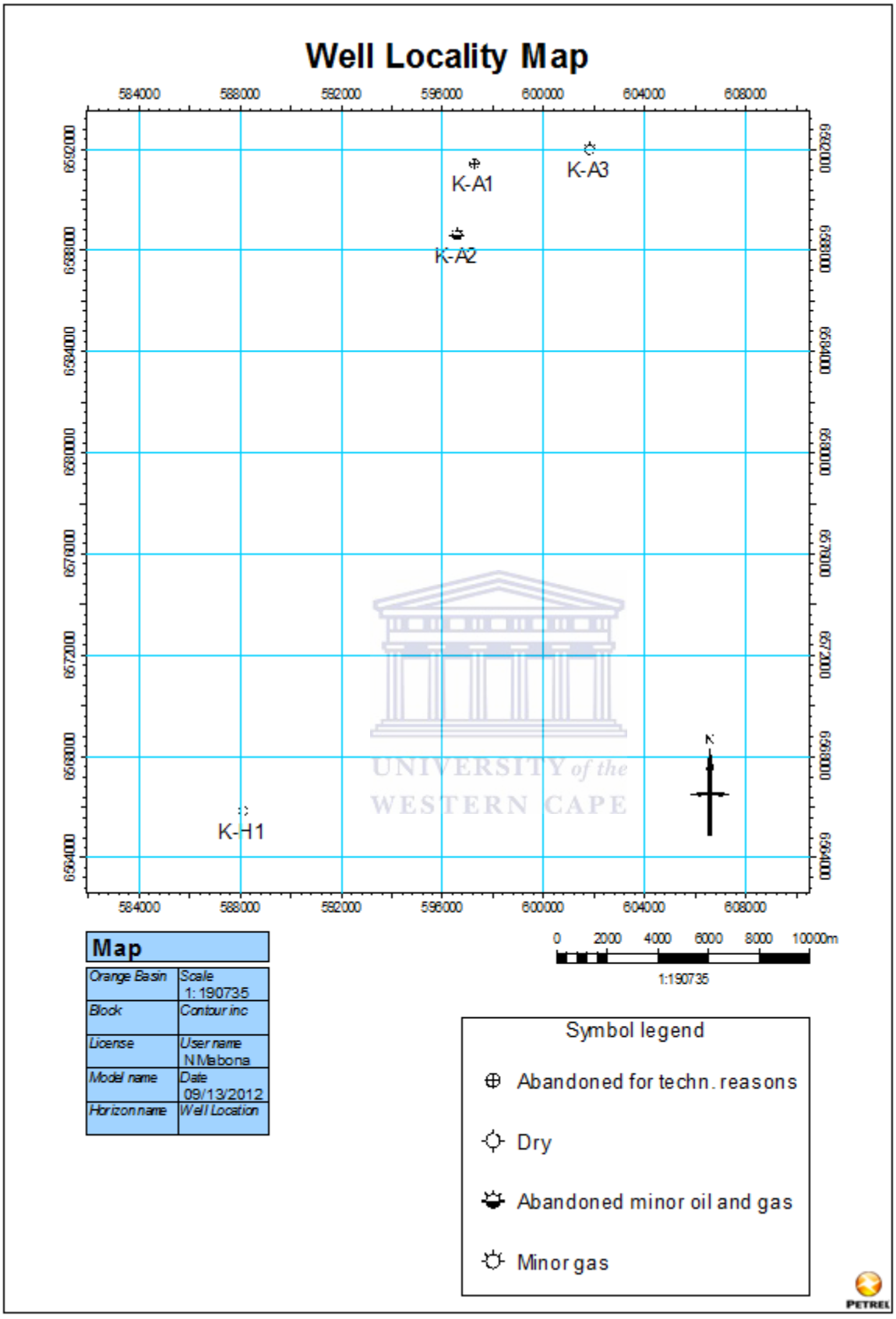

Figure 4: Well location map with well description (Generated in Petrel).

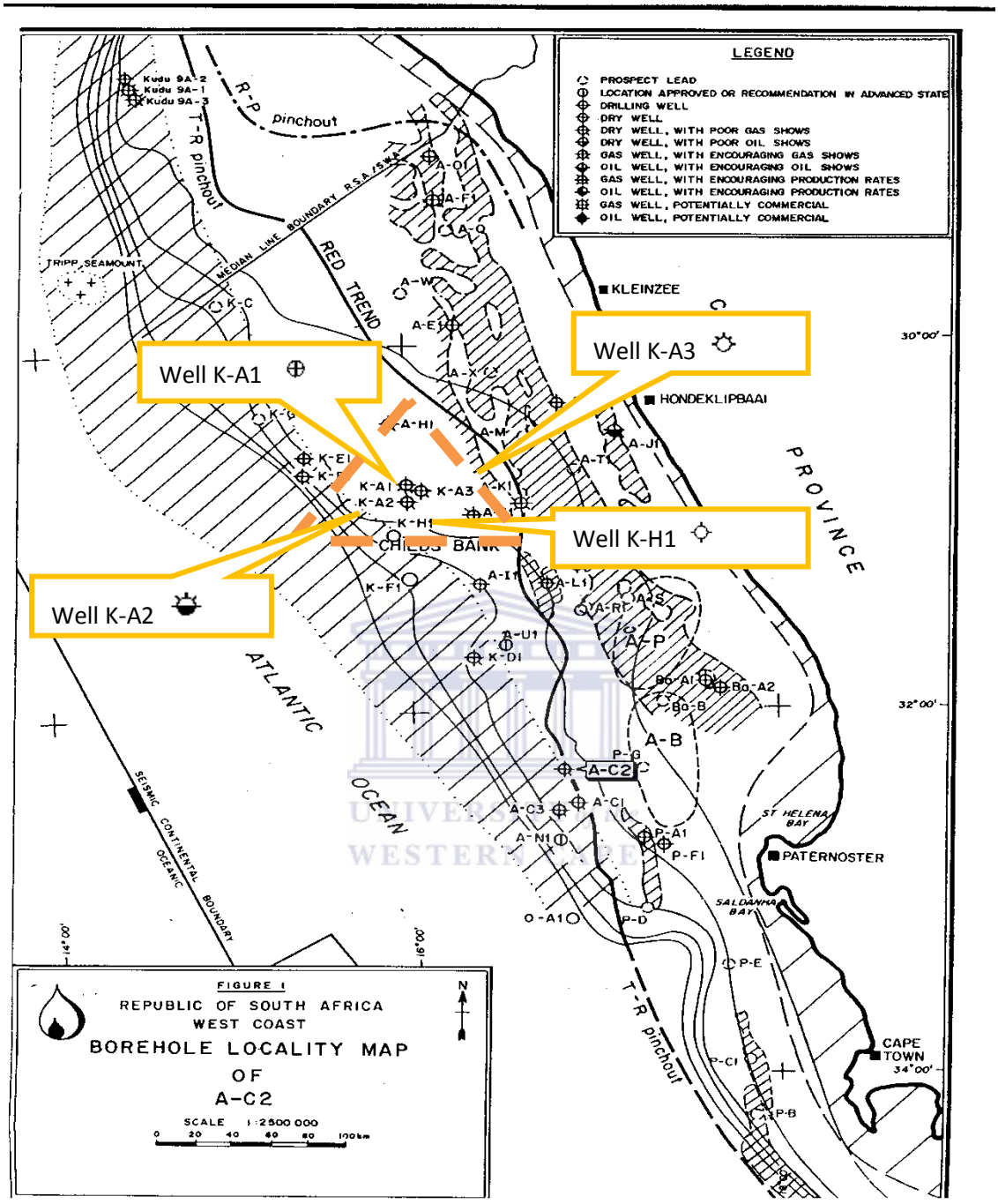

Figure 5: Borehole Locality Map of selected wells in the Orange Basin (Modified from PASA, 2003).

1.7 Geological background of the Orange Basin.

South Africa's coastline is about 3000km long. This comprises of the 900 km West coast which stretches from the Orange River to Cape Point and over 2000 km long from Cape Point further round the southern coast up alongside the western coast through Cape Town to the Southern Namibian Boarder (PASA Brochure, 2004/5).

Further beyond the coastline is the continental margin which constitutes the South African offshore environment. 20-160 km wide off the western coast is the immediate relatively shallower shelf area, 50-200 km wide off the southern coast and averaging 30 km wide on the eastern coast. The continental slope connects the shelf area with the deep marine environment. It follows a similar trend in width and widens on the west and south coast but becomes narrower to the eastern coast (Olajide, 2005).Figure 6, after (Broad 2004) provides a graphical representation of the geological background of the Orange Basin discussed in this sub-chapter.

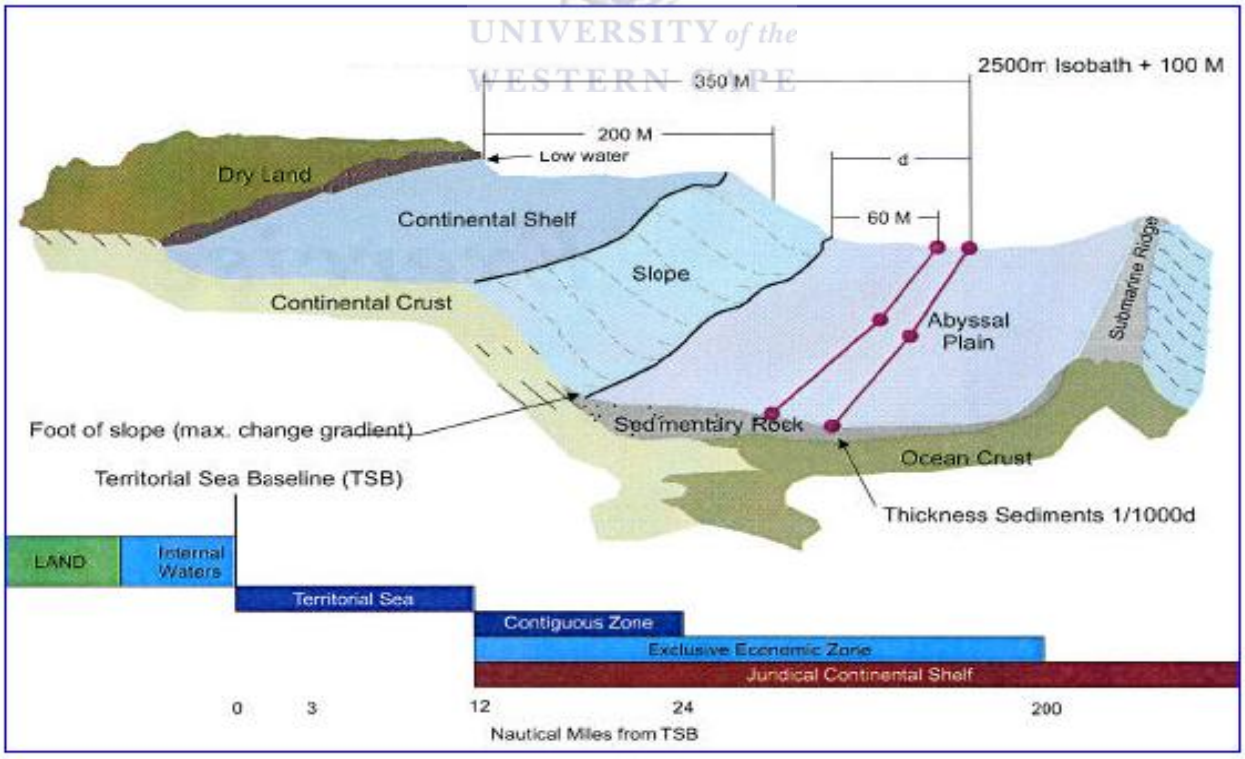

Figure 6: South Africa continental margin and oceanic crust (modified after Broad, 2004)

1.8 Previous Work on the Orange Basin

The Orange Basin is an under-explored area, the use of an integrated approach allows for a better comprehension of explored areas and more efficient and feasible manner of answering geological problems that are becoming more complex day by day. The use of an integrated approach in petroleum exploration has come into great use within the past few years. This is a result of more detailed analysis and decreases the uncertainty for when drilling.

The sparse data set of the Orange Basin with the majority of wells drilled on the shelf and widely spaced seismic data grid in the ultra-deep marine region coupled with proven hydrocarbon plays evidenced by the Kudu and Ibhubesi gas fields, makes the Orange Basin a good platform for frontier hydrocarbon exploration.

A study on the passive margin evolution and its controls on natural gas leakage in the southern Orange Basin, blocks 3/4, offshore South Africa was conducted by Kuhlmann et al. (2010). They made use of 2D seismic dataset that covered part of the southern Orange Basin offshore South Africa, and reconstructed the geological evolution of the basin. This evolutionary model was then used to investigate the occurrence of natural gas within the sedimentary column and the distribution of gas leakage features in relation to the observed sedimentary and tectonic structures developed in the post-rift succession since the Early Cretaceous (Kuhlmann et al, 2010).

Questions regarding the interaction of crust and mantle dynamics in the generation of margin geometries were still remaining. Hirsch et al. (2007) investigated the Orange Basin and developed a geological model to determine the position of the Moho for an isostatically balanced system.

The South Atlantic volcanic margins where further studied by, Gladczenko et al. (1997). Four main tectono-magmatic crustal units were interpreted. The interpreted seismic lines off Namibia reveal prominent seaward dipping reflectors and other tectono-magnetic features related to the break-up. Stevenson and McMillan

(2004) studied the succession of the proximal Orange Basin in the upper Cretaceous. They used seismic stratigraphic analysis of shallow seismic, lithological data, Sleevegun data, as well as cores obtained from sea-bed samples. The paleoenvironment of the incised valley was looked at in details. Results from the studies conducted shows fluvial incision, which is dominant within the Lower Turonian and Upper Coniacian ages. Fluvial flood plain facies reflects a waterlogged, highly reduced environment, which favours the formation of groundwater ferricretes. These observations are said to contradict previously published views that a dominant Orange River drainage system existed since the Albian at the position which the mouth is today.

Brown et al. (1999) discussed the morphological and geological characteristics of the South Atlantic margins of both Africa and South America. They explored the use of sequence stratigraghy as a strong complement to traditional exploration methods. Understanding the depositional response of cyclic sea level changes under various tectonic and sediment supply conditions provide the key for successful application of sequence ideas in all types of basins.

Paton et al. (2007) investigated the petroleum system within the southern Orange Basin. They created a basin model which aided in the prediction of present day gas seepage at the sea floor. This was calibrated with observed seepage events. Results obtained from the study indicated that the main period for hydrocarbon generation occurred in the late Cretaceous epoch. This event was then followed by erosion at the end of the Cretaceous period, deposition altered during the shelfbreak and sediment volumes prograded into the deep basin. This led to a second period of maturation which was mainly focused on prograding Tertiary wedges. The model predicts that the kitchen area is active up until the present day and is the source of hydrocarbons that are observed seeping from the sea-floor at present.

Schoen and Strack investigated the use of seismic inversion in successfully predicting the reservoir, porosity and gas content of a selected field in the Orange Basin. The use of attributes and other inversion techniques

were used reservoir properties and presence. The use of inversion is an attempt to predict rock properties like fluid content, hydrocarbon saturation and thickness from seismic data. This technique has proven to be very powerful and successful in the aim of diminishing the drilling of dry wells and wet wells.

CHAPTER 2: Geology of the Orange Basin

2.1 Regional Geology

In South Africa, hydrocarbon exploration began around 1940 and was mainly run by the corporate entity called SOEKER which is now known as PetroSA. At about 1974 there was the discovery of the Kudu gas field in southern offshore Namibia (Brown et al., 1995). In these many years of exploration, the Orange Basin is still relatively under-explored, with up to one well drilled per 400km (PASA,2006). It is South Africa's largest offshore basin with its sedimentary supply being obtained from river systems, with a rivalling delta to the north of the basin.

The recent availability of seismic data and basic geologic interpretation packages, renewed exploration interest in Namibian offshore petroleum basin.

The Orange Basin underlies the Atlantic Ocean offshore from south-western South African. The Orange Basin extends between Cape Town and Southern Namibian border at approximately 500km.

The Orange Basin is one of South Africa's offshore basins. South Africa's offshore basins can be divided into three distinct tectono-stratigraphic zones: The Southern offshore, Eastern Offshore and Western Offshore zones (PASA Brochure, 2003/4).

Figure 7 below shows the sedimentary basins found in Southern Africa's margins and also the structural elements are depicted.

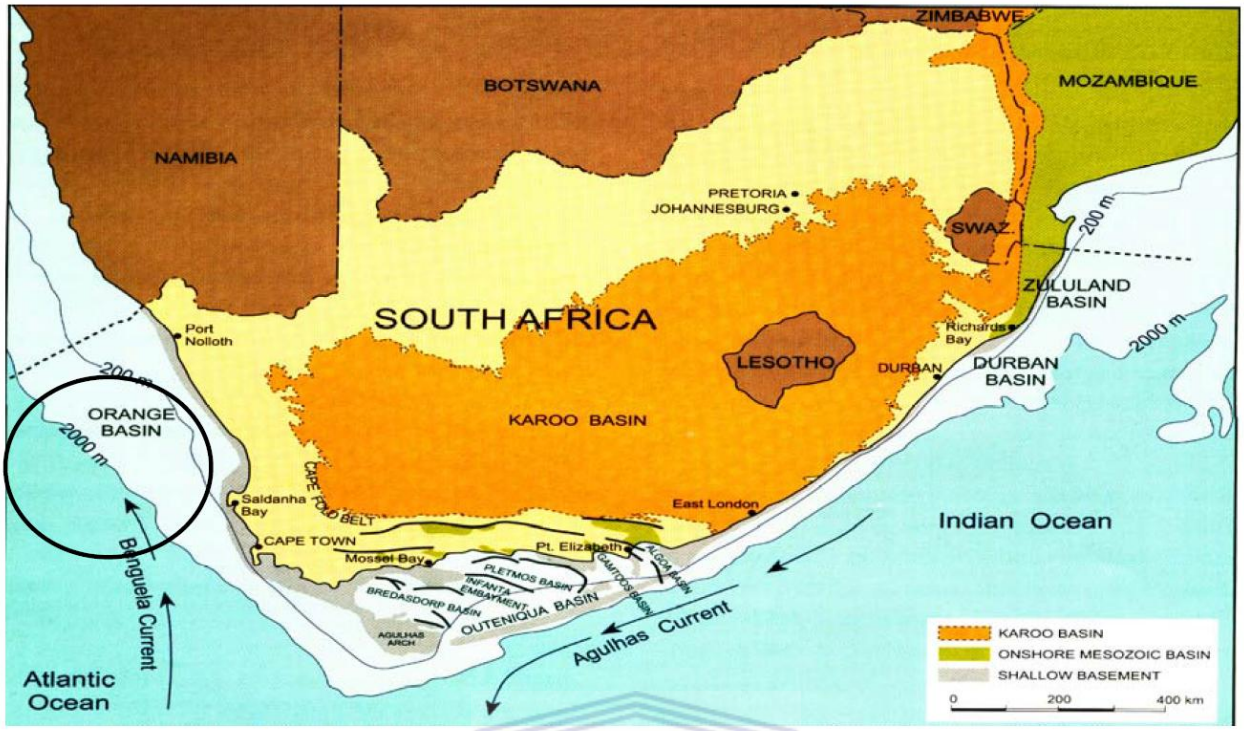

Figure 7: Structural elements and sedimentary basins of South Africa (PASA brochure, 2003)

The Southern Offshore zone is a large composite intracratonic rift basin, including a sub-basin, known as the Outeniqua Basin. During the Jurassic period the Eastern offshore which is a narrow passive margin was formed from the breakup of Africa, Madagascar and Antarctica from their supercontinent Gondwana. Two offshore basins are known as the Durban and Zululand Basins. These basins have seen limited exploration so far (van Van Vuuren et al., 2002).

The Western Offshore zone comprises of a broad passive-margin basin related to the opening of the South Atlantic in the Early Cretaceous period, known as the Orange Basin which is the subject of this study. The Orange Basin was formed by the breakup of Gondwana which initiated between 136 Ma and 126 Ma (Macdonald et al., 2003) with the development of the synrift to rift-stage sedimentary sequences up to the Hauterivian age.

2.2 Depositional Environment

The sedimentary inputs into the Orange Basin originate from the Orange River and Olifants River systems. Minor rivers entered the basin along coastlines aligned along the flank of Agulhas-Columbine Arch. Figure 8 from Bailey (2009) depicts a pictorial representation of the discussed area and Agulhas – Columbine Arch.

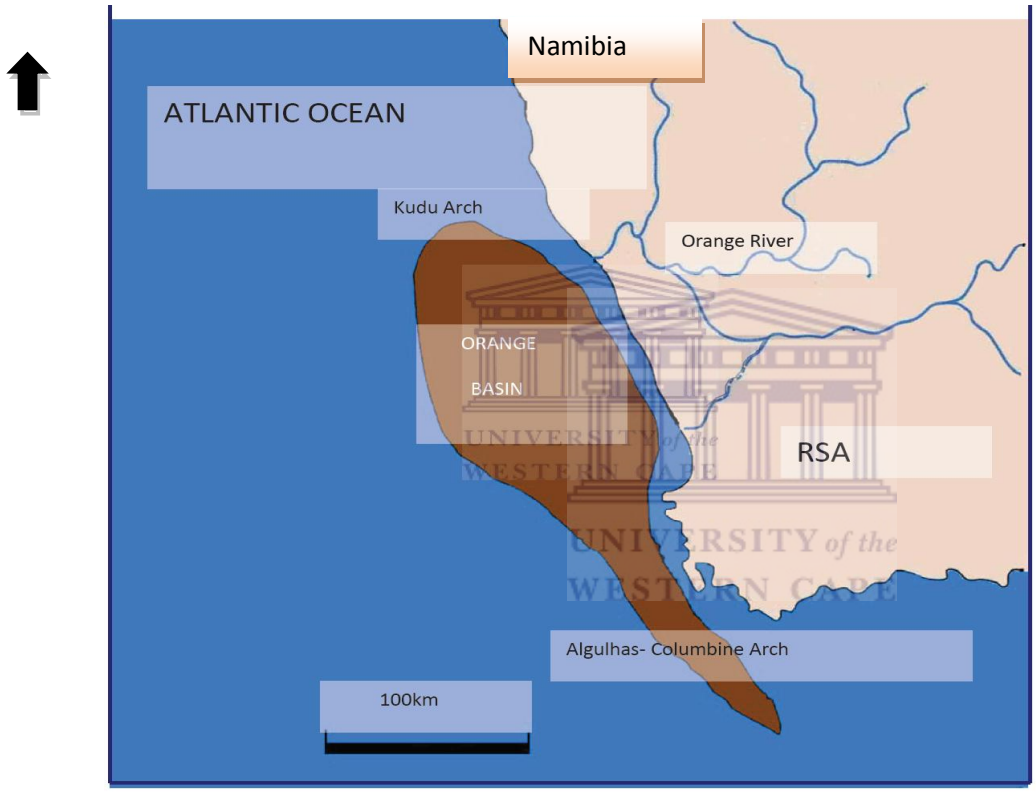

Figure 8: Map illustrating the locations of the flank of the South Western Agulhas- Columbine Arch. Also illustrated is the course of the Orange River, being the major sediment supplier to the Orange Basin. (Modified from van der Spuy, 2003)

The major contributor of the basin fill is the Orange River and early moderate influence is owed to the Olifants River (van der Spuy, 2003). The Olifants river system is a southern river system that entered the Atlantic by Lamberts Bay. The Olifants River contributed to filling the basin for approximately 13 million years from

117.5Ma to 103Ma (Brown et al, 1995) after which the Orange River became the sole contributor, post - 103Ma. The presence of major deltaic depocentres that are found adjacent to the mouths of the rivers 200km southwest of the Alexandra Bay provide evidence to support this fact (Dingle et al., 1983).

The basin developed under the long term influence of Orange fluvial and deltaic system. The Orange deltaic system progressively shifted laterally and prograded towards the west with increase in sediment supply.

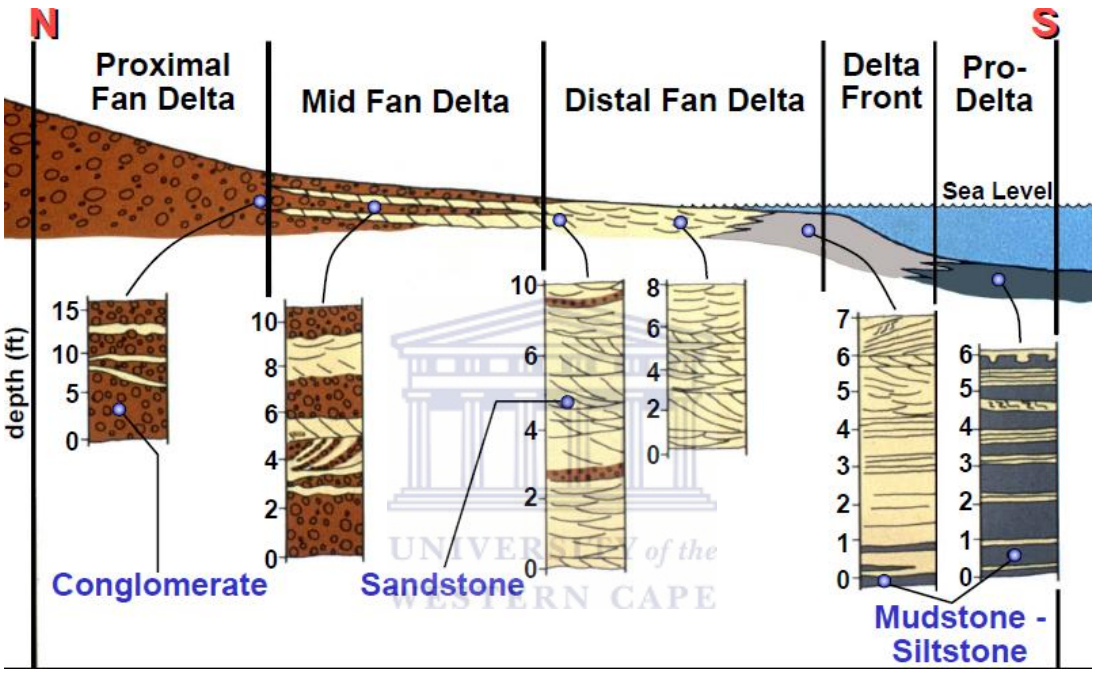

Figure 9: Sediments deposited in deltaic environment (McGowen & Bloch, 1985).

The Orange Basin consists of sediments from fluvial and deltaic environment. Figure 9 (McGwen & Bloch 1985) represents the sediments in the various transportation deposition zones in the area. The reservoir is heterogeneous consisting of massive sands with rare shale laminations and thinly bedded sand with plentiful shaly-silty inter-lamination. The alternating siltstone and mudstone with minor sandstone units constitute the Albian sequence. The average Albian sandstone reservoir thickness ranges from 3 m to 70 m. The sandstone appears greenish grey and shows the presence of glauconite apparently derived from marine conditions. The

sandstone is in the main well sorted, ranging in grain size from very fine to medium. The lower and upper contacts of sandstone are characterized by abrupt lower contacts, gradual bioturbated upper contact. The siltstones are thinly bedded and contain bioturbation (Derder 2002)

2.3 Regional Chronostratigraphy of Southern Africa offshore basins.

The rifting and breakup of Gondwanaland played a vital role in the formation and shaping of Southern African offshore basins. The Upper Palaeozoic period in this region was characterized by subduction during the Late Carboniferous to Early Permian along the southwest margin of Gondwana (PASA, 2004/5). This changed an old passive margin into a foreland basin known as the Great Karoo Basin. Sediments were fed into this basin from the south. The Cape Fold Belt formed during the Permo- Triassic period by the formation of an arc which thrusted the Cape Supergroup eastward onto the Karoo province (Figure 10, from Bailey 2009).

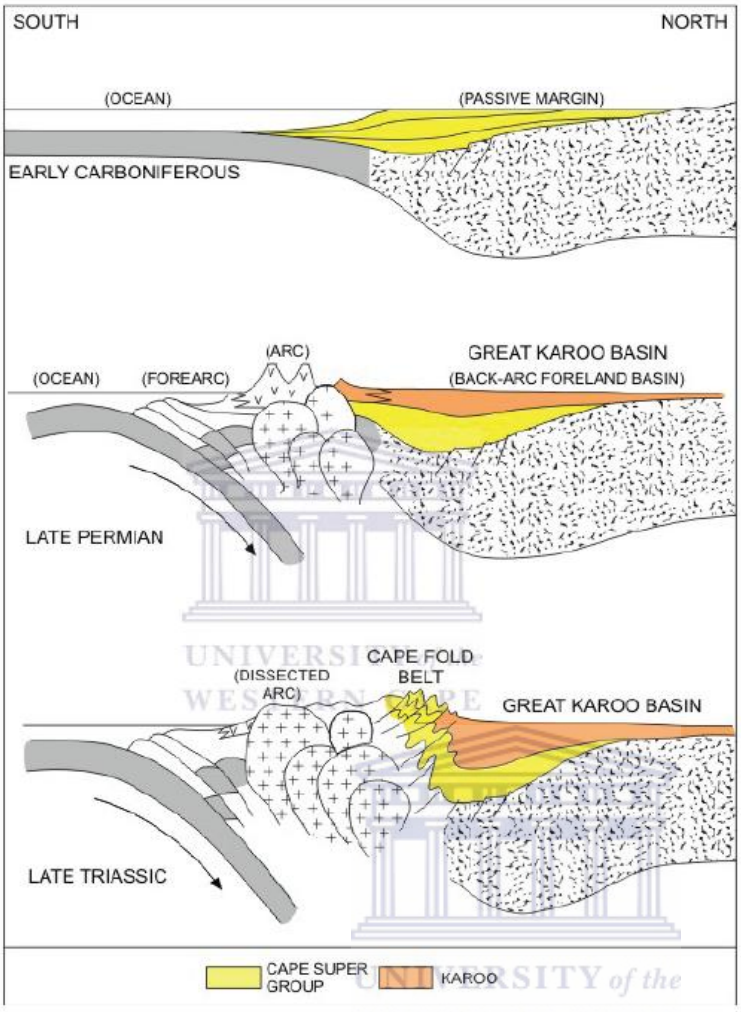

Figure 10: Evolution of the Cape Fold Belt. Source: Petroluem Agency SA, 2003

The Mesozoic era is characterized by volcanism in the Early to Middle Jurassic, which marked the end of erosion. This occurred in South Africa, the Falklands and Antarctica, and provides evidence of the Gondwana break up. The eastern margin of Africa started to break away with Madagascar and Antarctica pulling away. This caused the formation of the Durban and Zululand Basins.

Movement of microplates past southern Africa caused shearing between plates, namely the Falkland Plateau, during the early to Middle-Cretaceous moved towards the south west past the south coast of Africa which resulted in dextral shearing between the plates. This movement marked the formation of the sub basins of the Outeniqua Basin. The failed rifting created half grabens which began in the east and progressed towards the

west, resulting in the formation of the Algoa Basin followed by the Gamtoos, Pletmos and the youngest Bredasdorp Basins. The Orange Basin is a post-rift basin and overlies many rift basins of Early Cretaceous epoch. It is bounded on the northwest by the Kudu arch of southern Namibia and on the southeast of by the Agulhas-Columbine Arch (Brown et al, 1995).

2.4 Stratigraphy

Earliest sedimentation in the Orange Basin is dated as Pre-Hauterivian and is thought to have begun in the Kimmeridgian (~152-154 Ma) or Tithonian Brown et., al 1995. The Orange Basin contains the stratigraphic record from lithospheric extension and rift tectonics throughout a fully evolved post-break-up setting. The stratigraphy of the Orange Basin can be illustrated in terms of the prerift, synrift, transitional, drift and tertiary to present day successions de Vera et al., (2010). Figure 11 below provides a good illustration of the Orange basin's stratigraphy and tectonic setting.

The sedimentary fill of the Orange Basin is believed to be due to cyclic sea level changes, hence it is observed to be a broad prograding sedimentary wedge, subdivided by erosional unconformaties. The sedimentation in the Orange Basin was broadly due to the syn-rift and Drift phase of sedimentation processes (PASA.2005).

The prerift phases or basement rocks of the Orange Basin consist of high grade and low grade metamorphites in the south and granitic plutons and alkaline intrusives in the northern part (Broad et al,2007). The basement rocks are overlain by Pre- Barremian synrift successions (van der Spuy et al, 2007) that have been intersected in drill cores between horizons T and 6At. The succession is composed predominantly of basic lavas within the central rift sequences and coarse continental clastic, fluvial and lacustrine sediments along with volcanics within the marginal rift basins (Barton et al, 1993).

The synrift phase fills complex grabens and half-grabens which contain continental sediments, with volcaniclastics and volcanics in places and are subdivided into synrift I and synrift II (Broad et al., 2006). Additionally, late Hauterivian lacustrine organic-rich shales are also contained within this phase and represent the oldest sediments in this succession.

A Hauterivian age unconformity separates the rift geology from that of the post rift period (PASA,2005). Between Hauterivian (130Ma) and Mid Aptian (100 Ma) times, an early drift phase commenced which corresponds to unconformities 6At1 and 13At1. The succession is classified as intermediate with Barremian-early Aptian source (Campher et al., 2009).

The later drift phase marks the start of full drifting, with sediments ranging from continental red beds to marine sandstones and siliclastic deposists largely deltaic and turbidites sediments in the distal parts (Broad et al., 2006). This interval continues until offshore Namibia where changes to aeolian sandstones.

This drift phase is denoted by the 13At1 unconformity and contains large growth and, slump structures and associated toe thrusts along shelf edge. The source rock in this phase is associated with global Cenomanian-Turonian anoxic event. The non-marine to marine sedimentation transition is shown by the 13At1 unconformity (Hirsch et al.2007).

2.5 Tectonic Evolution

Three major tectonic phases can be recognized in the area (Gerrard and Smith, 1982). On regional terms they are referred to as pre-, syn- and post-rifts phases. During the pre-rift time until the Late Triassic, the area was dominated by compressional tectonism and formed part of the Gondwana foreland. Figure 11(Schalkwyk,2005) displays present day plate tectonic evolution model of the South Atlantic showing the boundary of the area covered by the Mesozoic palaeofacies maps.

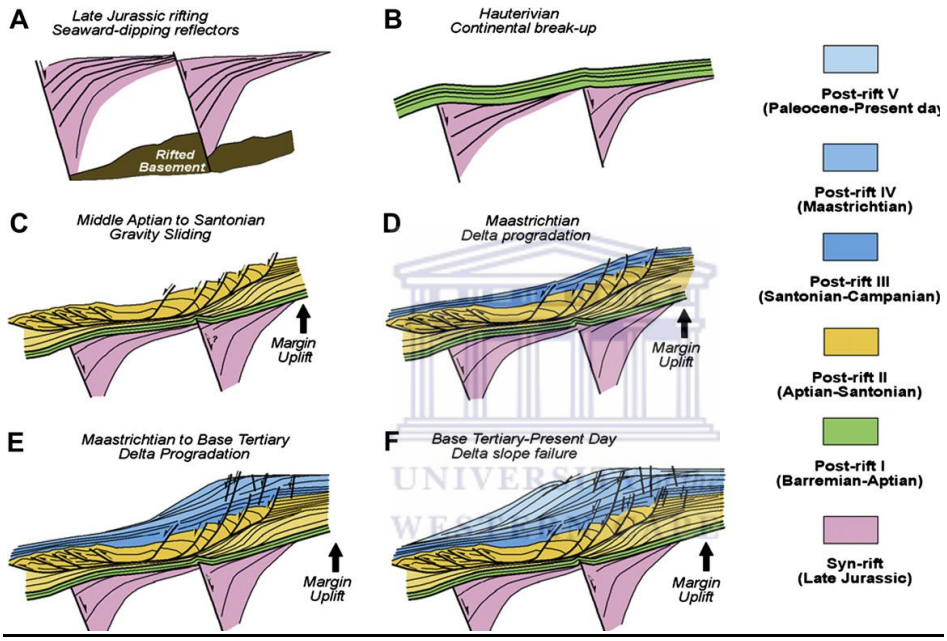

Figure 11: Synoptic basin evolutionary model for the gravity-driven system of the Orange Basin. A. Late Jurassic rifting (160–130 Ma). B. Hauterivian–Aptian (133–120 Ma). C. Middle Aptian–Campanian (120–75 Ma). D. Campanian–Maastrichtian (75–70 Ma).E. Base (de Vera et al 2010)

The southwestern margin of the South Africa is a divergent plate margin underlain by syn-rift graben basins and post-rift or passive margin Orange Basin (Muntingh 1993).

The Southern offshore is a large composite intra-cratonic rift basin, including a sub-basin, known as the Outeniqua Basin. During the Jurassic the Eastern offshore zone which is a narrow passive margin was formed from the breakup of the

supercontinent into Africa, Madagascar and Antarctica. Two offshore basins are known as the Durban and Zululand Basins. These large areas have seen limited exploration so far (van Vuuren et al., 1998).

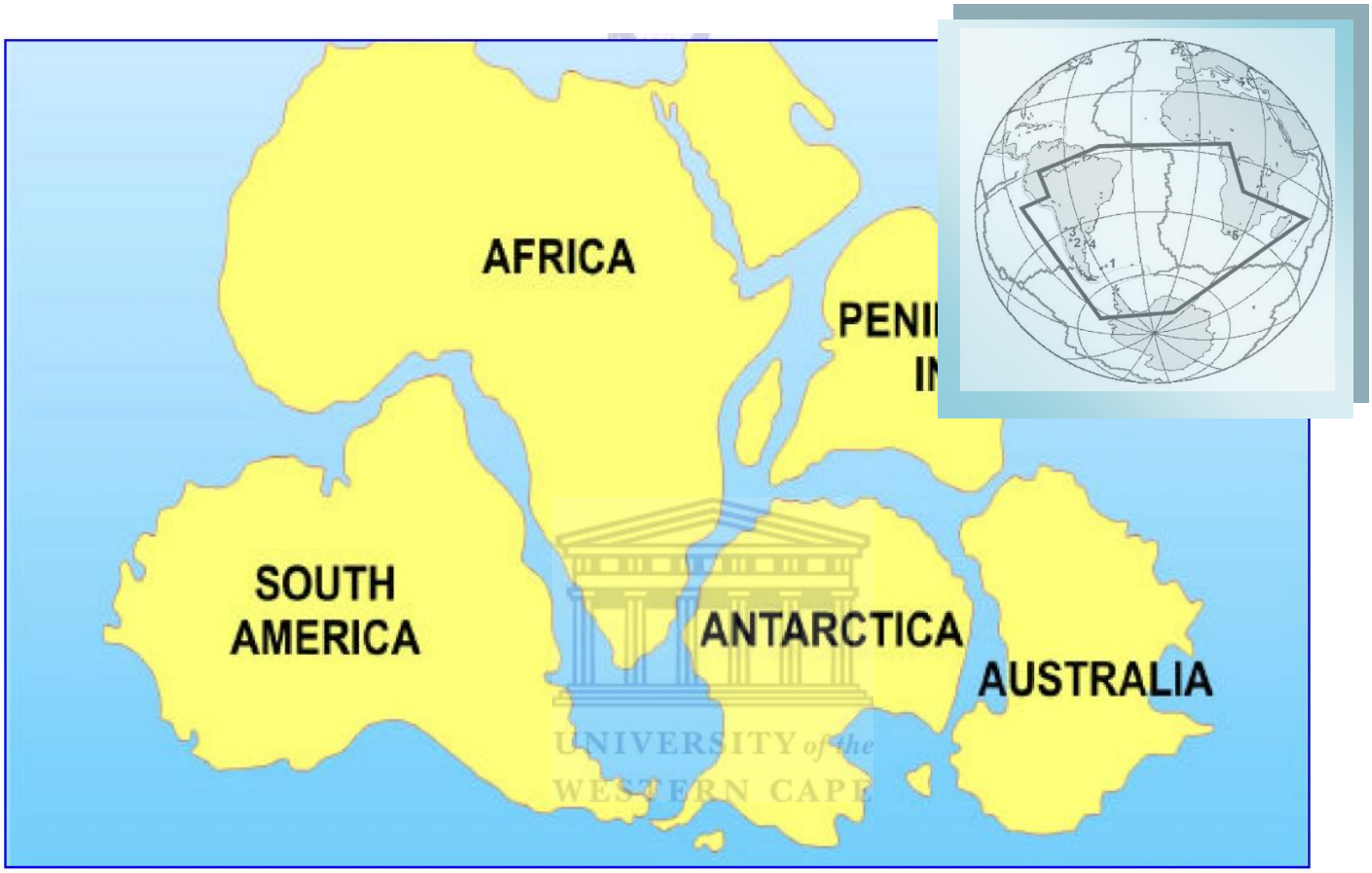

Figure 12: Continental rifting during Late Jurassic – Lower Valanginian (Broad, 2004)

The western margin of southern Africa is a passive continental margin formed by the breakup of Gondwana and the subsequent opening of the South Atlantic Ocean during the Late Jurassic to Early Cretaceous. (Figure 12) The break up initiated between 136 Ma and 126 Ma (Macdonald et al., 2003) with the development of the synrift to rift-stage sedimentary sequences up to the Hauterivian.

Rifting was accompanied by initial faulting and the creation of grabens and half-grabens aligned roughly parallel to the present coastline (Hirsch et al.2010). The rifting consists of an inner and outer zone of

predominantly coast parallel half graben, of which the latter extends westward into a marginal ridge and beyond into a series of wedges of seaward dipping reflectors.

There are several grabens formed by rifting of continental crust sub-parallel to the present coastline. Lower Cretaceous siliciclastic continental and lacustrine sediments filled the rift basin, but with some volcanic rocks present. The pre-rift basement of Precambrian or Palaeozoic is overlain by synrift strata resting unconformably (Brown et al., 1995; Jungslanger, 1999).

CHAPTER 3: Literature review

Based on previous studies, the Orange Basin requires the use of advanced techniques and methods in the understanding of its reservoir. This study will then create a framework and develop models which calibrate this data and utilize petrophysical analysis and geological models in advancing the geological comprehension and exploration of this area.

Petrophysical analysis has its strengths and weaknesses and the most output is received when this method is used with other techniques. The use of seismic with petrophysical analysis gives the lateral extent of the subsurface and geometry of the area.

No single method will meet the need of improved and accurate analysis and characterizing the reservoir, therefore new and existing technologies must be integrated to meet the need.

The use of petrophysical data goes beyond evaluation of porosity, saturation and permeability. Many disciplines use data that originate from well-bores; workflows become cross-domain in order to achieve their objectives. Combining core, log and seismic data brings added value for reservoir analysis.

In the past decade there has been a great improvement in the position of Petrophysics in seismic interpretation. This has resulted in vital improvements in seismic data processing techniques which consequently have a direct impact on the ability to estimate reservoir properties through the use of seismic inversion, amplitude versus offset methods and attribute analysis.

The petroleum industry is filled with many domain experts who at times are not integrated. Geologist's, petrophysicist's and geophysicist's work with each other's data very often but sad fact is that petrophysicist are unaware what geophysicist wish to do with log data and geophysicist rarely take advantage of the

operations logs are able to do. This is in essence a double standard and a disadvantage on exploration for the industry. (Veeken and Rauch-Davies, 2006)

These occurrences are the result of under evaluated reservoirs due to use of techniques independently of others. This realization means that the optimum petrophysical analysis should be capable of a wide range of analysis options and should be extendable across a broader scope of workflows; petrophysical data is involved in many stages of analysis from the well to the reservoir scale. Building strong, deep and efficient links between Petrophysics and seismic optimizes exploration and could result in breakthroughs.

The assessment of reservoirs has mostly been of single methods and techniques; this has resulted in pitfalls in acquiring advanced information on reservoirs. The study is not only worthy of academic investigation, but can also provide the industry with new insights on new techniques which better improve exploration.

3.1 Reservoir Characterization

Veeken and Rauch-Davies (2006) define Reservoir Characterization as a reservoir modeling technique that predicts the behaviour of a reservoir. It is best described as a process that includes integrating, analyzing and understanding all available data from the well. The optimization of well performance is a result of the understanding of reservoir characteristics and being able to extract valuable information from seismic and log data of the well to enable excellent well and field development planning. Advanced technology and expert knowledge provide accurate reservoir analysis and answers that simplify development decisions.

A key task of reservoir characterization is to quantify and map reservoir properties such as porosity, permeability, water saturation, and net pay in the wells of the basin. To accomplish this, traditional petrophysical methods combined with new techniques such as seismic and petrophysical tie and analysis, core and log interpretation and correlation are utilized.

Interpretation of the well data allows the estimation of reservoir parameters. Correlation is very important in reservoir characterization. Correlation of logs with core data provides a comprehensive understanding and identification of the reservoir. Correlation between the wells can become extremely difficult and traditional correlation techniques can prove to be inadequate hence the use of seismic and petrophysics as a calibration. Reservoir characterization through petrophysical analysis permits for vast seismic modeling and forms the basis for understanding the seismic signature. It helps in the prediction of reservoir characteristics away from well control points. Reliable estimation of petrophysical parameters is needed as input for such studies. These petrophysical estimates are an integral part of more advanced reservoir characterization and modeling.

The calibration of seismic to well data, allowed the integration of the petrophysical and production information to characterize reservoirs. In summary Reservoir evaluation encompasses various techniques of determining and analyzing properties exhibited by a petroleum reservoir, assuming it exists, usually referred to as reservoir characterization, in order to make volumetric estimates and to justify its commerciality.

3.2 Petrophysics

Petrophysics is the study of physical properties of rocks. These properties can be measured directly on rock samples retrieved from the borehole as cores (drill-cores). They can also be derived from electronic measurements carried out in the borehole while the well is being drilled or after the well has been drilled. The main properties of interest are porosity, fluid saturations and permeability, but there are many more. These parameters are needed to estimate the amount of hydrocarbon present in a well, and how much of it can be recovered economically.

The study will make us of petrophysical analysis and integration with seismic data. Hence the topic, Seismic Petrophysics is discussed.

Crain (2003) defines Seismic petrophysics as a term used to describe the conversion of seismic data into meaningful petrophysical or reservoir description information, such as porosity, lithology, or fluid content of the reservoir. Until recently, this work was qualitative in nature, but as seismic acquisition and processing have advanced, the results are becoming more quantitative. Calibrating this work to well log "ground truth" can convert the seismic attributes into useful reservoir exploration and development tools. Since there are infinite possible inversions, it is pretty important to find the one that most closely matches the observed reality.

3.3 Wireline logs

Wireline log is the main source of accurate information on the depths as well as apparent and real thickness of beds. They yield information on the subsurface geology including formation boundaries, lithology, fluid content, and porosity amongst others. The wireline log suite obtained for this study includes Gamma ray, Sonic, Resistivity, Neutron and Density logs (Crain, 2003). Figure 13 illustrates the signatures of these mentions wireline logs.

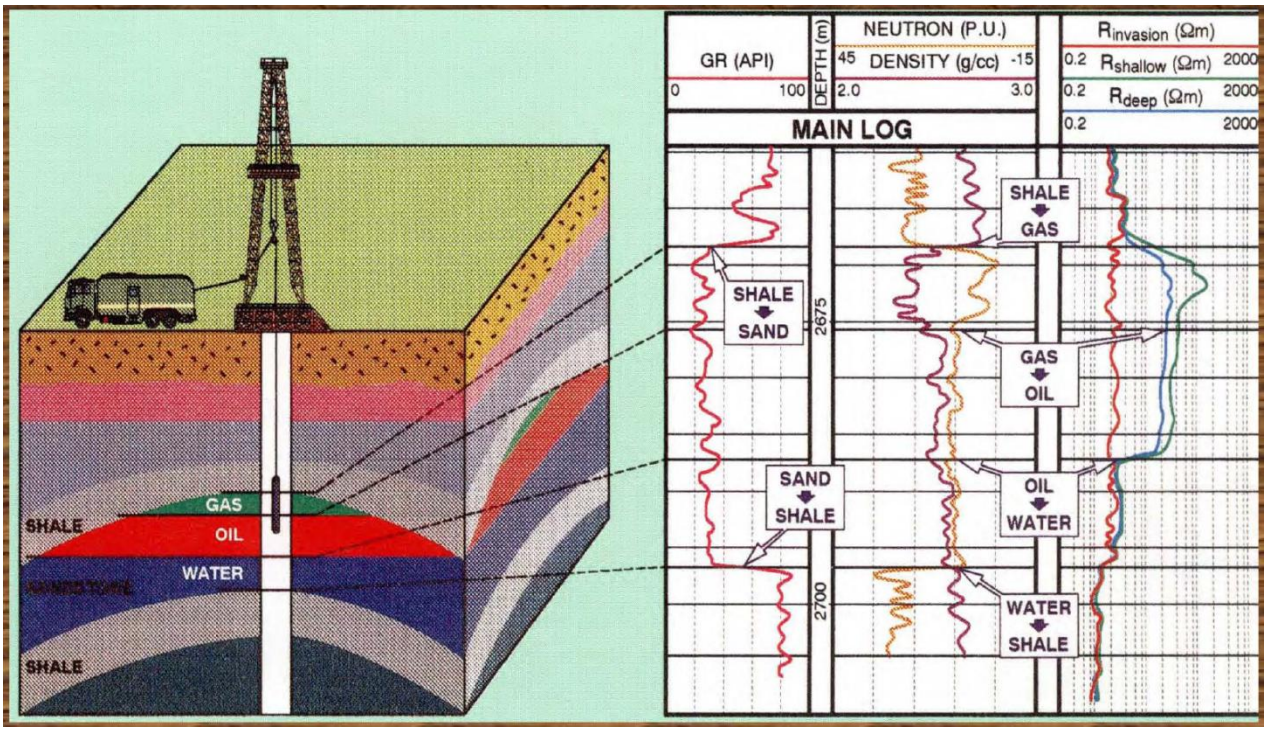

Figure 13: Graphical representation of logs and reference to subsurface and hydrocarbons. (After Van Ditzhuijzen, P, 1994)

The geophysical wireline logs are the continuous records of geophysical parameters along a borehole. They are products of wireline logging which involves inserting a logging sensor or a combination of sounding probes (Sonde) in the drill collar which is then lowered into the well bore by a survey cable and continuous physical measurements (electrical, acoustical, nuclear, thermal and dimensional) are made. Figure 14 below is a pictorial representation of the process discussed above, where the number three (3) is the Sonde in the borehole which has light emitting which represent the signals been given out and measurements acquired from readings made.

A sensor and its associated electronics are housed in a Sonde, which is suspended in the hole by an armoured electric cable. The sensor is separated from the virgin formation by the drilling mud, mud cake, and often by an invaded zone in the formation. Signals from the sensor are conditioned by down-hole electronics for

transmission up the cable to the surface electronics, which in turn conditions the signals for output and recording. As the cable is raised or lowered, it activates a depth measuring device which provides depth information to the surface electronics and recording devices. The data is recorded on digital tape, film or paper for analysis and interpretation.

Once a well is cased and in production, data missed in the original logging phase cannot be recovered anymore and costly work-over would be needed to find out what went wrong and where. It is therefore a false economy to cut corners during the original logging operation.

Some well logs are made of data collected at the surface; examples are core logs, drilling -time logs, mud sample logs, hydrocarbon well logs, etc. Other types such as movable oil plots, computed logs, et cetera, show quantities calculated from other measurements.

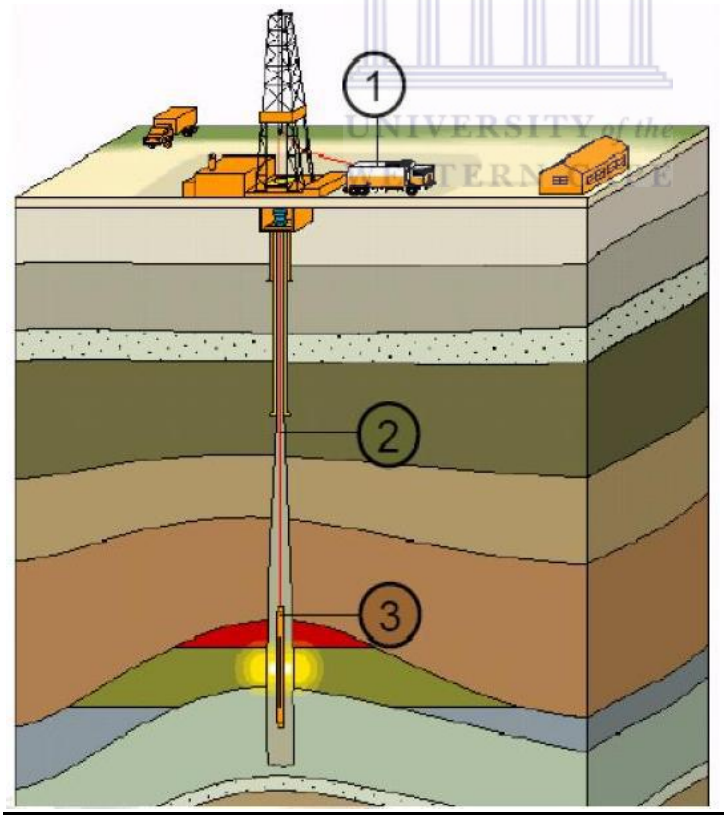

Figure 14: Well logging operations, and sonde in the formations. After Strack 2002

3.3.1. Gamma Ray Logs

Gamma ray logs are designed to measure the intensity of natural radioactivity in formations. The number of energy of the naturally occurring gamma ray in the formation is measured and distinguished between elements of parent and daughter product of the three main radioactive families: Uranium, Thorium, and Potassium (Figure 15). In sediments the log mainly reflects clay content because clay contains the radioisotopes of potassium, uranium, and thorium. Potassium feldspars, volcanic ash, granite wash, and some salt rich deposits containing potassium (e.g. potash) may also give significant gamma-ray readings. Shale-free sandstones and carbonates have low concentrations of radioactive materials and give low gamma ray readings. The standard unit of measurement is API (American Petroleum Institute)

Gamma ray log is usually preferred to spontaneous potential logs for correlation purposes in open holes nonconductive borehole fluids for thick carbonate intervals, and to correlate cased -hole logs with open–hole logs.

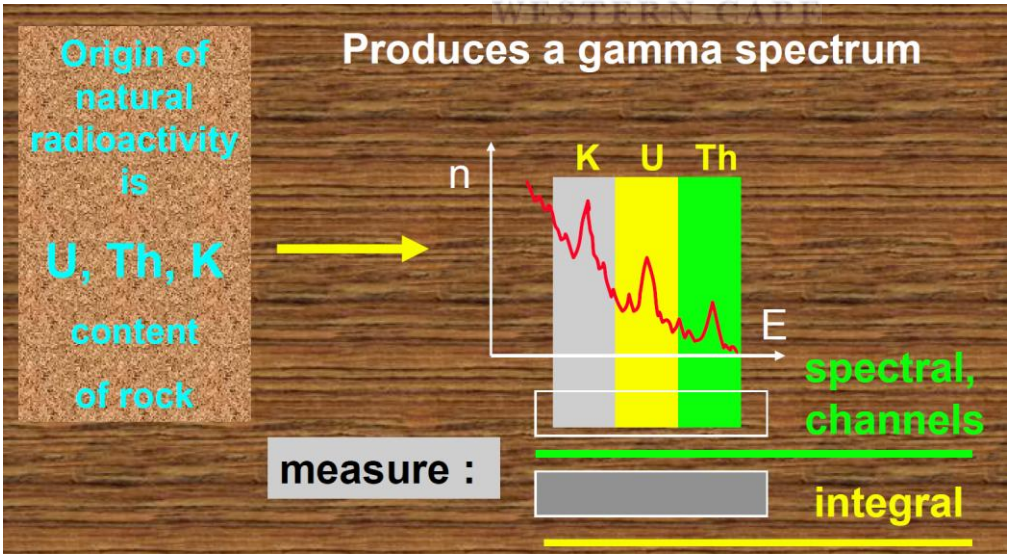

Figure 15: Gamma ray spectrum in spectral channels. Modified from Schlumberger 1972

Figure 16 below is a cross plot between Th/K (ratio of Thorium and potassium) and Pe (lead), from this the mineral classifications can be made and at times the high gamma ray reading will be a result of presence of mica, feldspars and glauconite in the rock.

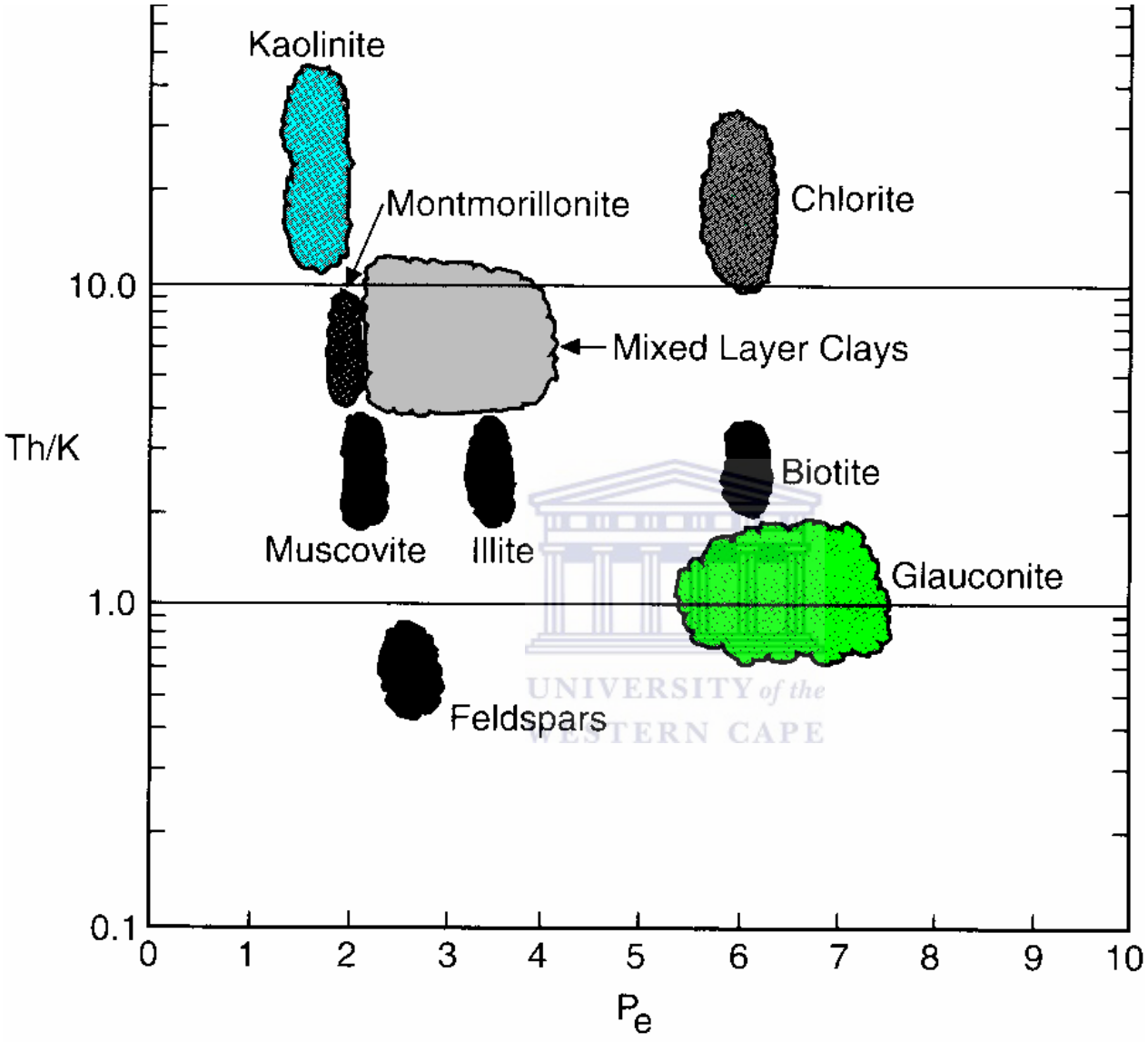

Figure 16: Th/K crossplot and mineral classification. (Schön, J.H, 1996)

3.3.2 Neutron logs

Neutron Logs measure the hydrogen content in a formation. In clean, shale free formations, where the porosity is filled with water or oil, the neutron log measures liquid filled porosity (ϕN, PHIN, NPHI).

Neutrons are emitted from a chemical source (americium –beryllium mixture). On collision with nuclei in the formation, the neutron loses energy. With enough collisions, the neutron is absorped and a gamma ray is emitted. (Figure 17 a)

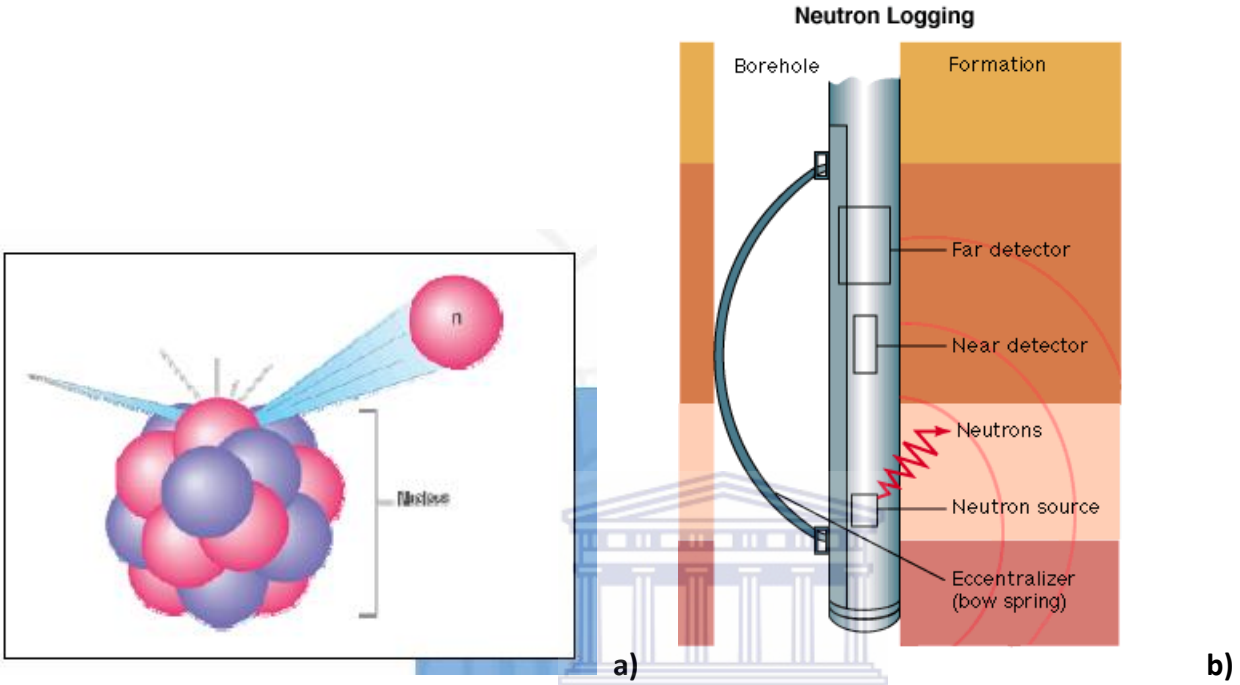

Figure 17: a) Neutron emitted from nuclei. Strack, 2002. b) Neutron logging tool from Schlumberger NeXT Basic logging course

Since a neutron is slightly heavier than a proton, the element which closely approximates to the mass of a neutron is hydrogen. In neutron-hydrogen collisions the average energy transfers to the hydrogen nucleus is about ½ that of contained in the neutron. Whereas, if the scattering nucleus was oxygen (mass16 amu) the neutron would retain 77% of its energy.

Materials with large hydrogen content like water or hydrocarbons become very important for slowing down neutrons. Since hydrogen in a porous formation is concentrated in the fluid-filled pores, energy loss can be related to the formation's porosity. Neutron curves commoly displayed in track 2 or 3 are displayed as Neutron Porosity (NPHI, PHIN, NPOR) (Figure 13).

Units: porosity units (p.u.) (calibrated with a standard, different for all tools), v/v decimal, fraction or %

Neutron logs are not calibrated in basic physical units. Therefore, specific logs need to be interpreted with specific charts.

3.3.3 Caliper Log

Caliper log is used to measure the hole size (diameter and shape of a borehole). The caving size and wash outs can be determined. It uses a tool which has 2, 4, or more extendable arms. The arms can move in and out as the tool is withdrawn from the borehole, and the movement is converted into an electrical signal by a potentiometer.

In the two arm tool, the borehole diameter is measured. This is shown in track 1, (Figure 18) of the master log together with the bit size for reference. Borehole diameters larger and smaller than the bit size are possible. Many boreholes can attain an oval shape after drilling. This is due to the effect of the pressures in the crust being different in different directions as a result of tectonic forces. In oval holes, the two arm caliper will lock into the long axis of the oval cross-section, giving larger values of borehole diameter than expected. In this case tools with more arms are required.

In the four arm (dual caliper) tool, the two opposite pairs work together to give the borehole diameter in two perpendicular directions. An example of a four arm tool is the Borehole Geometry Tool (BGT). This has 4 arms that can be opened to 30 inches (40 inches as a special modification), and gives two independent perpendicular caliper readings. The tool also calculates and integrates the volume of the borehole and includes sensors that measure the direction (azimuth) and dip of the borehole, which is useful in plotting the trajectory of the borehole.

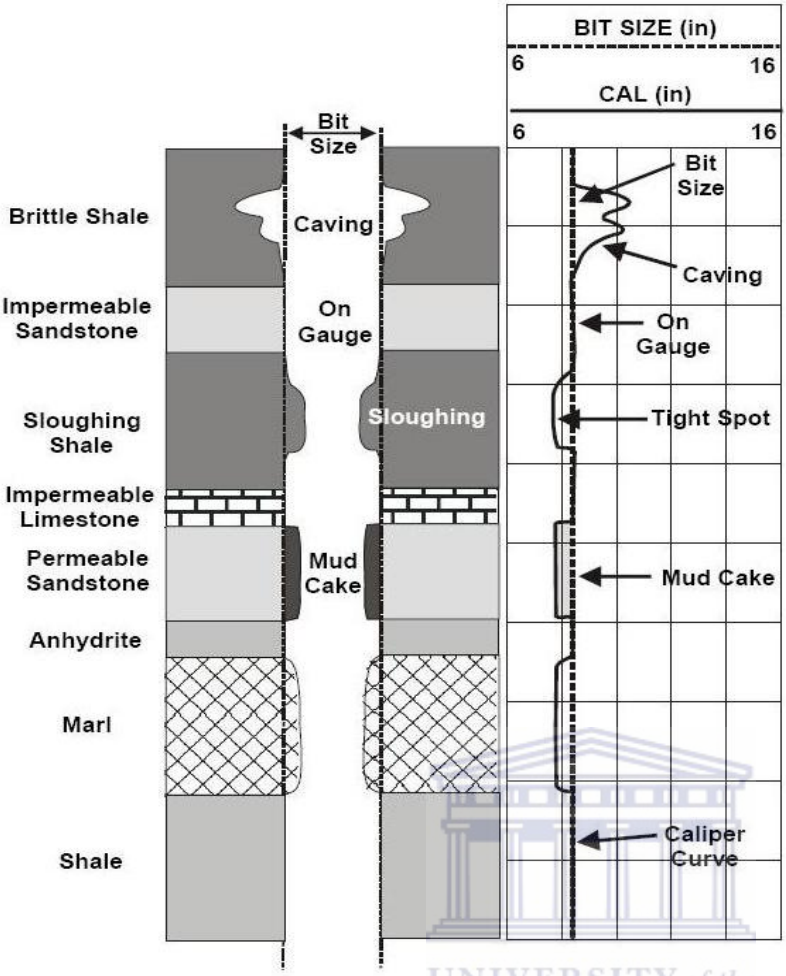

Figure 18: Typical caliper response to various lithologies. Western Atlas, 1992

In the multi-arm tools, up to 30 arms are arranged around the tool allowing the detailed shape of the borehole to be measured.

The caliper logs are plotted in track 1 with the drilling bit size for comparison, or as a differential caliper reading, where the reading represents the caliper value minus the drill bit diameter. The scale is generally given in inches, which is standard for measuring bit sizes.

Use of Caliper Log:

The commoner uses of the caliper log are as follows:

- ❖ Contributory information for lithological assessment.
- ❖ Indicator of good permeability and porosity zones (reservoir rock) due to the development of mudcake in association with gamma ray log.
- ❖ Calculation of mudcake thickness.

Indication of hole quality for the assessment of the likely quality of other logs whose data quality is degraded by holes that are out of gauge. Other log data can often be corrected for bad hole conditions using the caliper readings, but the larger the correction, the less reliable the final data will be. Centralized tools are designed to be about 4 inches in diameter for a standard 8.5 inch hole, and they are designed to work with 2.25 inches of drilling mud between them and the formation.

If the hole caves to 14 inches, which is not uncommon, the distance to the formation becomes 5 inches and the tool responses are degraded. This can be corrected for to some extent if the caliper value is known. Tools that work by being pressed up against the side of the borehole wall have even greater problems because the irregularity of the borehole wall makes it impossible to obtain reliable readings. The caliper log is additionaly used for the selection of consolidated formations for wireline pressure tests, recovery of fluid samples, for packer seating for well testing purposes, and for determining casing setting depths.

3.3.4 Spontaneous Potential Logs (SP)

Also known as self potential logs , it measures potential (DC voltage) difference between a movable electrode in the borehole and a distant reference usually at the surface .The SP results from the measurable voltage drop in the borehole produced by the flow of SP currents generated by electrochemical and electrokinetic potentials in the hole. The SP tends to follow a fairly constant shale base line in impermeable shales while in permeable formations. The deflection depends on the contrast between the ion content of the formation water and that of the following: Drilling mud filtrate, Clay content, Bed thickness and resistivity, Hole size, Invasion and Bed boundary effect.

In thick permeable, thick non-shale formations, the SP value approaches a fairly constant value (static SP), which will change if the formation water salinity changes. It varies in dirty reservoir rocks and a set of pseudo-static SP values is recorded (figure 19).

SP is most useful when:

- Drilling mud is fresher than the formation water,
- Good contrast exists between mud filtrate and formation water resistivity,
- Formation resistivity is moderately low.

The SP curve becomes featureless when the mud column becomes so conductive that it fails to display a demonstrable voltage drop which the tool can support. SP response of large negative deflection in permeable beds enhances easy sandshale discrimination, correlation, and under favourable conditions estimation of formation water resistivity (Rider, 1996).

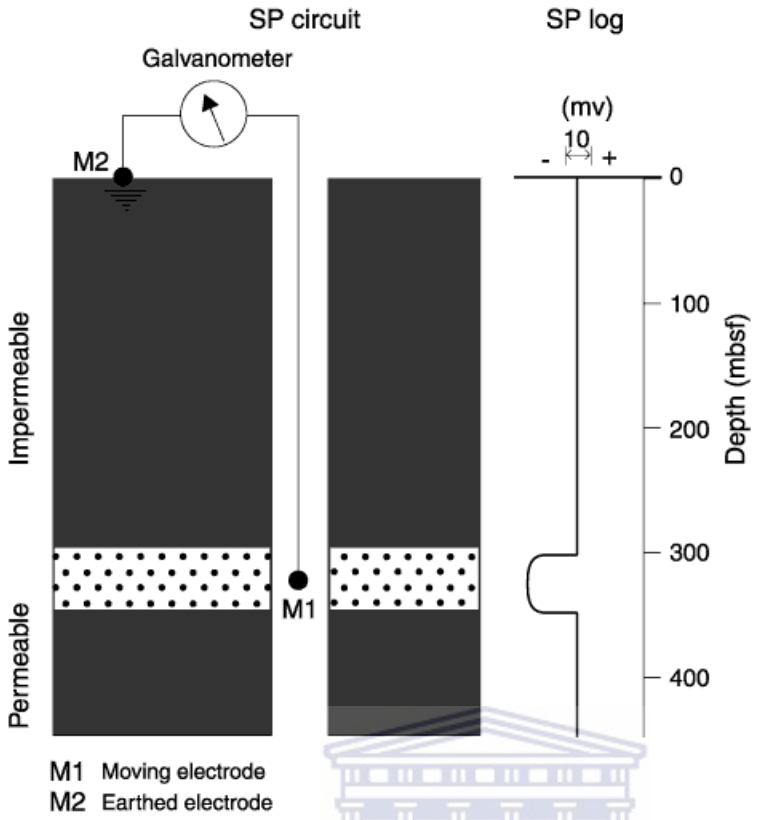

Figure 19: Spontaneous Potential logging tool (Rider, 1996)

3.3.5 Resistivity Log

The resistivity of a formation is a key parameter in determining hydrocarbon saturation. Electricity can pass through a formation only because of the conductive water it contains. With a few rare exceptions, such as metallic sulfide and graphite, dry rock is a good electrical insulator. Moreover, perfectly dry rocks are seldom found. Therefore, subsurface formations have finite, measurable resistivities because of the water in their pores or absorbed in their interstitial clay.

The measured resistivity of a formation depends on

- resistivity of the formation water
- amount of water present
- pore structure geometry

The resistivity (specific resistance) of a substance is the resistance measured between opposite faces of a unit cube of that substance at a specified temperature. The meter is the unit of length and the ohm is the unit of electrical resistance. In abbreviated form, resistivity is

$R = r A/L$,

Where,

R is resistivity in ohm-meters,

r is resistance in ohms,

A is area in square meters,

and L is length in meters.

The unit of resistivity is ohm-meters squared per meter, or simply ohm-meter (Ohm-m).

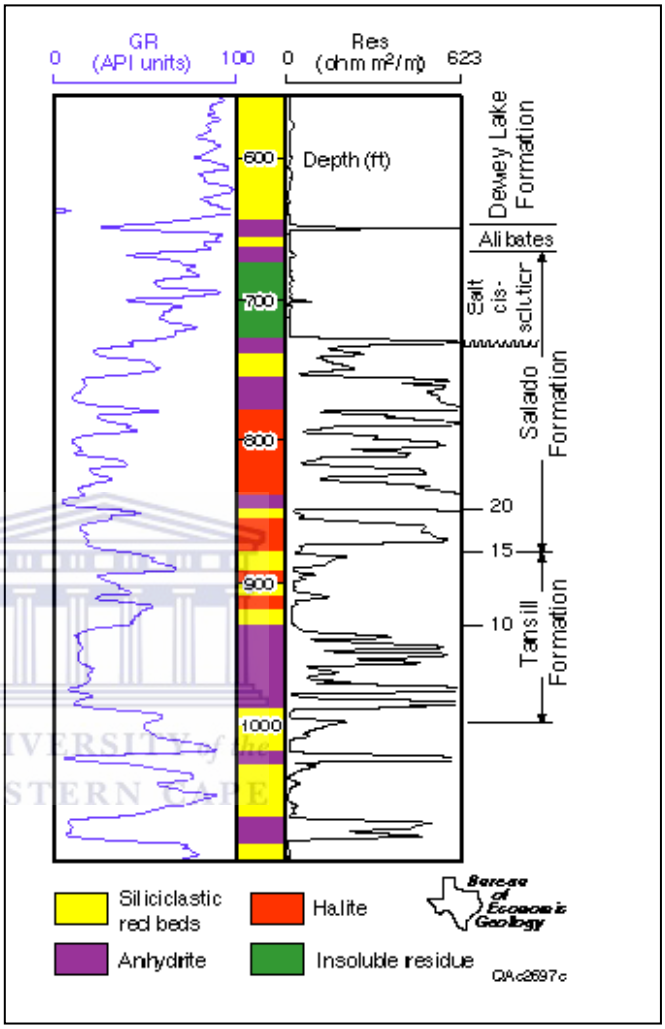

Figure 20: Resistivity signature response from different lithologies. Crain (2003)

3.3.6 Density Log

The formation density log measures the bulk density of the formation. Its main use is to derive a value for the total porosity of the formation. It is also useful in the detection of gas-bearing formations and in the recognition of evaporates. The formation density tools are induced radiation tools. They bombard the formation with radiation and measure how much radiation returns to a sensor.

The typical tool consists of:

• A radioactive source: This is usually caesium-137 or cobalt-60, and emits gamma rays of medium energy (in the range 0.2 – 2 MeV). For example, caesium-137 emits gamma rays with a energy of 0.662 MeV.

• A short range detector: This detector is very similar to the detectors used in the natural gamma ray tools, and is placed 7 inches from the source.

• A long range detector: This detector is identical to the short range detector, and is placed 16 inches from the source.

The gamma rays enter the formation and undergo compton scattering by interaction with the electrons in the atoms composing the formation. Compton scattering reduces the energy of the gamma rays in a step-wise manner, and scatters the gamma rays in all directions. When the energy of the gamma rays is less than 0.5 MeV they may undergo photo-electric absorption by interaction with the atomic electrons. The flux of gamma rays that reach each of the two detectors is therefore attenuated by the formation, and the amount of attenuation is dependent upon the density of electrons in the formation.

• A formation with a high bulk density has a high number density of electrons. It attenuates the gamma rays significantly, and hence a low gamma ray count rate is recorded at the sensors.

• A formation with a low bulk density has a low number density of electrons. It attenuates the gamma rays less than a high density formation, and hence a higher gamma ray count rate is recorded at the sensors.

The density of electrons in a formation is described by a parameter called the electron number density, ne. For a pure substance, number density is directly related to bulk density, and the relationship can be derived in the following way:

• The number of atoms in one mole of a material is defined as equal to Avogadro's number N ($N \approx 6.023 \times 10^{23}$).

• The number of electrons in a mole of a material is therefore equal to NZ, where Z is the atomic number (i.e., the number of protons, and therefore electrons per atom).

Since the atomic mass number A is the weight of one mole of a substance, the number of electrons per gram is equal to NZ/A. However, the number of electrons per unit volume is of relevance, and these can obtained from the number of electrons per gram by multiplying by the bulk density of the substance, ρb. Hence, the electron number density is

$$Ne = (NZ/A)\,\rho b$$

Where,

Ne = the number density of electrons in the substance (electrons/cm3)

N = Avagadro's number ($N \approx 6.023 \times 10^{23}$).

Z = Atomic number (no units)

A = Atomic weight (g/mole)

ρb = the bulk density of the material (g/cm3).

3.4 Seismic interpretation

Primary seismic reflections are generated in response to significant impedance changes along stratal surfaces or unconformities. The fundamental principle that seismic reflection follows is gross bedding and therefore approximate time lines are the basis for seismic sequence stratigraphy (Adekola,. et al 2009).

3.4.1 Seismic Acquisition

Offshore seismic is acquired when an air gun towed behind the survey ship transmits sound waves through the water column and into the subsurface (Figure 21). Changes in rock type or fluid content reflect the sound waves towards the surface. Receivers towed behind the vessel record how long it takes for the sound waves to return to the surface .Sound waves reflected by different boundaries arrive at different times. Seismic horizons represent changes in density and allow the subsurface geology to be interpreted.

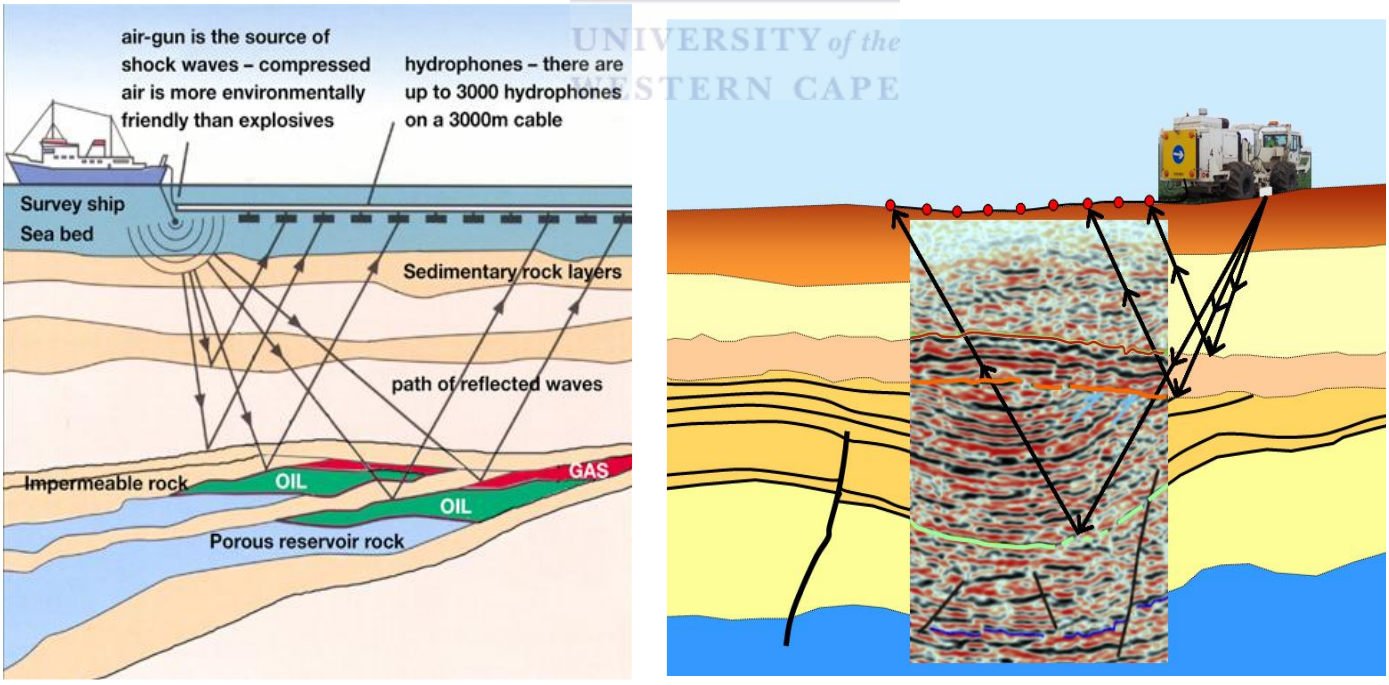

Figure 21: Seismic acquisition and reflection on a seismic trace exhibiting lithology changes and angular unconformity and. Source: University of Derby course notes

The ideal time to integrate seismic and petrophysical data is during the interpretive processing stage (i.e., interpretive processing of both petrophysical and seismic data). The earlier in the processing stream these two data types are compared and calibrated, the more likely a reasonable reservoir flow-unit characterization will evolve. If integration is pushed down, after completing the petrophysical characterization, and after seismic data is processed and handed off to the interpreter, the integration will become rigid; dependent on the assumptions built into both the petrophysics and seismic sides of the workflow.

Seismic Attribute Analysis

Seismic data provide information to characterize lateral variations of physical rock properties, such as porosity and permeability within a reservoir. The process of generating petrophysical rock type maps from seismic data involved several steps, namely,

a) Interpretation of key namely horizons. b) Extraction of seismic attributes from the intervals of interest c) Identification of relationships among the seismic attributes and reservoir properties from well data. d) Generation of rock types map between the actual values at the well locations and the integration of seismic attribute. Original amplitude attribute provided reasonable correlations and was used in the subsequent analysis.

3.5 Coring

The core analysis process has improved vastly in the past several years, with clear improvement of methods and techniques used to generate the core from the subsurface. Core analysis provides direct measurement of reservoir rock properties and forms a vital step in evaluating the formations and in reservoir engineering factors.

Coring is the term applied to the technique whereby relatively large samples (by comparison with the normal size of the drilling cuttings) of reservoir material are removed from their in situ state and brought to the

surface for physical examination (www.metu.edu.tr). Core analysis can provide us with information on porosity, permeability, water saturation and hydrocarbon saturation and structures including fossils.

There are many different types of drilling techniques applied to obtain the core, namely; rotary, diamond,wire-line,side-wall and conventional coring, just to name a few.

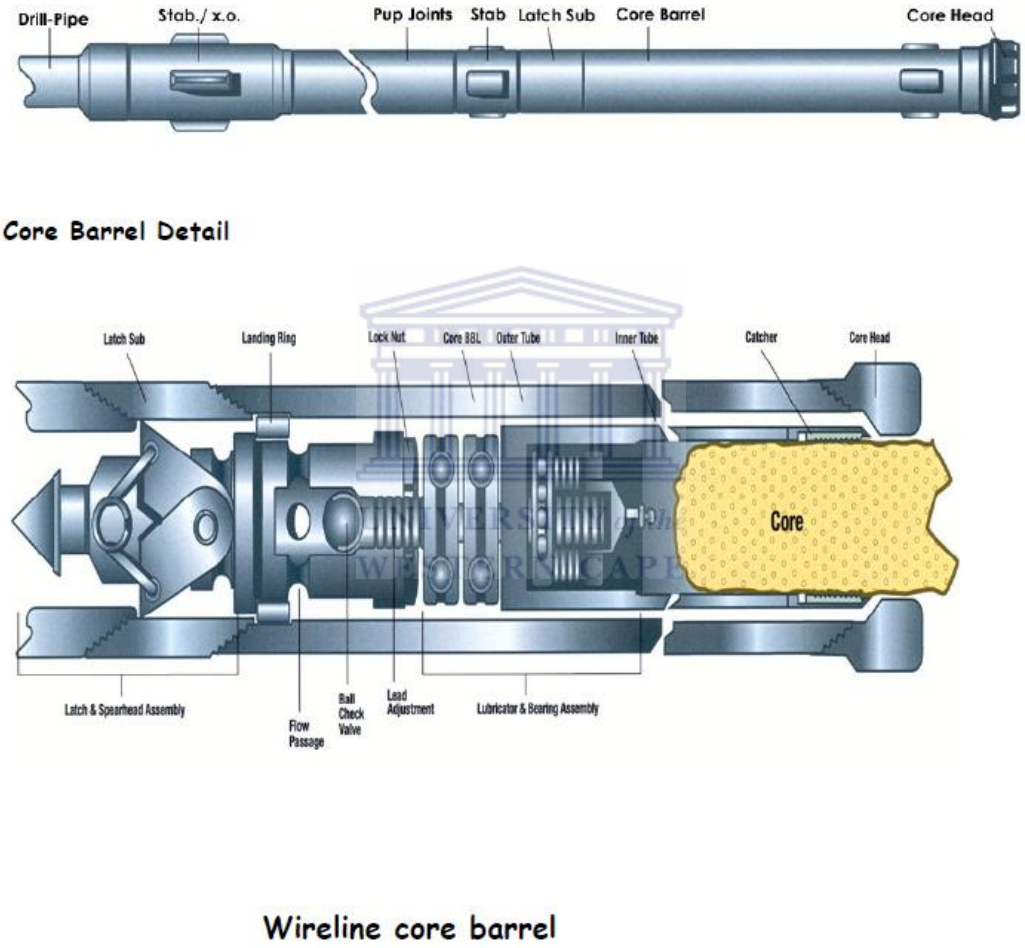

Figure 22: Wireline coring graphical example (www.metu.edu.tr)

Upon drilling, core can also be obtained, Figure 23 shows a technique of acquisition of core and Figure 24 below shows how the core looks in the trays and a summary of the information contained with the log graph of the core. It is important for interpretation to know the depths of the core, when and who took it and if any core was destroyed.

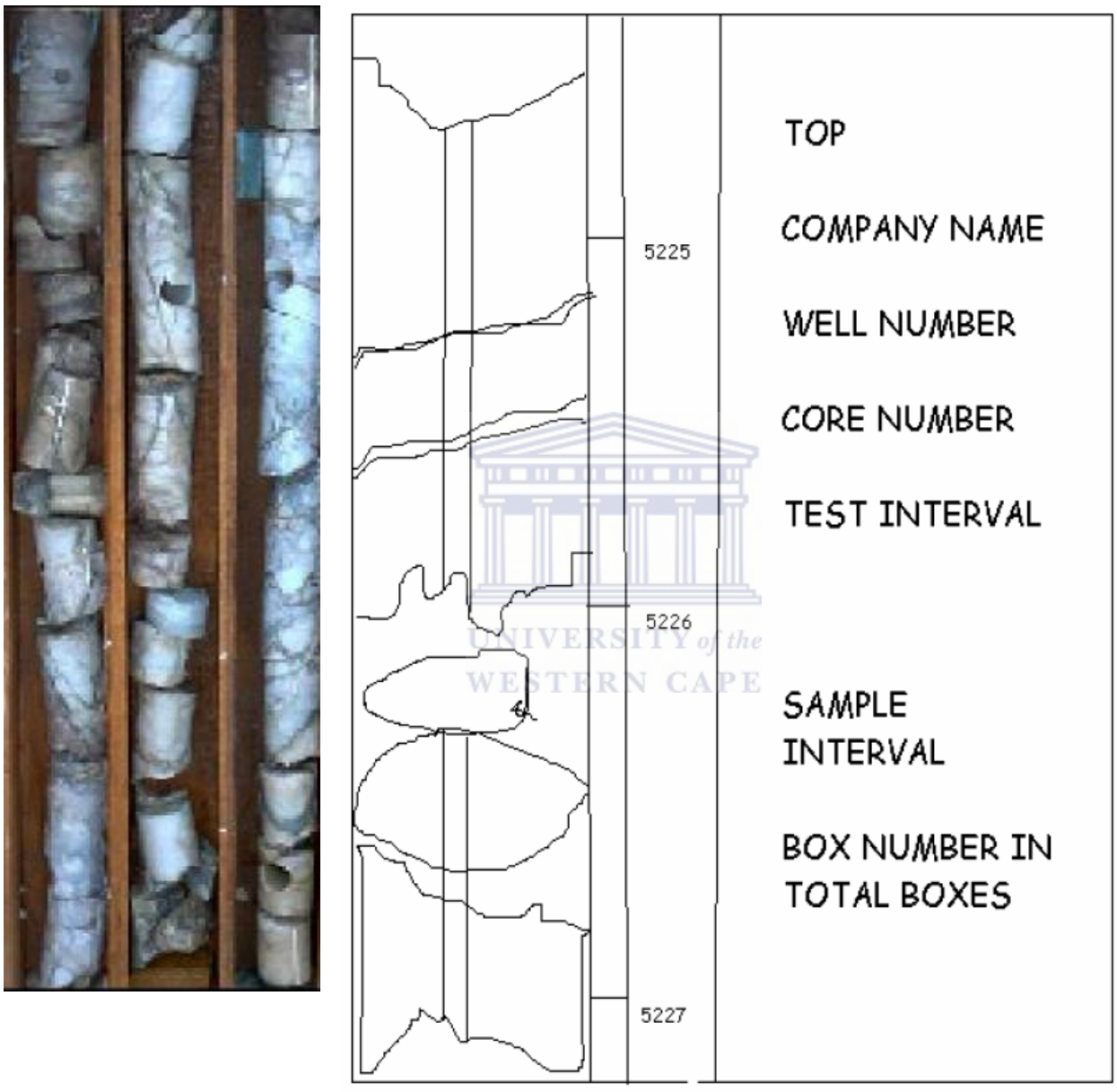

Figure 23: Graphical and pictorial represenation of summary log in core box. modified from. PEP course notes. Schlumberger (NeXT)

CHAPTER 4: Methodology

4.1 Materials

This chapter describes the techniques used for the study. Figure 25 presents the flow chart of the various methods that was used in the course of this study. The data set for this research was basically well data and seismic data. Seismic data provided information about inter-well heterogeneity that is not available when using only well data. The well logs, seismic lines and core samples were obtained from the Petroleum Agency SA and a table is available summarizing the reports used in this study (Table 2). The softwares used are Schlumberger PETREL and Techlog and Sedlog. These softwares were used to carry out various interpretation, modeling and analysis of the available digitized data.

DATA LIST

Orange Basin – Sungu Sungu Central Basin

Wells AK1, AK2, AK3 and AH1

1. **Geophysical Logs**

   The geological logs used were: Digital Wireline logs LAS format: Gamma Ray log, Density log, Spontaneous potential log, Neutron logs, Sonic logs, Micro-resistivity logs, (LSD,MSFL,LLS), Caliper log.

2. **Seismic Data (2D) SEG-Y format**

The seismic data used were:AK76 -026; A88-018; K80-015; AK76-028;AK76-032;AK76-011;AK76-007;AK76-009;AK76-015; AK76-01.

Well Reports

Table 2: Reports used for study

Data	Well Name			
	K-A1	K-A2	K-A3	K-H1
DIGITAL GEOLOGICAL DATA - CALCULATED TOC, LITHOLOGY DATA, LISTS OF BURIAL HISTORY DATA	*			
RECOMMENDATION TO DRILL IN THE CENTRAL ORANGE BASIN REPUBLIC OF SOUTH AFRICA.	*			
CORE PHOTOGRAPHS	*			
FINAL REPORT	*	*	*	*
CONVENTIONAL CORE ANALYSIS	*			
GEOLOGICAL WELL COMPLETION REPORT	*			
GEOCHEMICAL DATA AND SUMMARY REPORT		*	*	
SPECIAL CORE ANALYSIS			*	
CONVENTIONAL CORE		*	*	

4.2 Methods

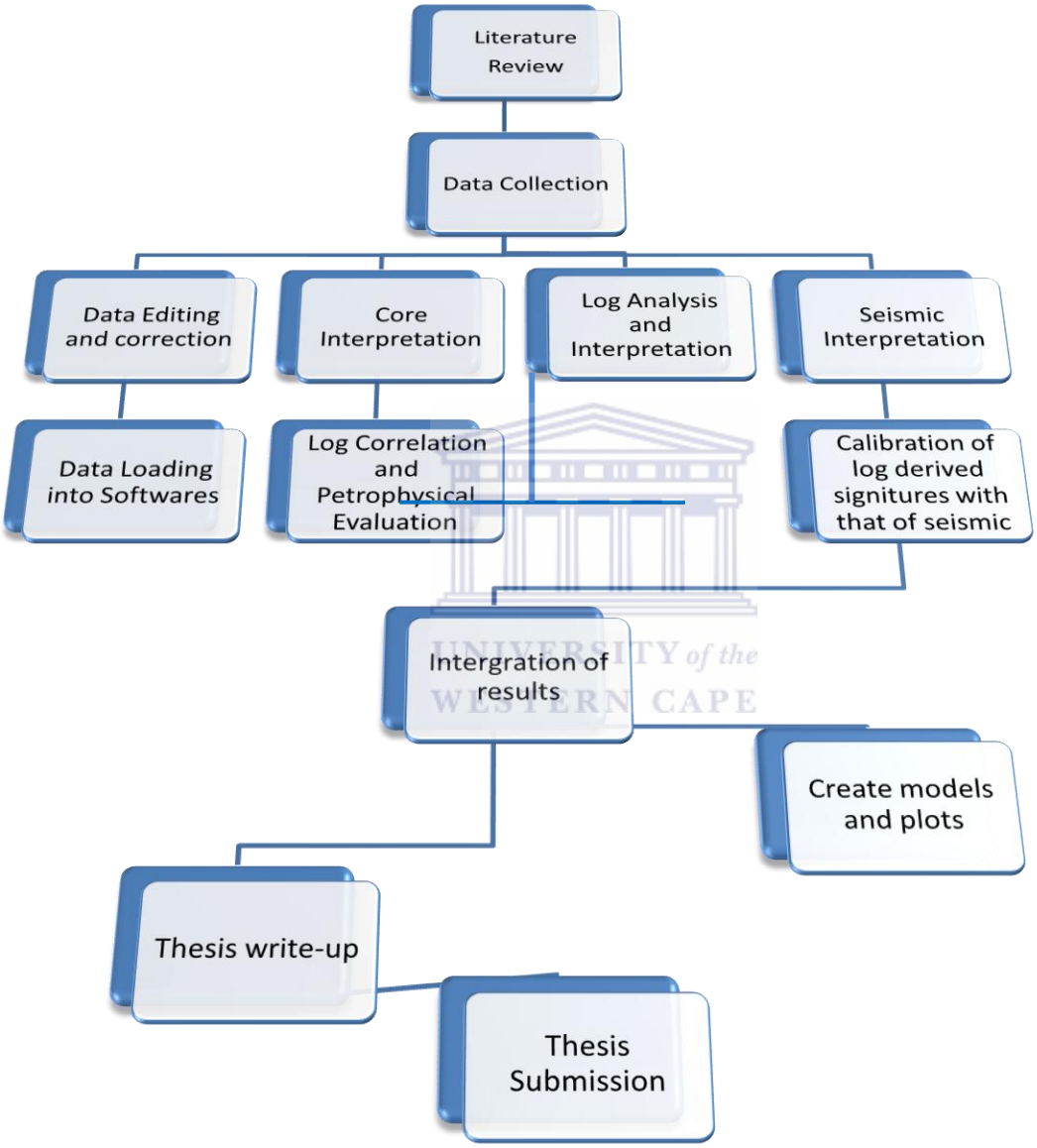

Figure 24: The flow chart of the research methodology

Table 3: Table of deliverables and summary of methods applied in the study

ACTIVITY	DELIVERABLE
General inspection of well,core and log data	
Literature review	Summary report of the study area and topics discussed
Well Log correlation	Brief write-up to describe the impedance nature of the reservoir. well log and seismic tie shot
Log/core analysis	Stratigraphic framework.
Seismic Interpretation	Snapshot of interpreted horizons from basemap, identification of onlaps, downlaps and truncations.
Generate Petrophysical Analysis	Petrophysical parameters and calculations utilised. (NTG, Sw, Porosity,etc)
Generate cross plots	porosity vs permeability, density vs Neutron porosity etc
Seismic and well line log ties	Snapshots

4.3 Data Loading

Petrel and Techlog were used for the loading and display of the log curves. The data were received in LAS format and was loaded directly into the Techlog where depth shifting, splicing and quality control were done based on the core description .These data were loaded into Petrel in ASCII format.

Data Control was conducted in Techlog which is an extremely powerful wellbore centric tool that can handle and wireline logs and petrophysical analysis very well. Petrel was used to display the seismic data as well as the seismic well tie as it is a visualization tool that can handle various data types and provide the shared earth model.

The minimum and maximum values on gamma ray log were checked and all null values and arbitrary values were removed. This was done for each well in conjunction with caliper log and other log types available. At the end of the editing the log is ready for interpretation.

4.4 Data Quality

Data quality can be commented upon on the basis of deviation of caliper from the bit size. In our data, the quality commonly shows a good trend however it is poor at certain regions. The borehole enlargement in these regions may be due to washout.

Table 4: Log scale

LOG SCALE:	**Unit**
SP log	In mV
GR log	In API
Bite Size	In Inches
Caliper log	In Inches
Resistivity log	In ohm-meter
Neutron-porosity log	In percentage
Density log	In gram/cc

The data sets obtained were prepared in SEGY format for each of the lines picked. The

10 lines are controlled by the Wells K-A1, K-A2, K-A3 and K-H1. These seismic lines are visible in Figure 26.

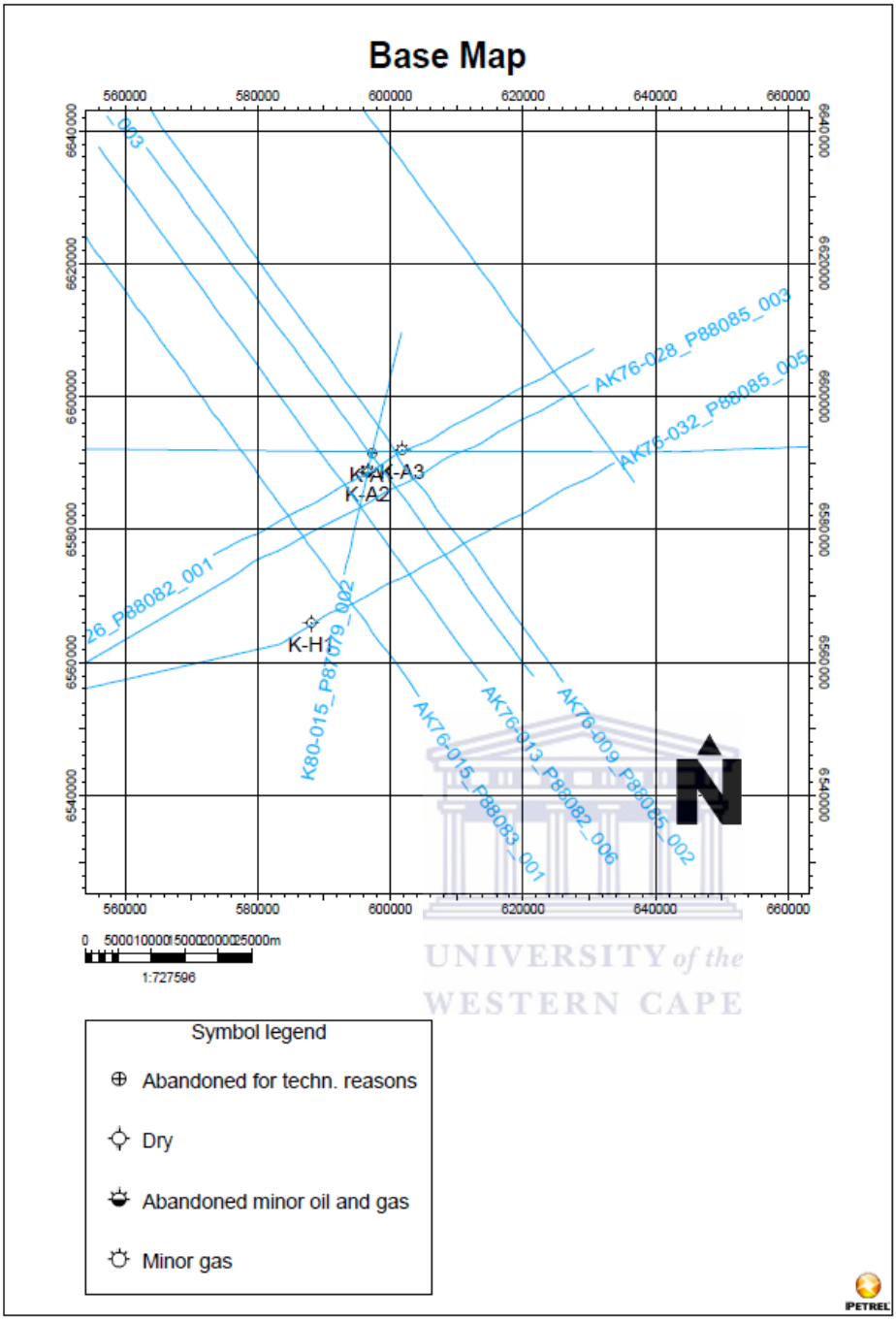

Figure 25: Base Map with seismic lines in the study area, controlled by 4 wells.

4.5 Core Description

Apart from wireline logs that come close to revealing the actual subsurface geology displayed by seismic lines, cores reveal this ground truth to a much greater detail. It is also important to test the usefulness of spectral

gamma ray logs in subsurface correlation, lithofacies identification/ description and the interpretation of depositional environments.

SedLog 2.1.4 software was used to illustrate the lithologies found in the core and to determine the various depositional facies as well as the various observed changes in the cores. The core description process started with by identifying the depths of interest and then the laying out of the cores. Core description comprises a combination of quantitative and qualitative data, which were concisely recorded. The quantitative information varies continuously down hole and best displayed as some type graphic plot (Sedlog).

The samples were laid in trays with the depths marked on the trays. Ten metres or more of the samples were scanned to observe the lithologic “breaks”. The samples were then examined in detail for textural, structural and other geological features. Wetting the samples not only cleans off mud and other contaminants, but also brought out the rock characteristics that were not apparent in the dry samples. All the details are recorded on a log sheet and photographs are taken of the cores and the features of interest. An example of this of this log sheets was created in for this study and is represented by figure 28 and the core photographs are seen in figure 26 a- f.

4.6 Seismic data interpretation (General principle)

The methodological approach used in arriving at the seismic interpretation is as follows:

The seismic data acquired for this study are 2D seismic sections and were used for structural and sequence stratigraphic analyses. Structural analysis involved the identification and mapping of faults. The seismic sequence stratigraphic analysis procedure entails the following:

- Identifying the unconformities in the area of interest. These generally occur at an angle to underlying and/or overlying strata surfaces.
- Drawing the unconformity surface between the onlapping and downlapping reflections above and the truncating and toplapping reflections (below).
- Extending the unconformity surface over the complete section. Where the boundary become conformable, its position was traced across the seismic section by visually correlating the reflections.

  This process of identifying the bounding unconformities was carried out on all the seismic profiles provided in the fields of interest and the interpretation was done to tie correctly along all correlation loops throughout the grid.
- Having identified the sequence boundary, the systems tracts (LST, TST, and HST) within each sequence were identified based on the aforementioned characteristic seismic and log signatures. Primary seismic reflections are generated in response to significant impedance changes along surfaces or unconformities.

- The seismic stratigraphy technique was employed in interpreting the stratigraphic information from seismic data.

  The fundamental principle of seismic stratigraphy is that within the resolution of the seismic method, seismic reflections follow gross bedding patterns are presented in time lines.
- A key message in seismic is that in which the correlative impedance contrasts are represented on seismic data from bedding interfaces but not lateral facies changes.

Major Seismic Reflection Termination Patterns

Reflections terminations are characterized by the geometric relationship between the reflection and the seismic surface against which they terminate. The features named below, first introduced by Mitchum et al. (1977) were mapped:

Lapout was mapped between the lateral terminations of a reflector (generally a bedding plane) at its depositional limit.

Baselap/downlap - lapout of reflectors was mapped against an underlying seismic surface. Baselap which consists of downlap, where the dip of the surface is greater, and downlap, seen at the base of the prograding clinoforms representing the progradation of a basin margin slope system into deep water, were also mapped.

Toplap - a termination of inclined reflections (clinoforms) against an overlying lower angle surface believed to represent the proximal depositional limit was mapped. An apparent toplap in which clinoforms pass upwards into topsets that are too thin to resolve seismically were also encountered.

Erosional Truncation - is a termination of strata against an overlying erosional surface, in which toplap developed into erosional surface, but truncations are more extreme than toplap and led to development of erosional relief and the development of angular unconformity. The erosional surface in marine setting such as the base of a canyon, channel or major scour surface, or of non-marine erosional surface developed in a sequence boundary was also mapped.

Apparent Truncation - is a termination of relatively low angle seismic reflectors beneath a dipping seismic surface in which the surface represents a marine condensation where termination process represents a distal depositional limit (or thinning) below seismic resolution, generally within topset strata, but sometimes also within submarine fan; it was also mapped.

Onlap is recognized on seismic data by the truncation of low-angle reflection against a steeper seismic surface. Two types of onlap were recognized in this study, namely marine and coastal onlaps.

Marine onlap represents a change from marine deposition to non-marine deposition or condensation. Marine onlap reflects a submarine facies change from significant rates of deposition to a much lower energy pelagic drape. The seismic surface of marine onlap was mapped as marine hiatus or condensed interval.

Coastal onlap, an onlap of non-marine, paralic, or marginal marine strata was mapped at a zone of deposition between basin margin (subaerial or shelf) erosion and non deposition.

Fault Truncation marked the termination of reflections against a syn or post depositional fault, slump, glide or intrusion surface.

Recognition of Stratigraphic Surfaces from Seismic Data

Determination of Sequence Boundary

Development of a high relief truncation surface; particularly one which erodes the topsets of older units indicates a sequence boundary. The downward shift in coastal onlap across the boundary was also used in the sequence boundary determination.

Determination of a Transgressive Surface

A transgressive surface marks the end of lowstand progradation and the onset of transgression. It was found associated with reflection terminations, and marks the boundary between a topset clinoform and the topsets interval.

Determination of a Maximum Flooding Surface

A maximum flooding surface was recognized on seismic data as a surface where clinoforms downlap onto underlying topsets, thereby displaying backstepping and apparent truncation.

Recognition of Systems Tracts on Seismic Data

The principle applied to recognise the system tracts from seismic data (systems Tracts) was based on the nature of their boundaries, and by the stacking pattern of their internal stratigraphy.

Recognition of Lowstand Systems Tract

A lowstand systems tract is bounded below by a sequence boundary, and above by a transgressive surface. It is also overlain by a transgressive surface (a transition to a retrograding topset unit and it contains a basinal fan unit), it was recognised as a mounded unit of a couple of reflection lower and more distal from the clinoform. The lowstand systems tract was divided into two parts; a lowstand fan and a younger lowstand wedge in which the fan was the most dominant in the basin.

Recognition Transgressive Systems Tract

Transgressive systems tract is bounded below by a transgressive surface and above by a maximum flooding surface. It was recognised on seismic section by retrograding topset parasequences. Transgressive systems tract often appears very thin, and consists of no more than one reflection as seen in this study. It is recognised as a transgressive systems tract as its base marks the transition from an underlying interval of mainly clinoforms, to an interval of mostly or entirely topsets. It also clearly showed internal retrogradational geometries. The transgressive systems tract overlain by a maximum flooding surface was recognized by the downlap of overlying clinoforms.

Recognition of Highstand Systems Tract

Highstand systems tract is bounded below by a maximum flooding surface and above by sequence boundary and exhibits progradational geometries. It consists of prograding topsets and clinoforms representing progradation and it overlies a maximum flooding surface, clinoforms within the system tract downlap topsets of the underlying systems tract. Apparent transactions were seen beneath the surface and the underlying systems tract infill erosional relief on an older sequence boundary.

4.7 Petrophysical analysis procedure/steps

The methods and formulas used in arriving at the petrophysical results are given in steps 1-12 is as follows:

Step 1
Selection of 'Zone of interest'

The primary objective of logging a well is to identify 'zones of interest' from hydrocarbon accumulation by integrating log responses of different geophysical tools. Although this is not always true and some exceptions can occur but in general the characteristic log responses that will indicate possibility of presence of Hydrocarbon (Oil or Gas or both) are: i. High Resistivity value, ii. Low Gamma ray value, iii. Negative deflection of SP log, iv. Mud cake formation, v. Low formation bulk density.

Step 2
Calculation of Formation Temperature

Formation temperature T_2 is given by the formula,

$T_2 = T_1 + \text{Geothermal Gradient} \times D$
T_2: Formation temperature of zone of interest
T_1: Mean surface temperature
D: Depth of interested zone (log depth)

Step 3
Calculation of Resistivity of Mud Filtrate at formation temperature (R_{mf} @ T_f)

1. Read Rmf from header file at surface temperature.

2. Determine the Rmf at formation temperature using the formula

$$R_{m2} = R_{m1} \frac{T_1 + 6.77}{T_2 + 6.77}$$ (temperature in degree Fahrenheit)

$$R_{m2} = R_{m1} \frac{T_1 + 21.5}{T_2 + 21.5}$$ (temperature in degree Celsius)

Here,
T_2 = Formation temperature and
T_1 = Mean surface temperature
R_{m1}=Resistivity of mud filtrate at surface temperature
R_{m2} = Resistivity of mud filtrate at formation temperature

Step 4
Calculation of Formation Water Resistivity (R_w) from SP log

1. Read value of SP deflection from log

2. Calculate R_{mf} at formation temperature

3. Convert R_{mf} at formation temperature to R_{mfe}

$$SSP = -(65 + 0..133T)\log \frac{R_{mfe}}{R_{we}}$$ (T in degree Fahrenheit)

a)Calculate R_{mf} @ 75^0 F using the above formula.
If R_{mf} @ 75^0 F is less than 0.1 ohm –m, then

$R_{mfe} = 0.85 \times Rmf$ (approximation)

If R_{mf} @ 75^0 F is greater than 0.1 ohm –m , then

$R_{mfe} = (146\ R_{mf}^{-5})/(337\ R_{mf} + 77)$

b) Determine the value of R_{we} @ 75^0 F
If R_{we} @ 75^0 F is greater than 0.12 ohm-m,then

$Rwe = -0.58 + 10(0.69.Rwe - 0.24)$

If R_{we} @ 75^0 F is less than 0.12 ohm-m,then

$R_{we} = (77.R_{we} + 5)/(146 - 377.R_{we})$

Step 5
Calculation of Shale Volume (V_{sh})

Shale volume present in the zone of interest or in the reservoir can be determined by GR log.

Vsh from GR log can be calculated as using the relation:

$$I_{GR} = \frac{(GR_{log} - GR_{min})}{(GR_{max} - GR_{min})}.$$

This Gamma Ray Index (I_{GR}) and V_{sh} are related, and the relation becomes non-linear for both structured clays and dispersed clays. Wide varieties of non-linear relationships exit between I_{GR} and V_{sh}. But none is universally accepted. Three common types of this non-linear relationship is illustrated below.

Linear $V_{sh} = I_{GR}$
Clavier $V_{sh} = 1.7 - [3.38 - (I_{GR} + 0.7)^2]^{1/2}$
Steiber $V_{sh} = 0.5 \times [I_{GR} / (1.5 - I_{GR})]$

Step 6
Determination of Porosity

The porosity *f* of a formation can be obtained from the bulk density if the mean density of the rock matrix and that of the fluids it contains are known.

The bulk density *ρb* of a formation can be written as a linear contribution of the density of the rock matrix *ρma* and the fluid density *ρf* , with each present is proportions (1- *Φ*) and *Φ* respectively :

$$\rho_b = (1 - \Phi)\,\rho_{ma} + \Phi\,\rho_f$$

where,

ρ_b = the bulk density of the formation

ρ_{ma} = the density of the rock matrix

ρ_f = the density of the fluids occupying the porosity

Φ = the porosity of the rock.

Determination of Neutron Porosity and Density Porosity

1. Effective porosity (Φ_e) is calculated by combining Neutron Porosity and Density porosity.

2. Neutron Porosity can be read directly from log.

3. Density porosity needs to be calculated from Density log using the formula as below-

$$\Phi_D = \frac{(\rho_{ma} - \rho_b)}{(\rho_{ma} - \rho_f)} \quad .$$

Here,

ρ_{ma} = density of matrix of the formation

ρ_f = density of formation fluid in the vicinity of borehole (mud filtrate)

ρ_b = bulk density of the formation

Step 7
Correction of Neutron porosity and Density porosity for the presence of shale

Neutron porosity as read from the log and density porosity as calculated need to be corrected for volume of shale present in the formation.

1. Corrected Neutron porosity is given by Φ_{NC} as follows.

$$\Phi_{NC} = \Phi_N - V_{sh}\Phi_{Nsh}$$

2. Corrected Density porosity is given by Φ_{DC} as follows

$$\Phi_{DC} = \Phi_D - V_{sh}\Phi_{Dsh}$$

Step 8
Calculation of Effective Porosity (Φe)

Effective porosity (Φe) is calculated by combining corrected neutron and density porosities using the formula,

$$\Phi_e = \sqrt{\frac{\Phi_{NC}^2 + \Phi_{DC}^2}{2}} \quad .$$

Step 9
Determination of Formation Factor (F)

Formation factor "F" is calculated as:

$$F = a / \Phi^m ,$$

Where,
a = tortuosity factor,
m= cementation factor,
For sandstones , a = 0.62 , m = 2.15 .

Step 10
Determination of Water Saturation (S)

For clean formation it can be easy to determine water saturation using "**Archie's Equation**"

$$S_w^n = \frac{F * R_w}{R_t}$$

Where,
S_w = water saturation
n = saturation exponent (usually taken as 2)
R_t = true resistivity, as read from the deep resistivity log;
F = formation factor .

Step 11
Determination of Hydrocarbon Saturation (S_{hc})

It is very easily determined from the relation,
$S_{hc} = 1 - S_w$
Where,
S_{hc} = Oil saturation of the zone of interest.

Step 12
Determination of Movable Hydrocarbon

Water saturation in the flushed zone (S_{xo}) is given by,

$$S_{xo} = \sqrt{\frac{F * R_{mf}}{R_{xo}}}$$

R_{xo}= Resistivity of the flushed zone given by Micro-logs,

$(1 - S_{xo})$ gives the hydrocarbon present within the flushed zone, i.e. immovable hydrocarbon.

This enables us calculating 'movable hydrocarbon' by subtracting the residual hydrocarbon.

$(1 – S_{xo})$ from total hydrocarbon saturation S_{hc} or $(1 – S_w)$
$S_{hcm} = (1 - S_w) – (1 – S_{xo})$
$= S_{xo} - S_w$

(Crain's Petrophysical Handbook).

The software's used where able to help automate this process and perform the calculations. Knowing the equations and methods assisted in the quality checking process of the study.

4.8 Wireline log interpretation

High resolution sequence stratigraphy from outcrop, core and wireline log data were run by Van Wagoner et al. (1990). This process has been beneficial to the industry and is now widely applied. Two wireline logs are vital in sequence stratigraphic analysis, namely, gamma ray log and resistivity logs with respect to overall log response or characters. The log responses are initially used in identifying, matching and tying sequence stratigraphic surfaces (sequence boundary, (SB), maximum flooding surface (MFS), and transgressive surface (TS) and subsequently in interpreting the stacking patterns of the vertical sedimentary sequences. Figure 27 displays the log responses discussed.

Application of sequence stratigraphic principles to well logs permitted complex lithologies in reservoirs to be interpreted. These lithologies are ones which are sometimes too thin to be recognized by seismic reflections alone.The general principles and procedures of wireline logs are hereby presented and employed in the data analyses. This was taken from Adekola (2009) and the source is Emery and Myers (1996).

Sequence Stratigraphy from Wireline Logs:

Wireline log data provide a better tool of analysing subsurface conditions. Log data provide information on lithology and depositional environment of a particular borehole, and when tied with seismic sections or correlated with other wells such data can provide better subsurface understanding. Trends in log response may equate to trends in depositional energy and thus can help to infer basin infill history (Adekola 2009). A number of distinct log trends can be recognized on wireline logs. Of all of them, the gamma ray log provides a good response for identifying lithology. The major log trends used in this study that is the Cleaning up trend, dirtying up trend, Boxcar trend, Bow trend and Irregular trend. These trends are discussed below.

The Cleaning up Trend

The cleaning-up trend shows a progressive upward decrease in the gamma reading representing a gradual upward change in clay-mineral content. In shallow marine settings the cleaning-up pattern is usually related to an upward transition from shale-rich to shale-free lithologies, owing to upward increases in depositional energy, upward shallowing and upward coarsening. Sporadically, cleaning up units were seen as a result of a gradual change from clastic to carbonate deposition of a gradual decrease in anoxicity, neither of which need be necessarily related to upward shallowing or propagation of a depositional system.

The Dirtying up Trend

The dirtying up trend showed a progressive upward increase in the gamma reading related to a gradual upward change in the clay-mineral component. This is a lithology change from sand to shale or an upward thinning of sand beds in a thinly interbedded sand-shale unit. Both imply decrease in depositional energy. Upward fining predominates within meandering or tidal channel deposits, in which it represents an upward decrease in fluid velocity and energy within the channel. The largest fining up units was found in coarse fluvial succession and in estuarine fills. Channel deposits have a basal lag which affects the gamma response when the lag contains shale clasts or heavy minerals. In shallow marine settings the dirtying-up trend reflected the retreat or abandonment of shoreline-shelf systems, resulting in upward deepening and decrease in depositional energy. The dirtying up trend occurs also as a result of gradual increase in anoxicity or gradual change from carbonate to clastic deposition.

Box Car Log Trend

This trend type is also known as a cylindrical motif. Box car trends were recognised by sharp-based low gamma units with an internally relatively constant gamma reading, set within a higher gamma background unit. The boundaries with the overlying and underlying shales were abrupt. The sonic readings from the sands had

higher and lower transit time for the shales, depending on cementation and compaction. Turbidite boxcar units generally showed a much greater range of thickness than boxcar fluvial channel units. Shallow marine sand bodies had truncated bases due to faulting or sharp bases as a result of falls in a relative sea level or other factors.

The Bow Trend

It is also known as barrel or symmetric trend. The bow trend consists of a cleaning up trend, overlain by a dirtying up trend of similar thickness and with no sharp break between the two. A bow trend, formed from the waxing and waning of clastic sedimentation rate in a basinal setting where the sediments are unconstrained by base level, was encountered. The bow trends were found developed in shallow marine settings, where base level constraints led to thicker progradational and thinner transgressive units.

Irregular Trends

Irregular trends were found to have no systematic change in either baseline or lack the clean character of the boxcar trend. They represent aggradation of a shaly or silty lithology, typical of shelfal settings; a lacustrine succession or muddy alluvial overbank facies. There is evidence of a subtle and systematic shift in the base line which appears to be an irregular trend. Irregular log trends were not recognised in shelfal or paralic facies because cyclic changes in water depth are likely recognised as cyclic log trends and identified as parasequences.

The Log Response of Clinoforms

On well logs, the clinoform unit had a cleaning upward pattern that reflects upward shallowing. The base of the cleaning up trend was equivalent to a downlap surface. Confirmation that this log response represents a prograding clinoform pattern supporting upward shallowing because upward shallowing in clastic systems

occur through progradation. The base of a clinoform unit was reported as a downlap horizon. This was recognized as a distinct base to the cleaning-up unit, with a log facies diagnostic of marine condensation, with high-gamma shale and a cemented horizon. The top of a cleaning-up clinoform trend was marked by an abrupt increase in shale content (gamma reading) resulting from abrupt deepening across the transgressive surface and overlain by topsets. An abrupt increase in the shale content within the clinoform trend implies an abrupt jump to a deeper facies, resulting from lobe switching or transgressions, during relative sea level rise. Similarly, an abrupt decrease in the gamma response implies an abrupt jump to shallower facies, identified as sequence boundary, a normal fault or slump.

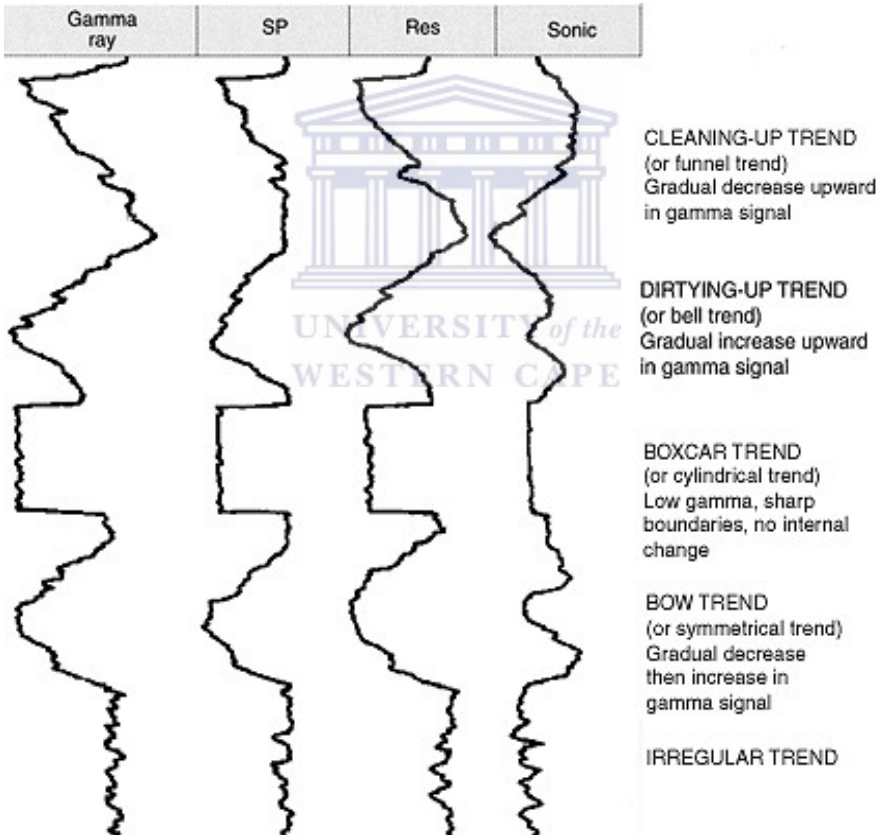

Figure 26: Well log response character (Emery and Myers, 1996).

4.9 Methodological Approach

This study made use of an integrated approach by integrating petrophysical and seismic data in the reservoir characterization and geological modeling. The main work was done by integration and combined interpretation of well logs, core data and surface seismic data. This approach combines the complementary strengths of two or more independent methods of measurements. The combination of these measurements creates significant synergy and provides a new dimension in petrophysical characterization.

This methodology can be used in other fields where seismic data, petrophysical data from core and well logs are available. In addition, seismic data will provide information about interwell heterogeneity that is not available when using only well data.

A quantitative petrophysical analysis using log suites has been developed with the abundant core and core-analysis data available. The initial approach was from traditional methods of log interpretation and integrate them with new methods for (1) determining true formation resistivity (*Rt*) from Deep Laterologs (LLD) and (2) calculating saturation exponent (*n*) using core porosity and water-saturation values from relative permeability curves.

Gamma Ray logs, Neutron porosity, Density, Resistivity (shallow and deep), Sonic and Caliper logs will be utilized. These logs are essential in determining various parameters. For example, Gamma ray log and Spontaneous log were used to calculate shale volume.

Secondly, core data was analyzed and merged with wireline data. A depositional setting may be established from this. Identify depositional environment/s within sequence stratigraphic framework.

The wireline was then overlain on 2D and 3D seismic lines to produce models. Various calculations of thickness and time-depth conversions were made.

In areas with poor incomplete data, there is probably no unique solution to log interpretation that will definitely be successful. Here seismic and log tie may suffice. Schlumberger's Techlog and Petrel Software's were used dependently in the completion of this project.

4.10 Deliverables

It is expected that this study will end successfully. The expected results and deliverables of the project in the end will be a successful petroleum reservoir analysis with the determined component aspects that include:

- Facies/sedimentary log model,
- Calibration of porosity,
- Seismic well Tie,
- Petrophyical Models,
- Cross plots.

CHAPTER 5: Results and Interpretation.

5.1 Core Analysis and interpretation

Apart from wireline logs that come close to revealing the actual subsurface geology displayed by seismic lines, drilled cores reveal this ground truth to a much greater detail. Conventional cores provide us with samples of what lies beneath the surface and detailed studies of them can assist in the reduction of uncertainty associated with reservoir and seal distribution and quality.

Core analysis and description form is a fundamental starting point for reservoir characterization. This chapter presents the detailed description of the core of three wells K-A2, K-A3 and K-H1. Well K-A1 is a wild cat and no cores were cut here. The preceding well is K-A2 and it is expected it will provide us with sufficient information. An interpretation of facies is generated based upon lithology characteristics. Graphic descriptions of core at various scales were done in order to integrate with logs. The core stratigraphic sequence described herein is organized on the basis of lithology, sedimentary structures, facie distribution, texture and grain size variation, bioturbation and fossils present.

The various cores were observed for their various depositional facies. SedLog 2.1.4 software was used to disciminate the various depositional facies and the various observed changes in the cores. (Figure 26 a –f)
Five main facies were defined and observed in this study. Five different large–scale lithologies were delineated by this study. These lithofacies are based on distinguishable sedimentary structures, textures, grain size and primary mineralogy.

The list below shows the different lithofacies defined by this core examination.

- Facie 1: Tight fine grained sandstone
- Facie 2: Medium grained clean sandstone
- Facie 3: Shale
- Facie 4:Fine Interlaminated Siltstone and sandstone

❖ Facie 5: laminated silt/shale

Figure 26: a) Tight, fine grained sandstone that is close to silt. b) Fine to medium grained clean sandstone typically massive I the core. c) Fossil trace and bioturbation shale. Very fine grained. d) Interlaminated shale and silt with some load casts and laminations. e) Coarse sandstone with mud drapes. f) Wavy laminations of mud in siltstone. Lenticular and flaser bedding structures with bioturbation and burrowing.

LITHOFACIES OF K-A2 CORE 1 and CORE 2

Core 1 and core 2 are characteristic of fining upward cycles (Figure 27), ranging between siltstone and sandstone. All sandstones are mostly very fine grained and bordering closely to siltstone. Sandstone between core intervals 2801 and 4094m comprise of a series of coarsening upward cycles and is less tight, so could be as good reservoir rock. These facies are characteristic of delta front and pro delta depositional environment sediments. Refer to Figure 9 in the Geology section.

Facies 1: Tight fine grained sandstone

This sedimentary rock facies was observed throughout the core (Figure 26 a). It is a light grey colour and grain size ranges from fine to silty. It has angular to sub angular grains and of some quartz and calcite material. This sandstone also shows a well sorted grain arrangement. The facies is assumed to be tight in terms of porosity

evaluation due to the inability to absorb dilute HCl added to it. The addition of dilute HCl to the samples generally showed reaction confirming the presence of calcareous material.

This facie occurred at a core horizon of approximately 3990.70m – 3991.42m. This attributes to a thickness of about 63cm. This facie reoccurs continuously on the log and is also visible at the top at 3982m for 50cm.

Different sedimentary features are also evident in this facie. Burrows, moderate to intense bioturbation, parallel laminations, claystone drapes were observed in the upper depths (3984,86m – 3982m) while some vertical burrows, load casts, soft sediment deformation features, planar lamination and erosional surfaces were noted at the deeper depths. Uneven base of silty sandstone with load structures is evident at 4078.735 – 4078.75m.

Facies 2: Massive clean sandstone

This sandstone consists of a well sorted arrangement of grains and is coarse to fine grained. It has thickness ranging from 40cm – 60cm at depths 3988.91m and 3985.45m respectively in the core. The cycle shows a coarsening upward sequence. It has minor bioturbation and is eroded in some parts. There are not few sedimentary structures visible. An irregular dark band at 3980.57 is present which could be due to a change in cement.

Facies 3: Shale

The facies is black and very fine grained with a sub-angular shape grains in well sorted grain arrangement. The dark colour of this shale is a function of its high organic carbon content. The observed minerals include chlorite, glauconite, mica and some coaly materials. A 2mm coal band is evident at 3986.62m depth. There was no reaction with dilute HCl signifying absence of calcareous material within that facies interval. Sedimentary structures like bioturbation and burrowing features, load casts, undulating, and planar laminations, capped ripple marks and cross laminations. At the deeper depths, the shale appears micaceous

and contains pyrite and a rippled contact with sandstone at 4079.8m grading to sandstone over 3cm. The intensity of bioturbation ranges from extreme to moderate, the degree of bioturbation is important as it introduces sand and silt and increases the vertical permeability. Fossil burrows from burrowing or feeding animals that leaves traces generally parallel to bedding were evident in the cores.

Facie 4: Fine Interlaminated Siltstone

This rock facies is light grey and is argillaceous. The sedimentary structures evident are bioturbations, burrows with pyrite filling and laminations which have become wavy and contoured with depth. There is also evidence of slumping at shallow depths. From 3985.25m the laminations are parallel and there is presence of interlaminations with shale and some shale clast. This facies is available at upper depths, above 39861m and also at the deeper depths 4080m. This faces could mark some transition.

Facie 5:Silt\shale laminated

There is also present of shale that laminates with siltstone. This facie is medium to light grey and has a sub-angular grain arrangement. It consists of laminated rippled contact and no cross laminations is visible. At 3984, 29 m there is presence of a sharp contact and a 10cm thick black, shale and siltstone laminated bedding with bioturbation and it grades downwards to a more apparent shale and siltstone.

Refer to Appendix A for the Legend of lithology types for the log interpretation.

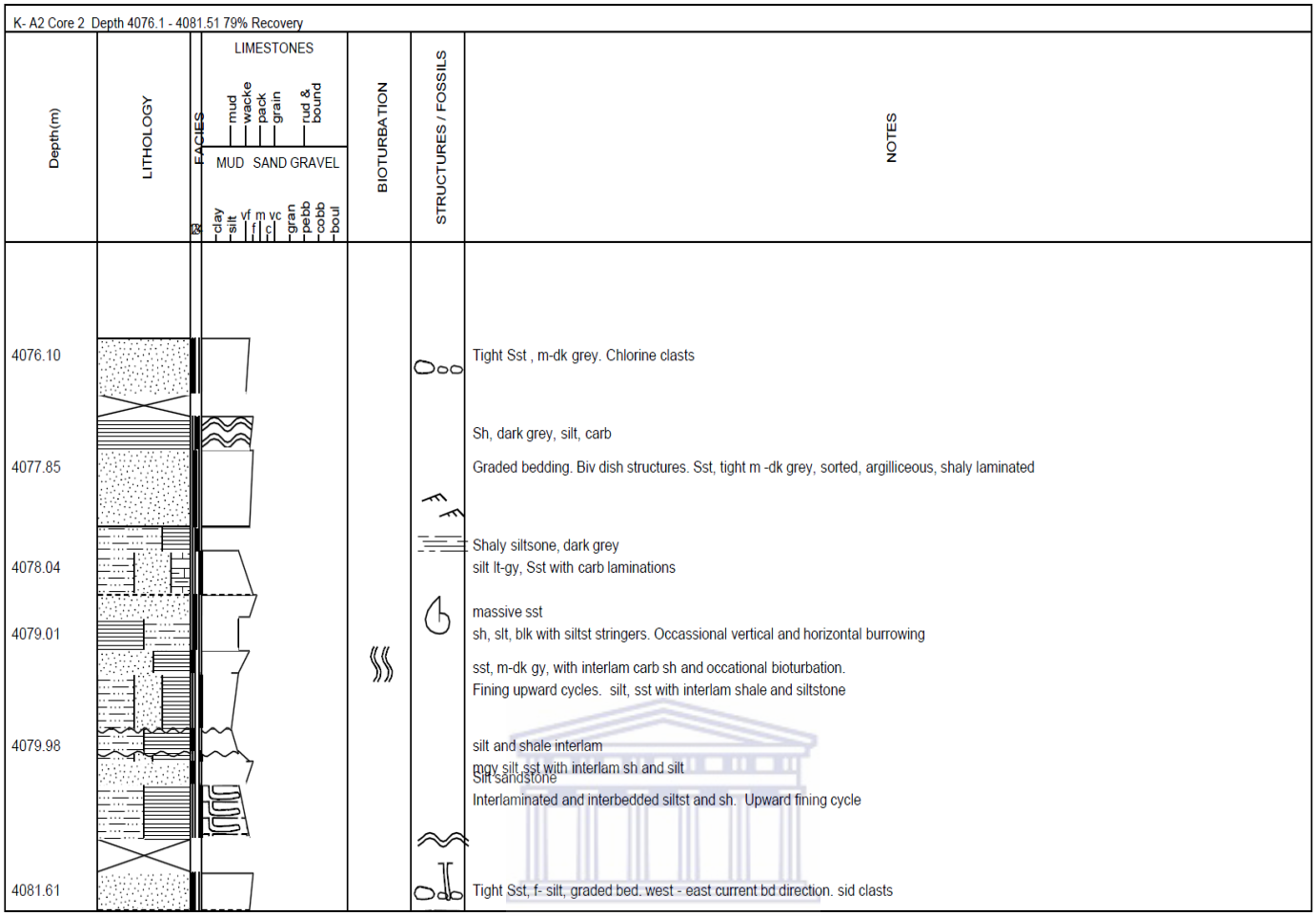

Figure 27: Summary log section of well K-A2 core 2. Scale 1:100

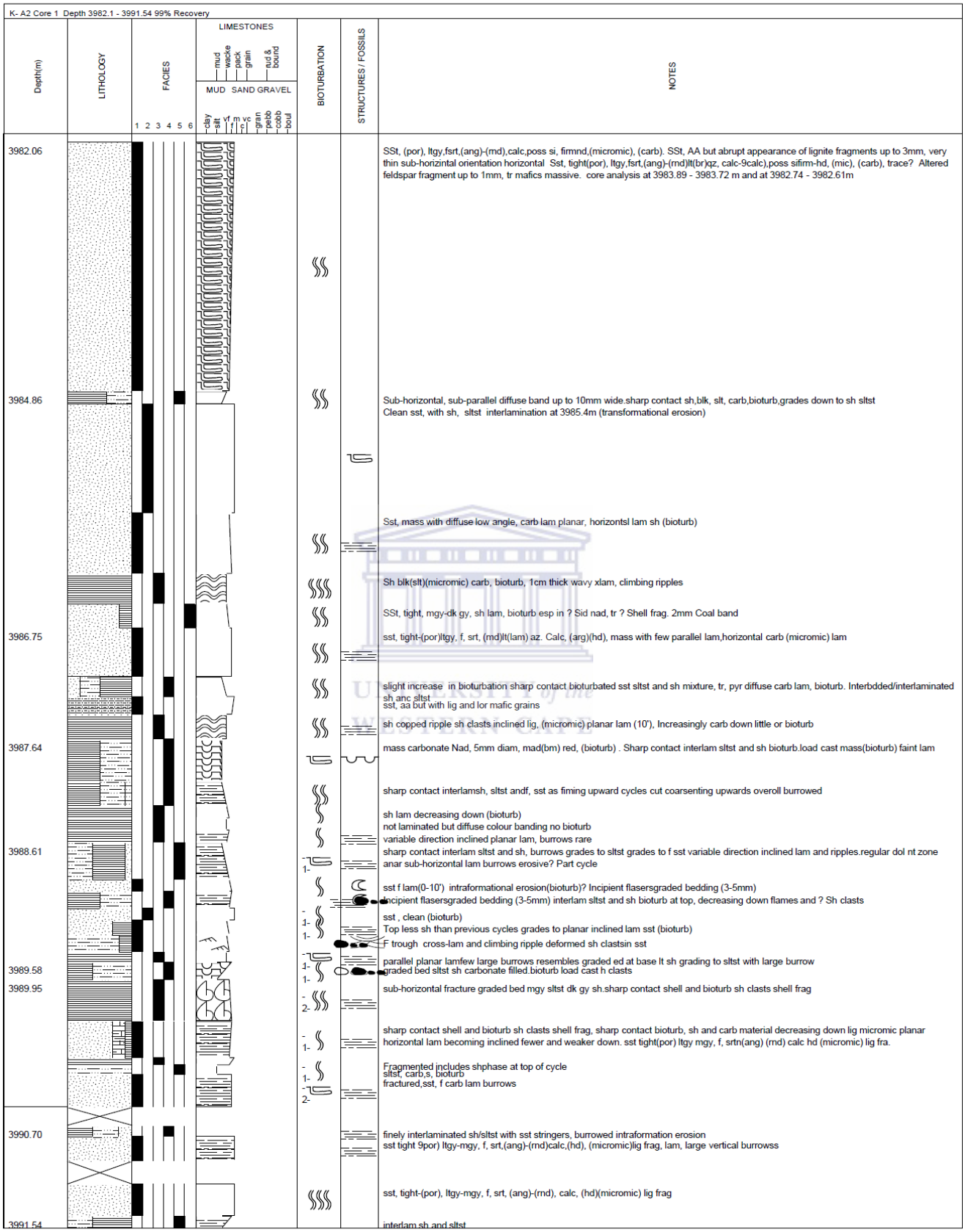

Figure 28: Fully interpreted log section of well K-A2 core 1

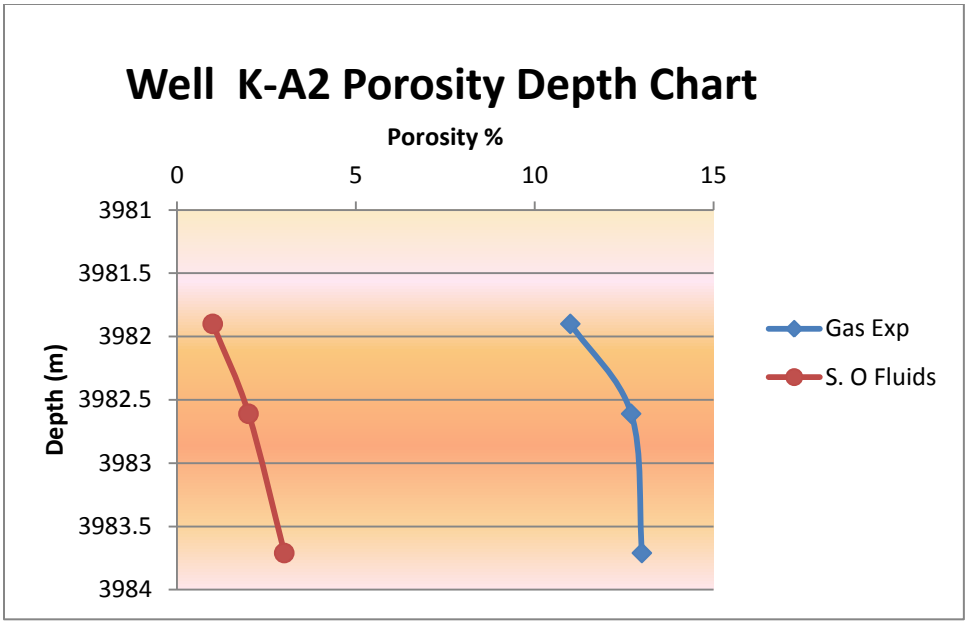

Figure 29: Core porosity chart for well K-A2

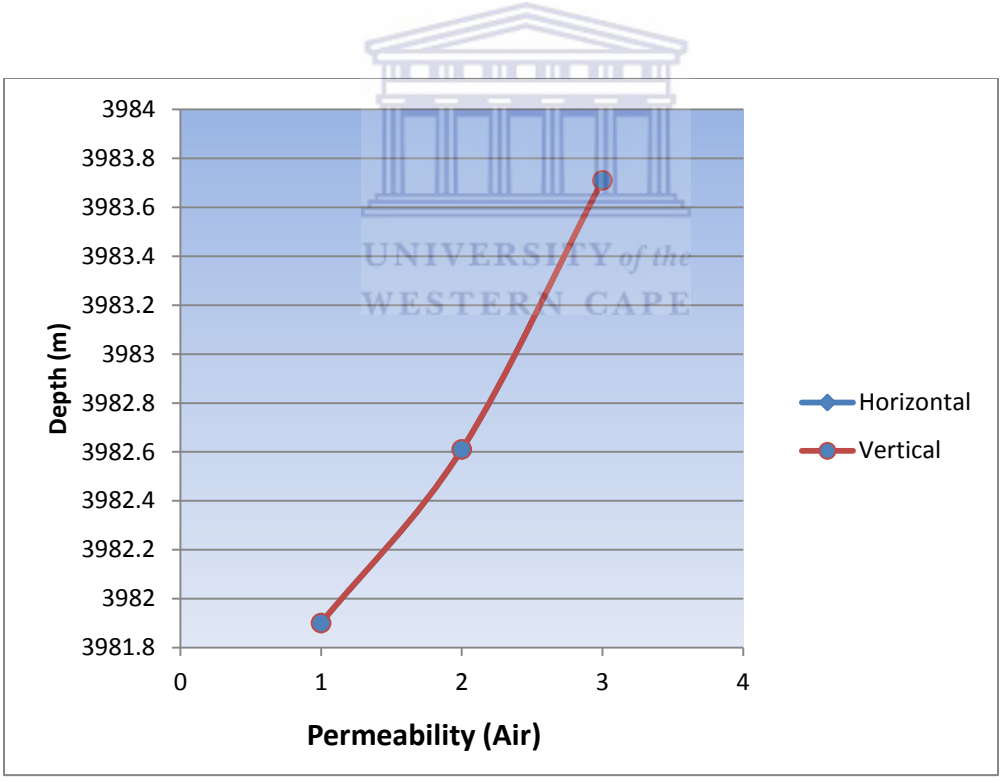

Figure 30: Core Permeability chart for well K-A2.

Figure 29 and 30 graphically represent the two very important petrophysical parameters of well K-A2 (Porosity and permeability). They show that gas expansion, increases slightly with depth but still remains below 5%. The

saturation of fluids in the core also shows an increase with depth. The porosity values range from 11 to 15.8 % (11 – 13% in the upper core and 8 – 9% in the lower core). Permeability values are very low (0.1md). This could possibly suggest that the reservoirs with more potential are available at deeper levels. The increase in porosity could be a result of gas but permeability's suggest water saturations. This can be later confirmed by our geophysical logs. It is noteworthy that the core logs exhibited tight sandstones at this depth, hence the low porosity and permeability values.

LITHOFACIES OF K-A3 CORE 1 and CORE 2

Core 1 and 2 Summary: (Figure 31 & 32) This core consists of a series of finely interbedded sandstones, siltstones and shales. The individual sandstones are about tens of cm's thick which are very thick. This is not the case in core 1 as the entire lithology consists of fine sandstones and some interbeds of siltstone. There are two sandstone types present also in this core and are represented as facie 1 and 2. The tight fine grained sandstone consists of lamination and interlaminations of silt.

Facie 1: Tight fine grained sandstone

The distinction between Facie 1 and 2 in this well is not very clear because of the thin laminations. This facie is characteristic of tight pores and is light grey in colour. It is medium to fine grained but predominately fine. The arrangement is sub rounded and is well sorted.

The visible sedimentary structures include cross bedding. At 2911.65m there is visible flaser bedding with mudstone. These sands exhibit a coarsening upward cycle. There is presence of calcite and dolomite cement in variable quantities. Glauconite and carbonaceous matter is also present. The carbonaceous material is found as some lignite fragments.

Facie 2: Medium grained clean sandstone

It is pale to light grey. There is some presence of pyrite in the sandstone is clean with little to no clay matrix. The sorting is generally good to well with angular to rounded arrangement. At 3880.91 the sandstone consists of a graded bed with an erosional contact 6cm below the grading. There is presence of some shells, bioturbation and micro faults.

Facie 3: Shale

This facie occurs mainly at two significant depths, namely (2906.98 and for more than 10cm at 3879.65). The grain size is very fine with a sub rounded grain shape. This shale is very rare in both cores 1 than core 2 (Figure 31 and 32 respectively). The shale is black and has micro mica and parallel laminations. Pyrite (FeS2) is a common sulphide mineral product of early diagenesis in organic-rich sediments.

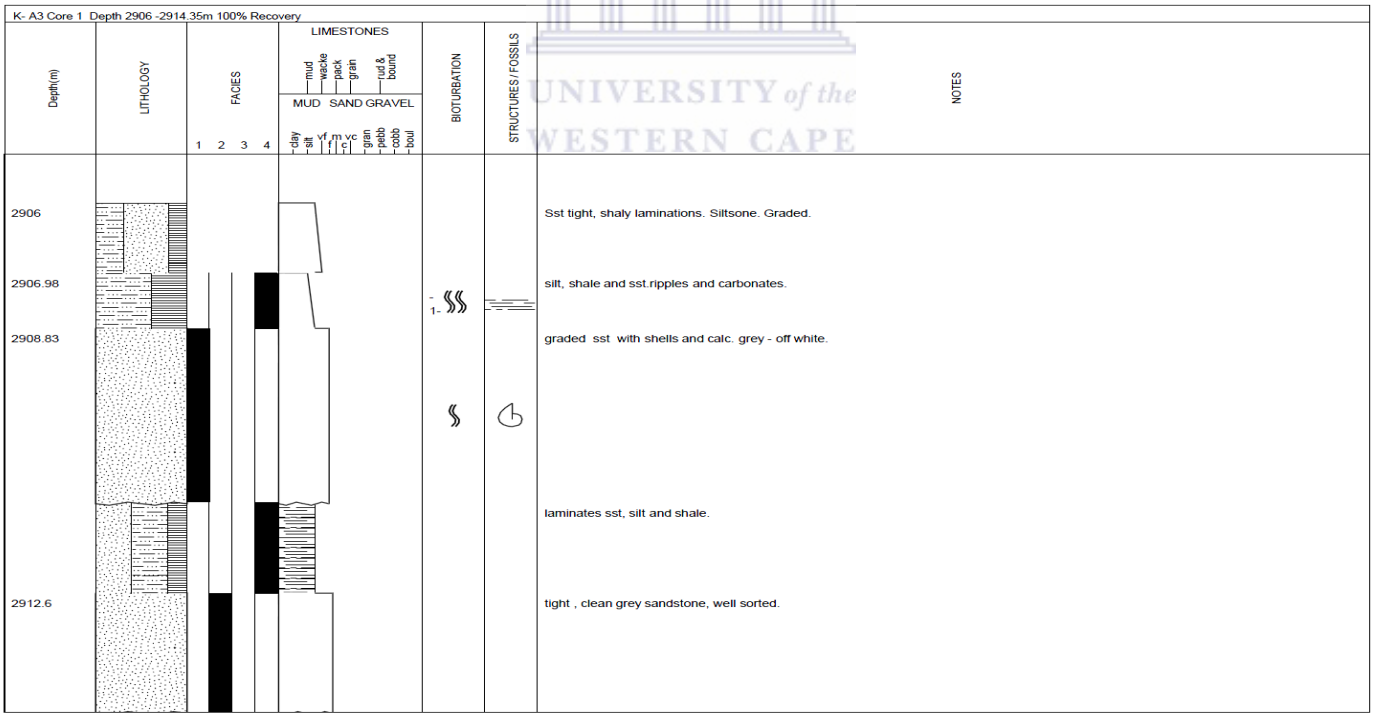

Figure 31: Summary log section of well K-A3 Core 1

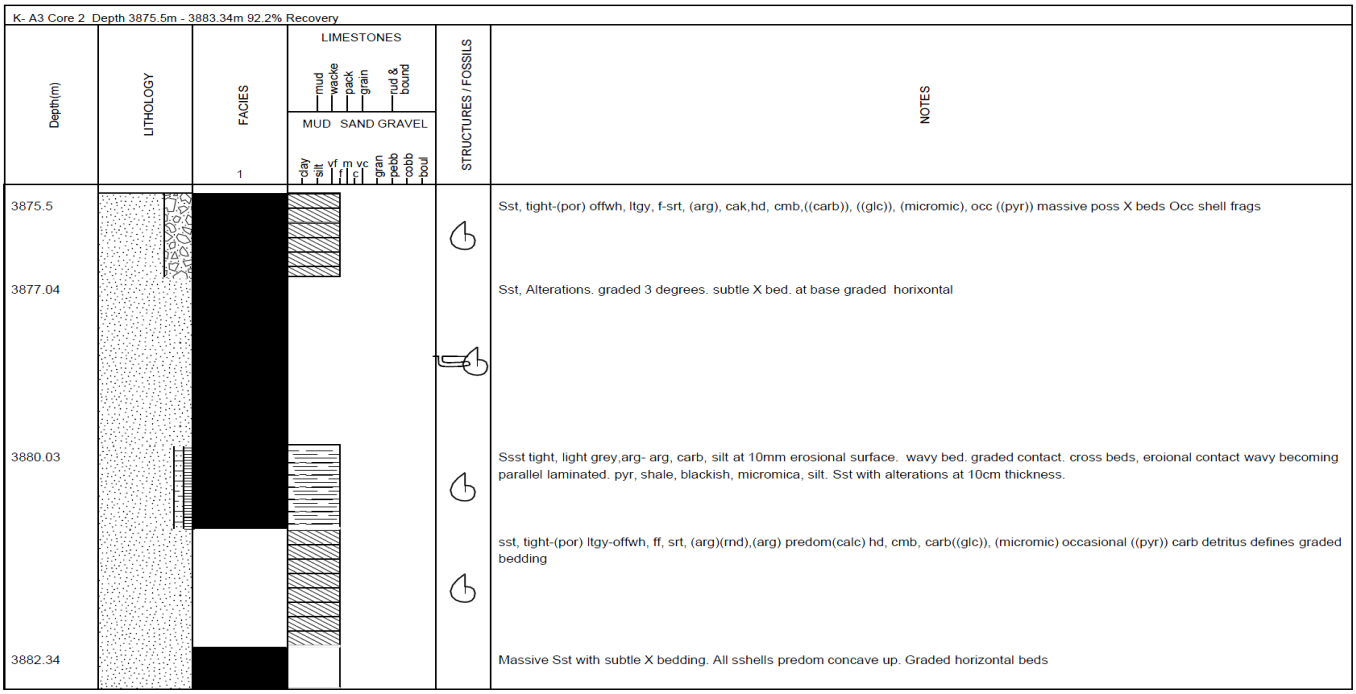

Figure 32: Summary log section of well K-A3 core 2.

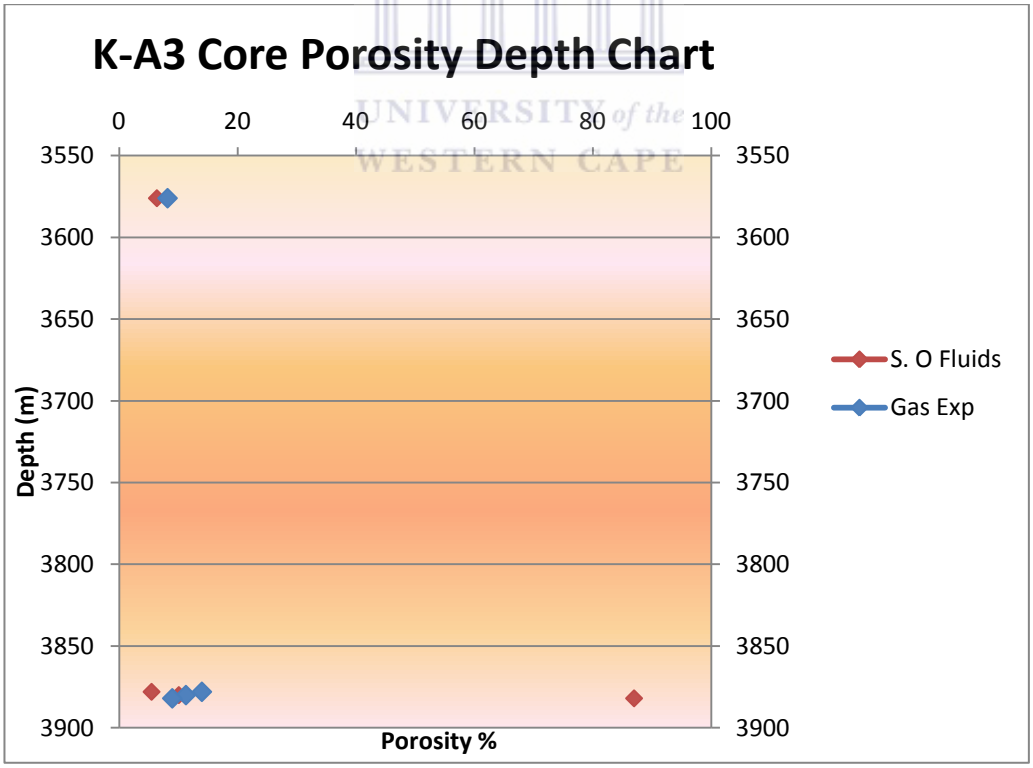

Figure 33: Core porosity chart for well K-A3

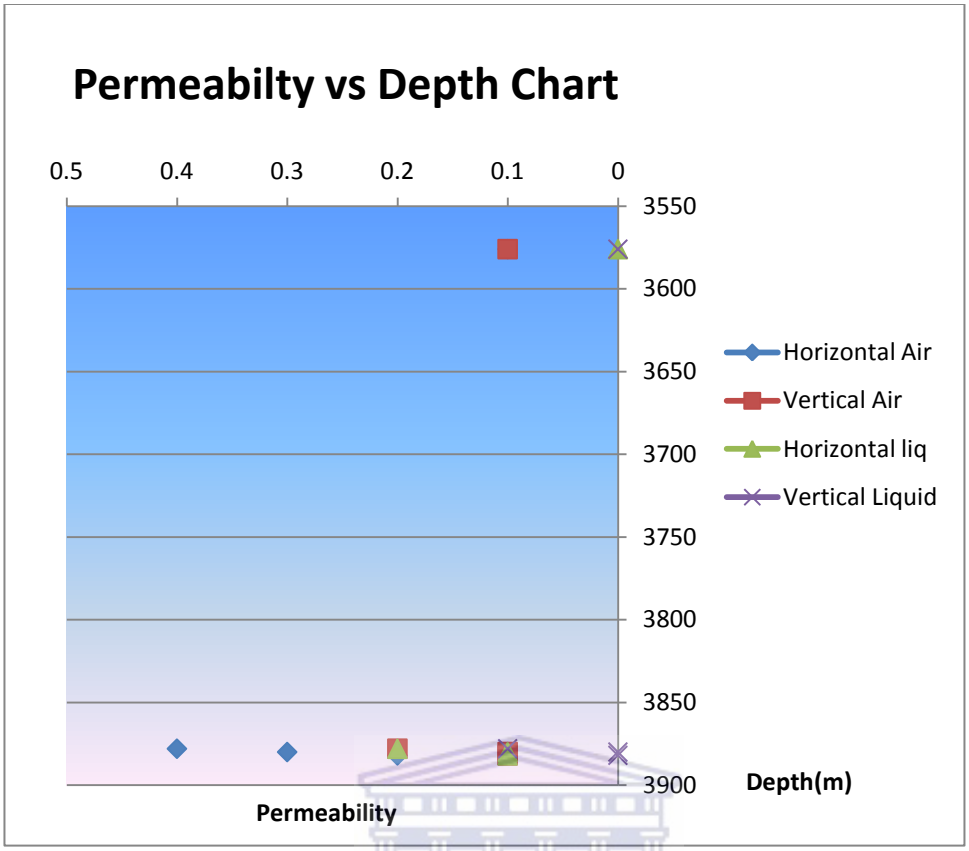

Figure 34: Core Permeability chart for well K-A3

The porosity values for well K-A3 are good and average at 18%. The core shows averages of permeability of 48md at shallow depths. But nonetheless the core shows very high water saturation results of approximately 74%. Thing to note is that both core 1 and core 2 of this well consist predominately of sandstone. A significant increase in porosity at 3877.45m – 3877.54m is apparent (Figure 33). The in surrounding porosity here sits at 15%. Permeability values of this total core are relatively very low and range below 1md (Figure 34).

LITHOFACIES OF K-H1 CORE

Core summary: The core KH1 consists of new facie that do not fall under the previously identified facies, namely; sandstone, siltstone, claystone and fossiliferous limestone. Facies at the core depth of 3080m – 2960m consist of stacked coarsening up sequence of claystones, siltstones and sandstone (Figure 35).The core

consist mostly of sandstone and claystone. At 3074m there is presence of fossiliferous limestone with an erosional contact

Tight sandstone

The sandstone is grey – pale and very clean. It has fine grains and consists of no calcite but contains carbonaceous material. The sandstone is intensely bioturbated and contains some load casts. At 3070m of the core there is evidence of a 10mm calcite vein along a fracture. Intensely bioturbated sandstone exists at a depth of 3066m. This sandstone is argillaceous and the characteristics mentioned above could suggest a formational environment characterized by the start of progradation of inner shelf and shoreface sediments over the outer shelf clays.

Claystone

Dark grey – black, very fine grained claystone. Fine grain size sediments consisting of planar bedding, ripple cross laminations. Large amount of carbonaceous material and bioturbation indicate deposition in a lower shoreface environment. There is also presence of burrows and siltstone lamination

Fossiliferous limestone (lime Mudstone)

Dark brown and grey with cross laminations and some sandstone clasts. There are also dolomite pellets and carbonate fragments.

.

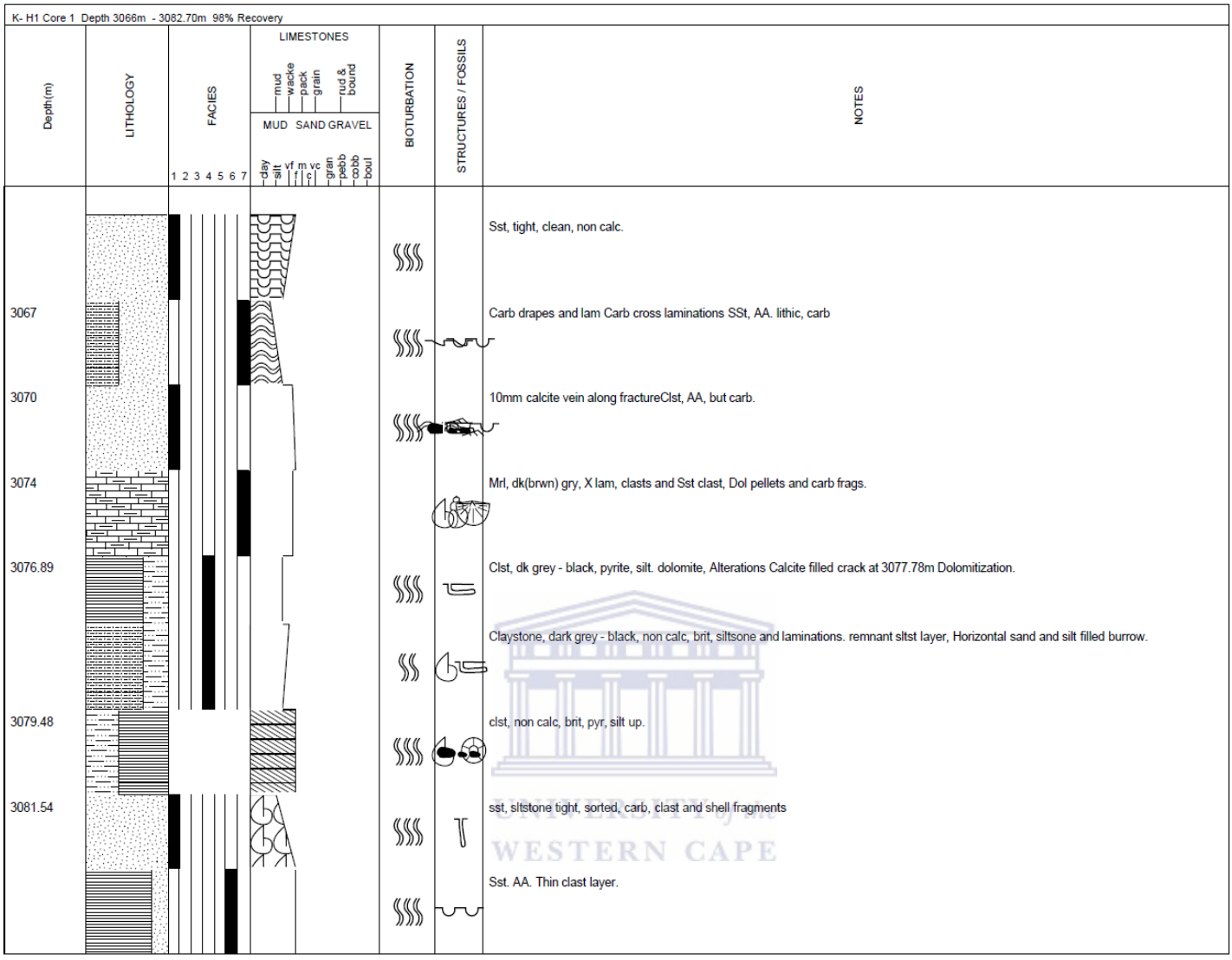

Figure 35: Summary log section of well K-H1

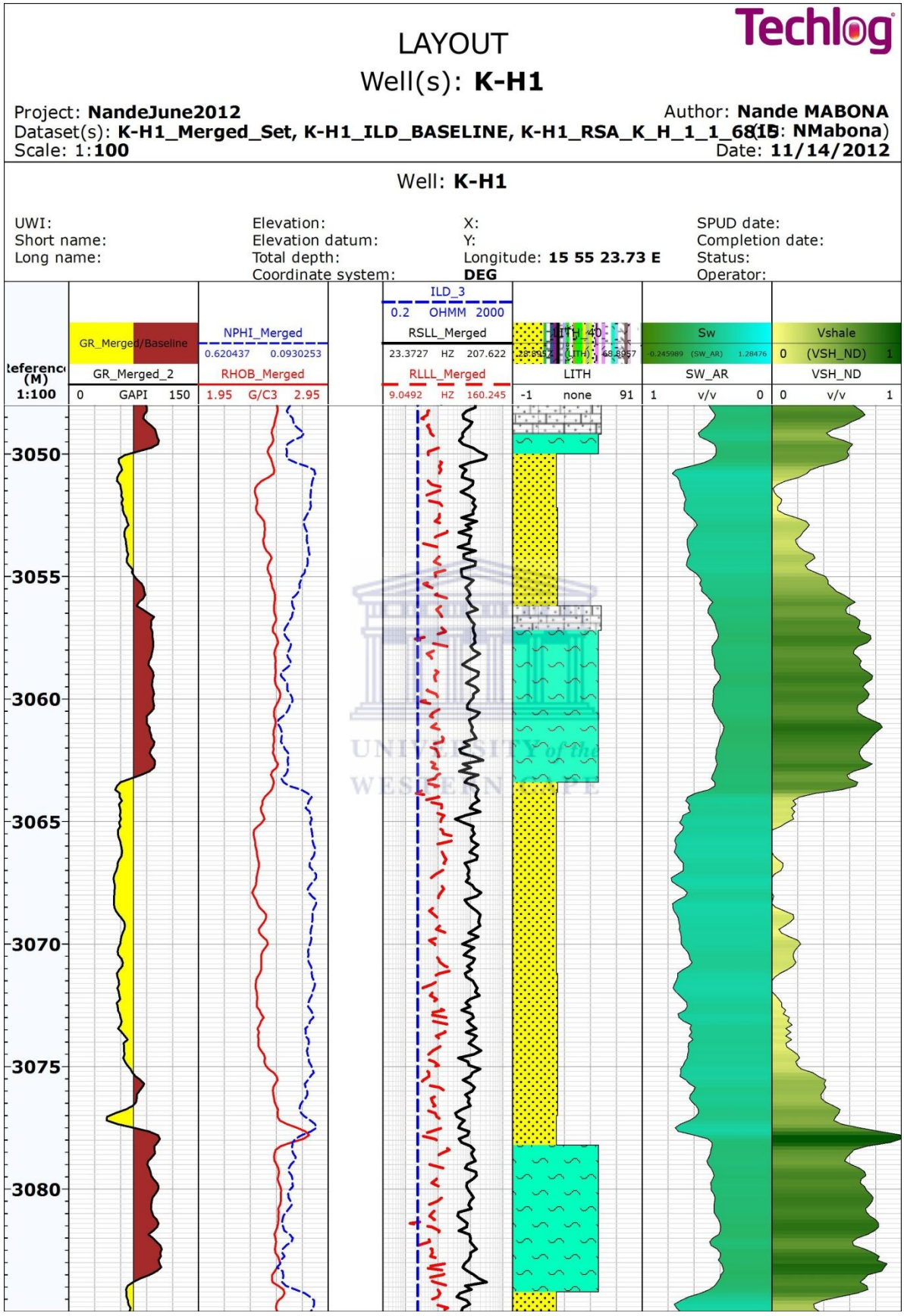

Figure 36: K- H1 Log summary, depicting what was described in the core log.

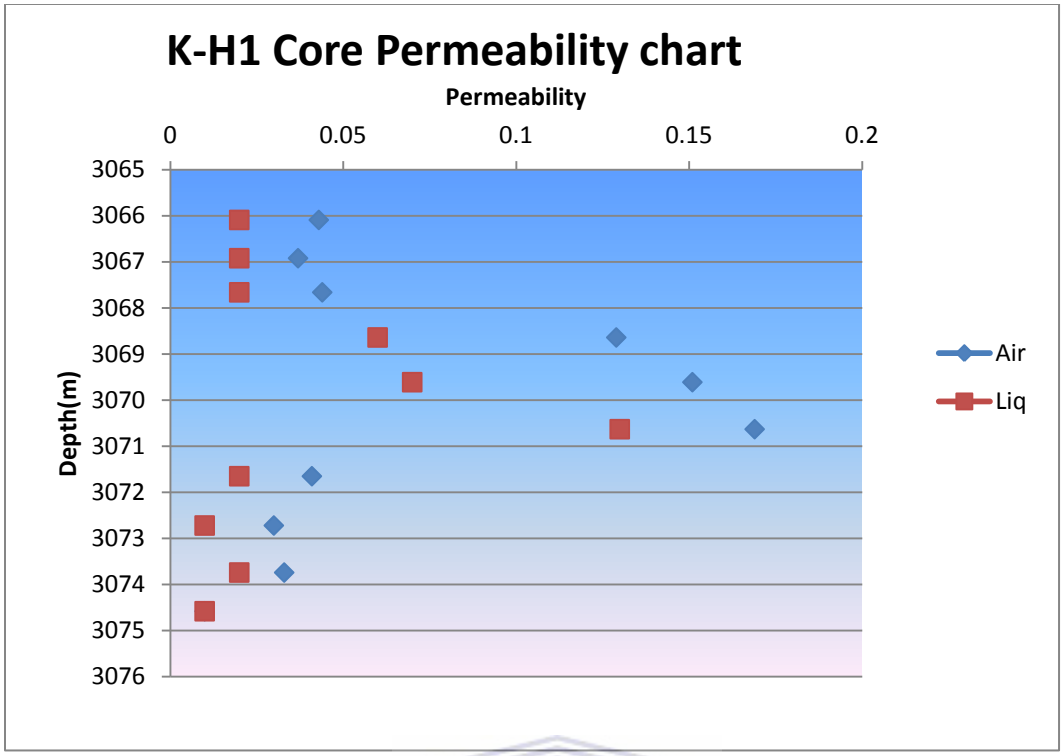

Figure 37: Core Permeability chart for well K-H1

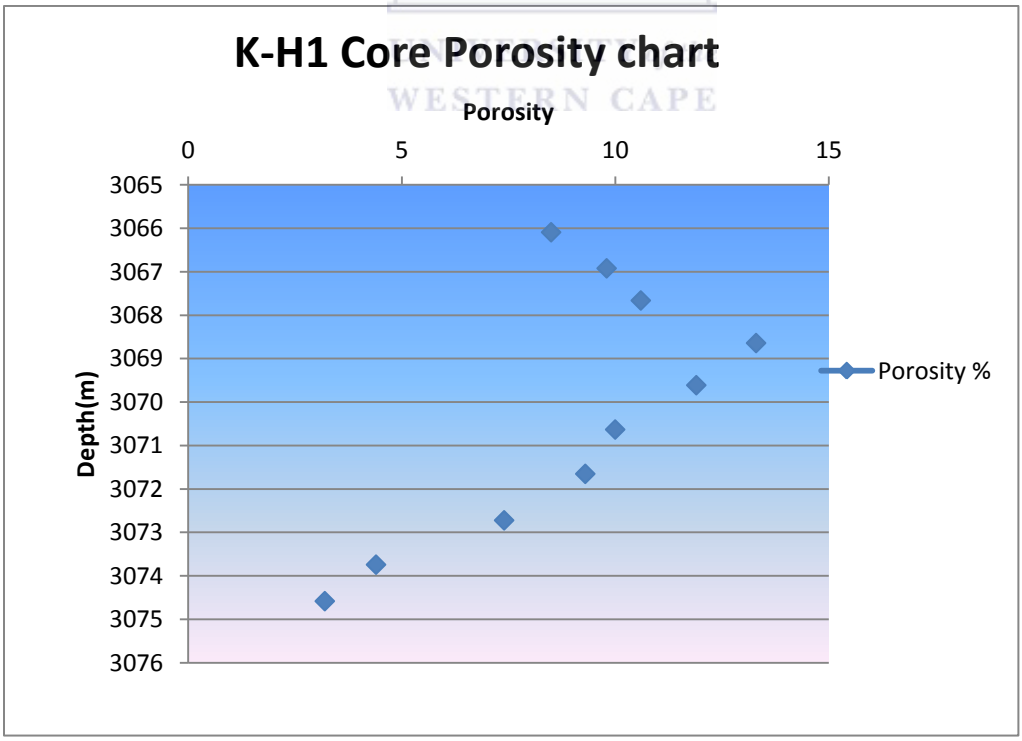

Figure 38: Core porosity chart, Well K-H1

Well K-H1 shows figures and data predominantly poor porosity and permeability (poroperm) qualities (Figure 38). The porosity and permeability decrease with depth. And from the core description it can be understood that this is a result of the claystones and interbedded and interlaminated sandstones present in the core. Permeability values are below 0.2md and porosity values range between 4 – 13%. The poroperm values confirm that this well could possibly be a dry well.

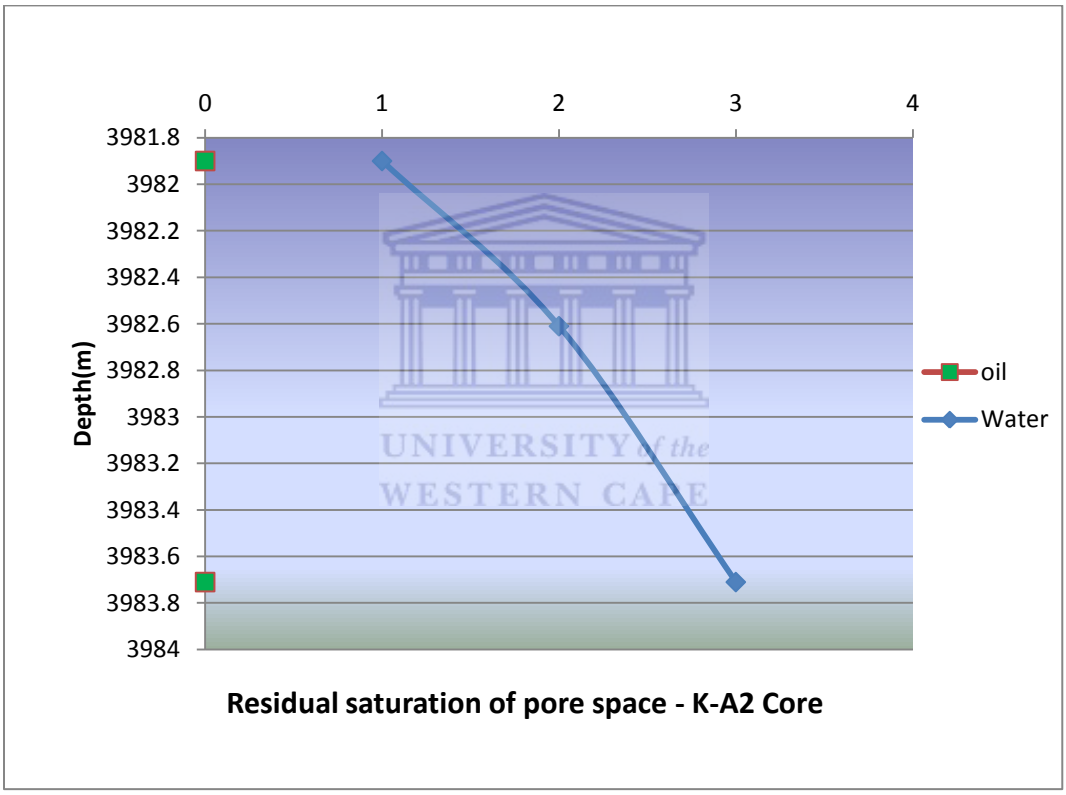

Figure 39: Water and Oil saturation of core K-A2

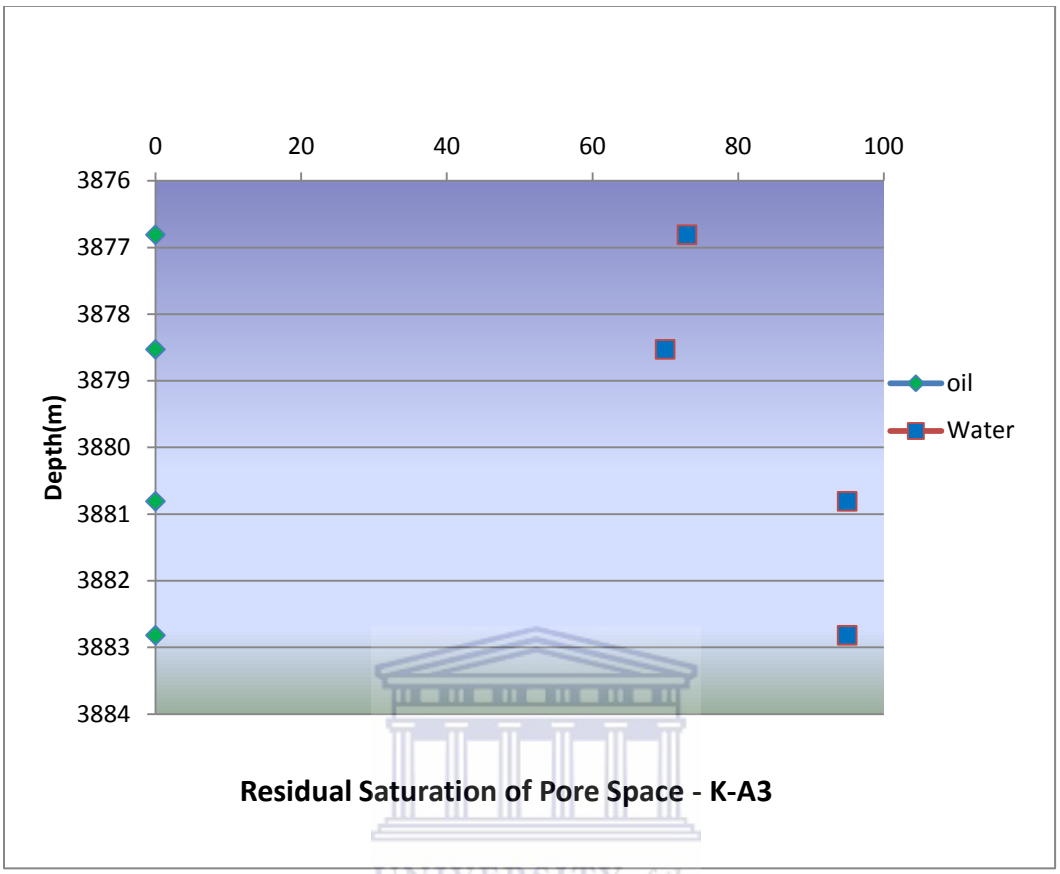

Figure 40: Water and Oil saturation of core K-A3

In well K-A2 the oil saturation is zero, meaning there is no oil in the area and the water saturation is very high and increases with depth. The saturation values are low and remain below 5% for oil meaning there is no oil within this sampled plug (Figure 39).

Well K-A3 depicts even higher residual saturation values for water. Residual water saturation is extremely high and values average at 80 %. It is also visible that with increasing depth there is an increase in the water saturation with oil saturation remaining at Zero.(Figure 40)

5.2 Poroperm Plots of Sampled zones

Core plugs were taken from the core at depths of interest. These plugs were then sampled to give information on core porosity, saturation of fluids, permeability etc. From the data in the study only K-A2 and K-A3 contain full sampled core data and hence there are some plots generated.

The core porosity was calibrated with the neutron and density and showed best fit with the density log (Figure 42 and 45). This method of calibrating core porosity with density is a good way of reducing the inaccuracy of data. The core porosity was graphed as points against the continuous Density and Neutron Logs.

Porosity and permeability are graphed together as a means of control. Porosity controls permeability very well. This is a result of the theory that the more porous a sand body is then the wider the pathways which will allow for fluid flow. Yes at most times this is not the case because there are clays and mineralization that affects permeability.

When interpreting these poroperm plots the trend that is depicted by the scattering of the points is of interest. It is always advised to know which lithology you are looking into so that you see the trend. In this study the sandstone in the delineated reservoir zones are of particular interest.

The diagram below (figure 41) has assisted in the determination and comprehension of poroperm relationships.

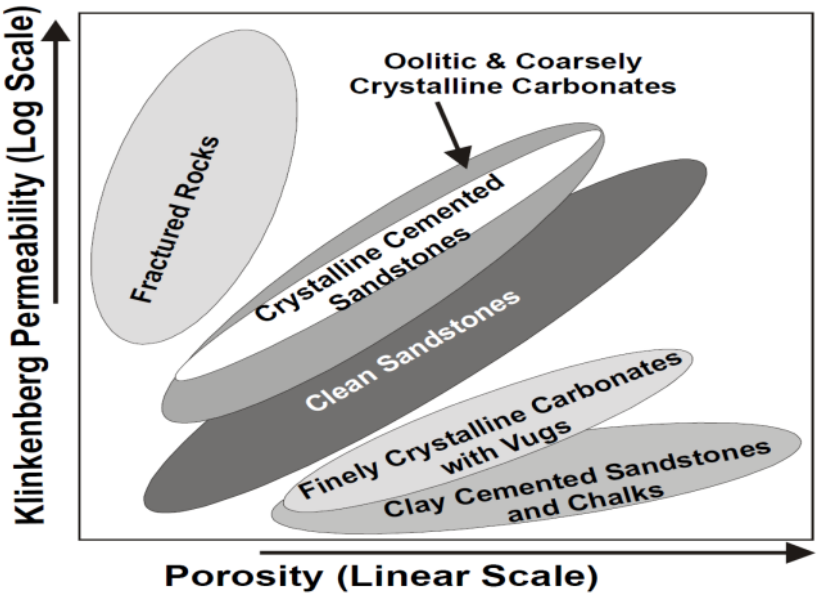

Figure 41: Permeability vs Porosity cross plot depicting lithology types. Basic Logging Course Notes. Schlumberger

Poroperm trends for different lithologies can be plotted together, and form a map of poroperm relationships, as shown in Figure 41.Fractured rocks fall above the sandstones because their porosity (fracture porosity) is very low, yet these fractures form very connected networks that allow the efficient passage of fluids, and hence the permeability is high. Such permeability may be directional because of preferred orientations of the fractures. By comparison, clay cemented sandstones have high porosities, but the porosity is mainly in the form of micro-porosity filled with chemically and physically (capillary) bound water which is immobile. This porosity does not take place in fluid flow, so the permeability is low. The sandstones in our study thus fall majorly within the crystalline cemented sandstones and partly within the clean sandstone, hence in the tighter sandstone porosity and permeability values are low and in the massive sandstones the porosity values are higher.

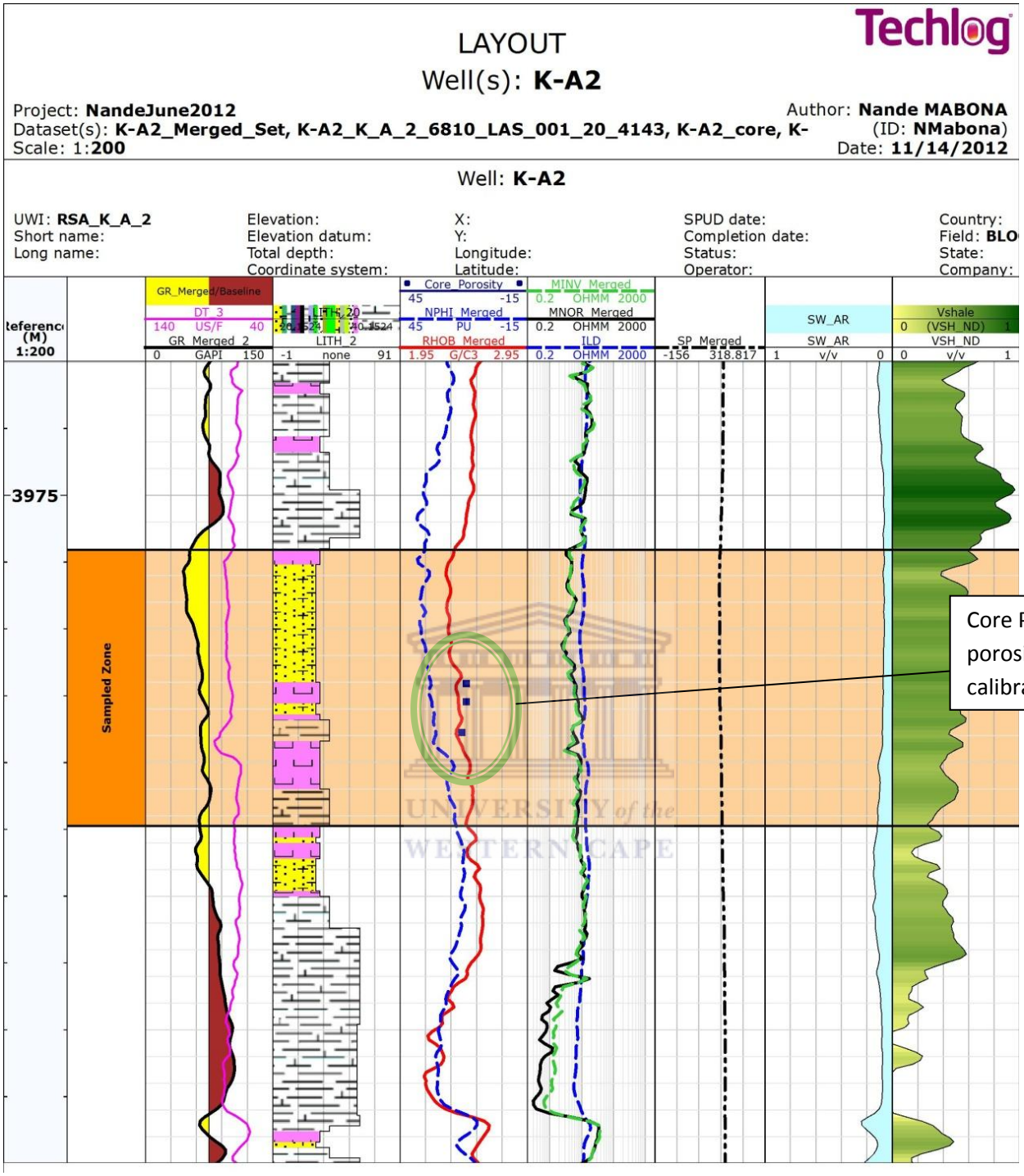

Figure 42: Log section showing Core plug sampled zone and calibrated core porosity in well K-A2

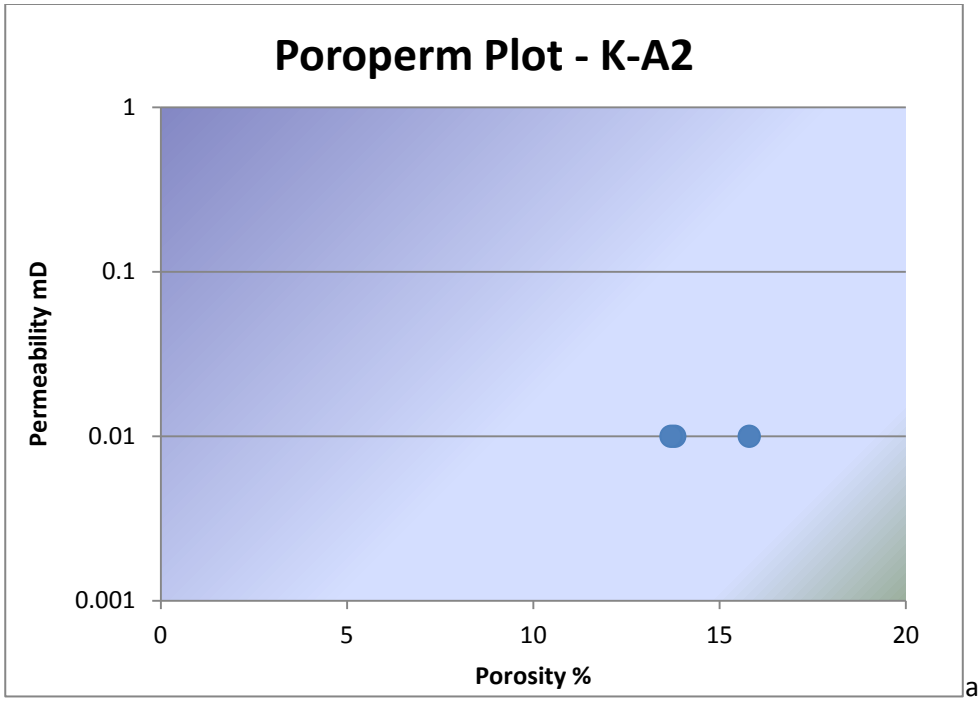

a)

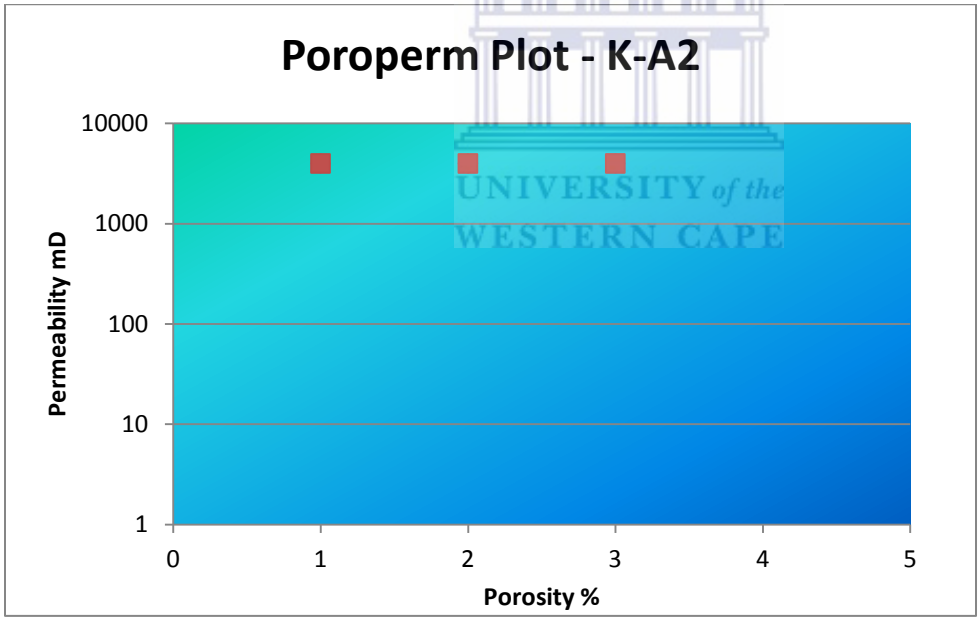

b)

Figure 43: Poroperm plot for a core plug in well K-A2 a) core 1, and b) core 2.

The poroperm plot for K-A2 was sampled at a depth of 3981.90m – 4081, 14m. The trend shows that the lithology is clay cemented sandstone. Looking at the Log interpretation this trend can be confirmed. The

permeability values are very low and range between 0 and 0.01mD. The porosity values are higher at lower depths averaging at 14% whereas at the deeper levels they range between 3.4 – 5.3%.

The poroperm plot for K-A3 was sampled at a depth of 3876.74 m– 3882.72m (Figure 44). Within this zone the range in permeability values is very drastic. Above 3876.74m depth there are very high permeability values ranging between 31md – 58mD, whereas below that depth the permeability values are average of 0.1mD. The trend depicted by this poroperm relationship at this depth indicates that the lithology is clean sandstone and grading into the crystalline cemented sandstones.

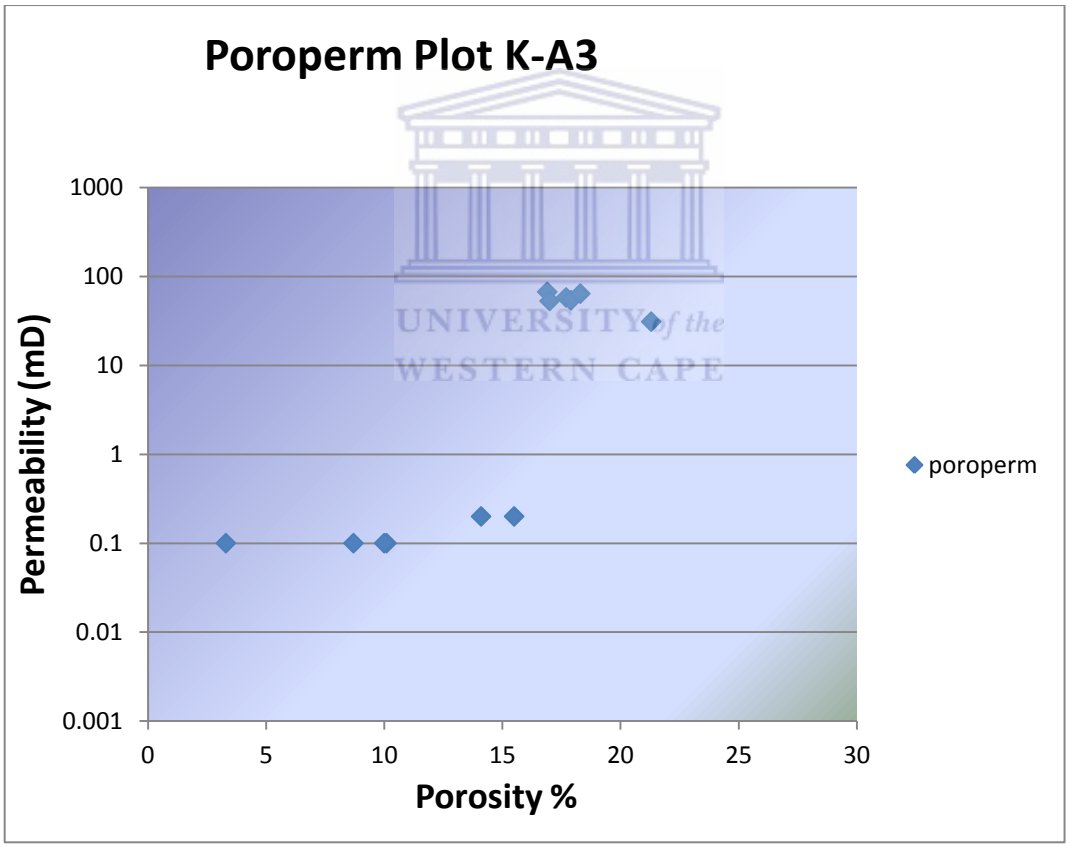

Figure 44: Poroperm plot for a core plug in well K-A 3

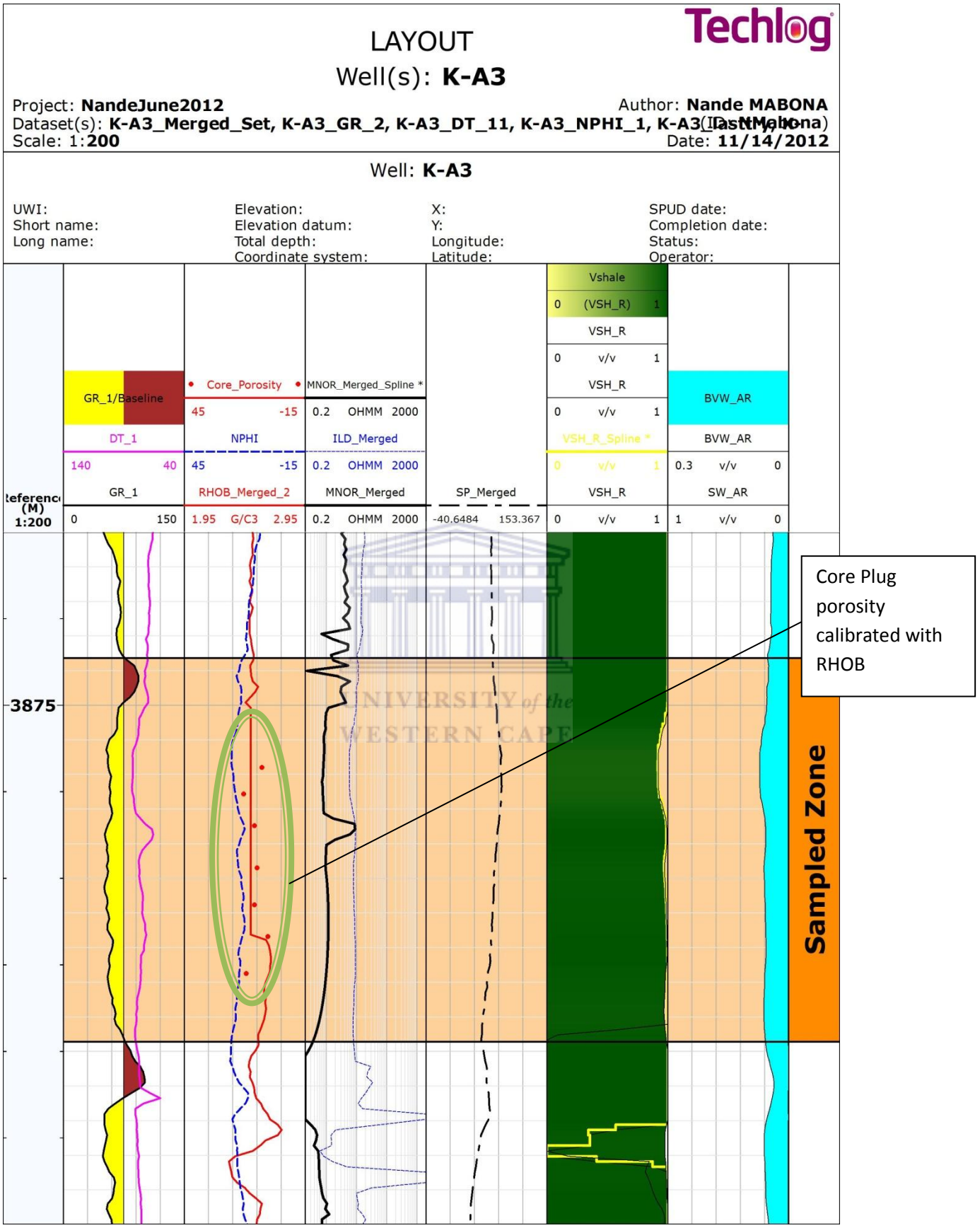

Figure 45: Log section showing Core plug sampled zone and calibrated core porosity in well K-A3

5.3 Petrophysical Analysis

Wireline log is the main source of accurate information on the depths as well as apparent and real thickness of beds. It comes second to core data as core data provides the exact ground truth. Wireline logs yield information on the subsurface geology including formation boundaries, lithology, porosity, shale volume etc. The wireline log suite obtained for this study includes Gamma ray, Sonic, Resistivity, Neutron and Density which were used in lithostratigraphic and seismic interpretation of the wells in the Orange Basin.

Figure 48, below is the chronostratigraphic correlation chart of sequence stratigraphic studies of the Orange Basin (Adekola 2009). It provides a geological framework, using the time scale of Haq et al.,(1988) and is useful for understanding the distribution of lithofacies through time (Broad et al. 2006).

5.3.1 Well Correlation and Stratigraphic Analysis

The reservoir tops are defined through the use of a stratigraphic approach. The intervals are useful in delineating the parameter intervals (reservoir zones). The comparison of wells in an area is an important part in understanding the distribution of lithologies, structural modeling and facies at different locations where data is available. In the study the well tops are used to correlate wells K-A1, K-A2 and K-A3.

5.3.2 Log Correlation description

From the correlation it is apparent that well K-A3 was drilled deeper that than K-A1 and K-A3 hence correlation with the selected surfaces was not possible. The distribution of the horizons within a west-east direction is visible. From the stratigraphic correlation well developed sandstones occur above 15AT1 but those at 16AT1 seem to be argillaceous. Sandstones within the 14B2t1 – 14At1 interval are less well developed in well K-A2.(Figure 46)

Looking at the gamma ray signature, it is possible to tell that sandstones within the 13At1 interval are poorly developed, but directly below this interval there is a cleaning upward sequence that could hold as reservoir zones.(Figure 47)

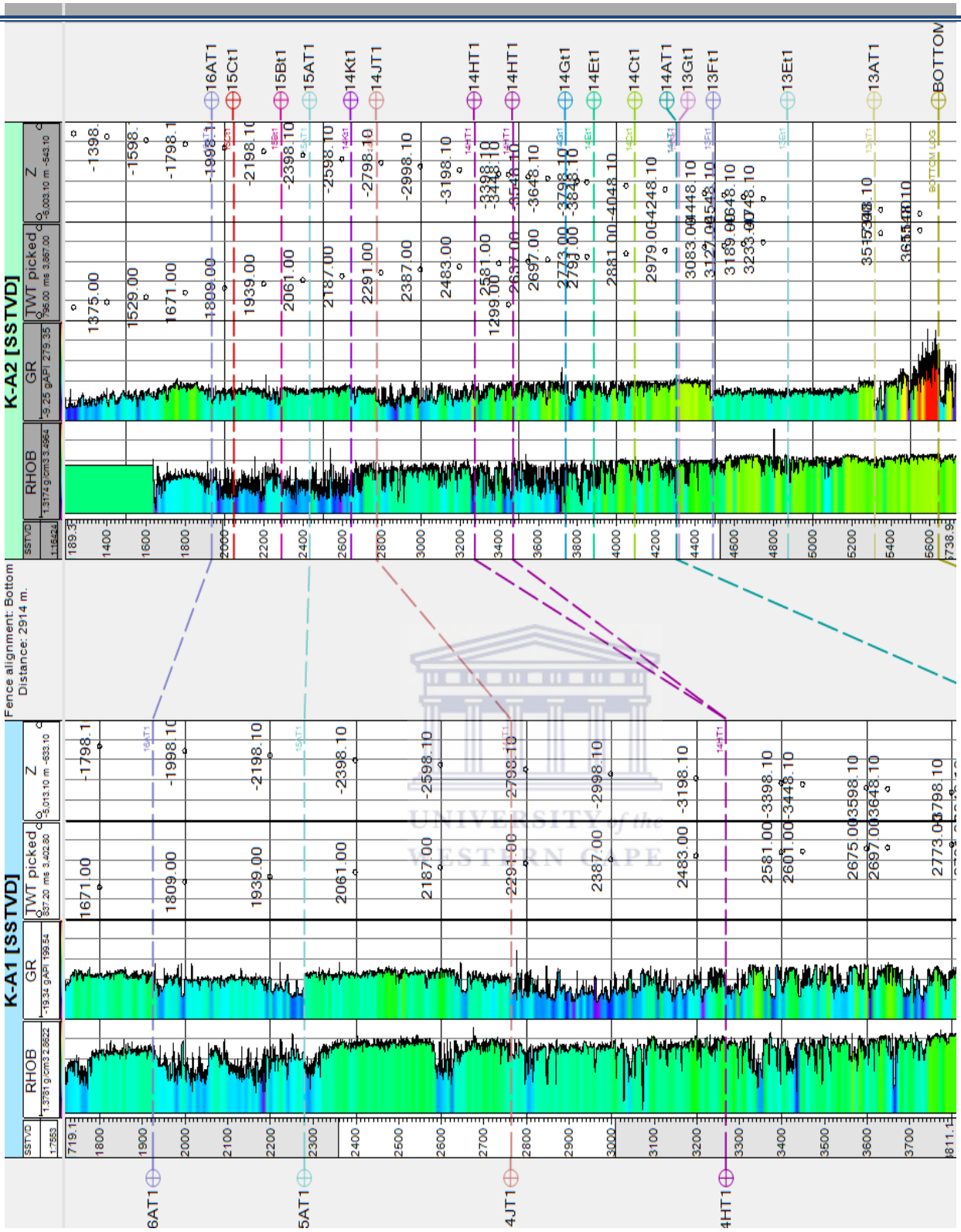

Figure 46: Well correlated stratigraphic section of K-A1 and K-A2

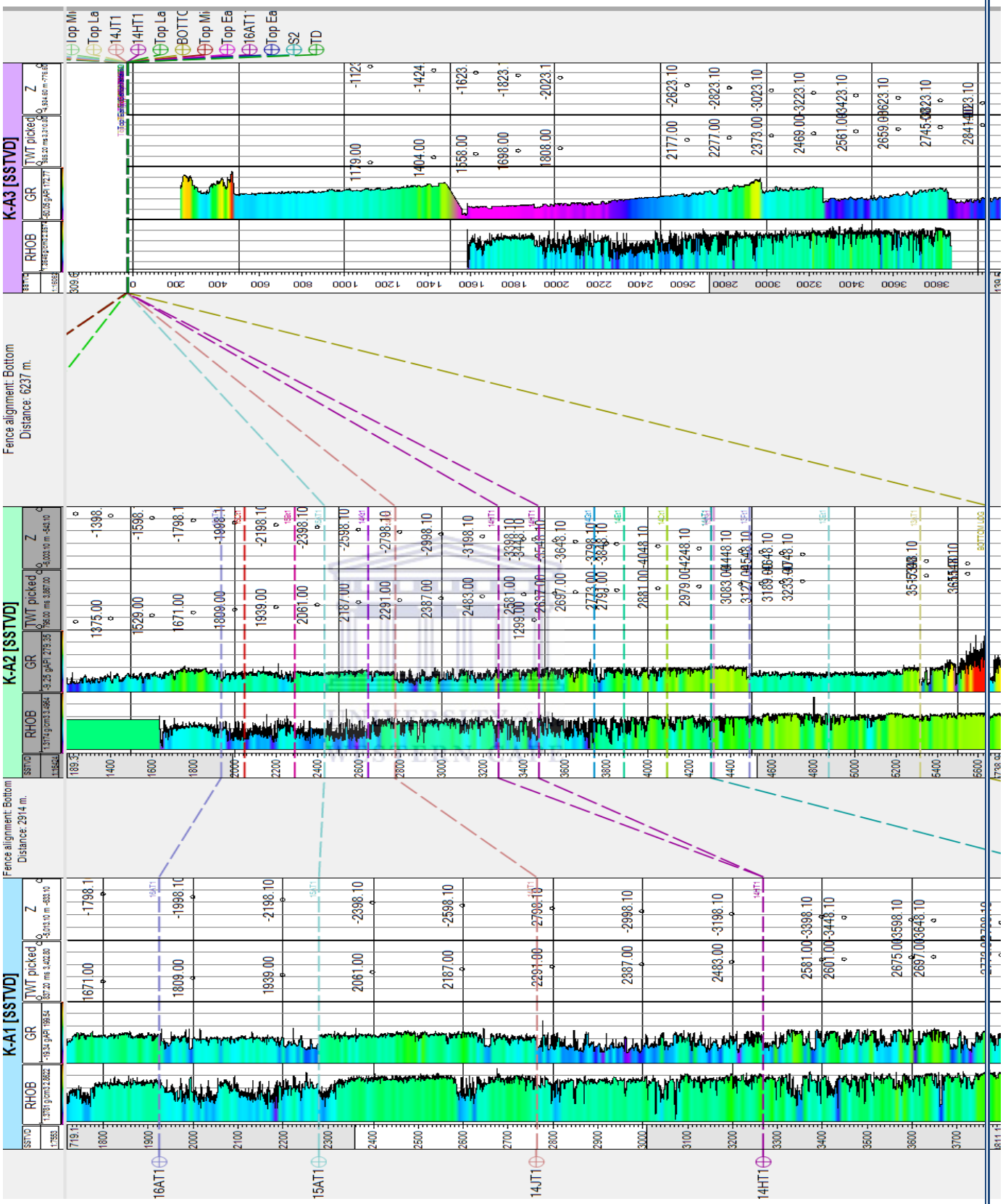

Figure 47: Correlation of stratigraphic section of Wells K-A1 , K-A2 and K-A3

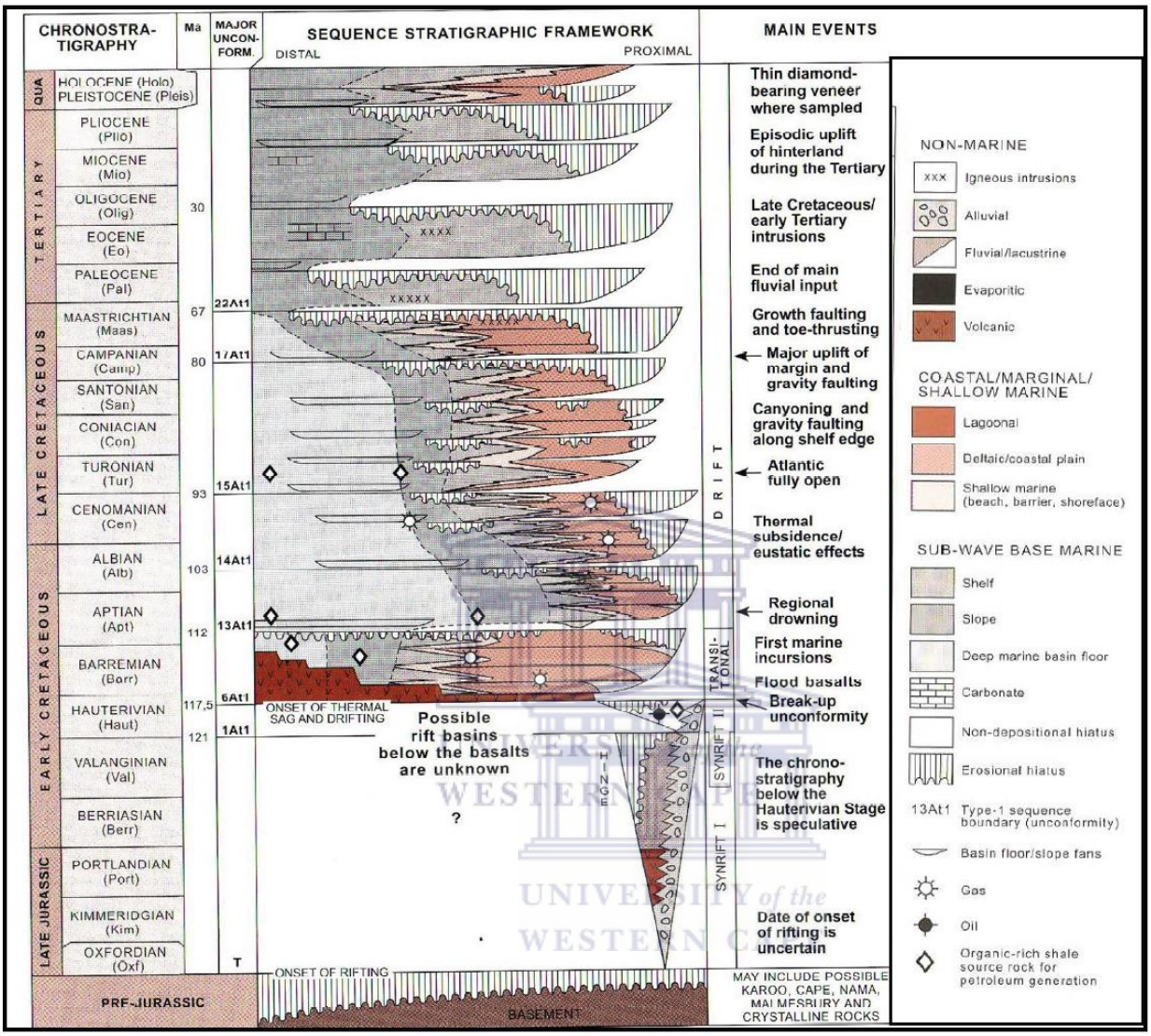

Figure 48: Generalised chronostratigraphy and sequence stratigraphy of Orange Basin offshore Mesozoic basin, based on results of sequence stratigraphic studies (Broad et al., 2006).

Petrophysics encompasses the analysis of well logs run on wireline and drillstring, conventional and special core analysis, mud logging, and formation testing and fluid sampling (Crain, 2003). It provides the building blocks for integrated reservoir models (Archie Reservoirs). Petrophysical interpretive procedures usually are described in terms of a typical clastic reservoir, which is the textbook reference and is sometimes termed an "Archie" reservoir because it broadly matches the requirements for the application of the fundamental Archie equations that provide the quantitative basis for well log analysis (Worthington et al., 2011).

The attributes of an Archie reservoir are listed in Table 6.1.Although these conditions were not itemized explicitly by Archie (1942), they are understood in the use of the Archie equations on the basis of many years of application. Through the examination of the core data, it is apparent that in the Orange Basin an ideal Archie type reservoir is not clearly visible as the lithologies in the basin are argillaceous , silty and contains pyrite, glauconite and laminated sedimentary beds.

Table 5: Criteria for Archie Reservoir. Worthington et al 2011.

TABLE 1—CRITERIA FOR AN "ARCHIE" RESERVOIR		
No.	Archie Criteria	Non-Archie Conditions
1	Single rock type	Multiple electrofacies or petrofacies: thin beds
2	Homogeneous	Heterogeneous (e.g., variable mineralogy/texture)
3	Isotropic at micro- and mesoscales	Anisotropic (e.g., ellipsoidal grain shape, laminations)
4	Compositionally clean	Clay minerals
5	Clay free	Argillaceous
6	Silt free	Silty
7	No metallic minerals	Pyrite and other minerals
8	Unimodal pore-size distribution	Multimodal pore-size distribution including microporosity
9	Intergranular porosity	(Micro)fractures/fissures/vugs
10	High-salinity brine	Fresh water
11	Water-wet	Mixed wettability
12	I_r is independent of R_w	I_r varies with R_w

5.3.3 Wireline logs

The geophysical wireline logs are the continuous records of geophysical parameters along a borehole. They are used to identify and correlate underground rocks, determine their mineralogy, generate their physical properties and the nature of the fluids they contain. It is able to delineate possible reservoir zones from the wireline logs.

K- A1

Two possible reservoir zones could be delineated from this well at the interval of 3930 and 3910m (Figure 49) .A strong negative deflection is apparent on the SP long and the gamma ray exhibits a short cleaning upward trend. The dirtying up trend is dominant in the log and is distinctive of a funnel shaped signature. Following this is a dirtying upward trend caused by the shale and silt laminations. The well seems to be highly saturated in water. The volume of shale in the reservoir zones is less than 50 meaning that the Vsh is not too high in the log. The Sp log depicts a negative deflection at the reservoir zones and all zones have the gas effect bounding them. The deep resistivity signature is relatively constant at 20ohm, but at a depth of 3965m there is a spike and the deep resistivity reached approximately 2000ohm which also has a corresponding lower water saturation signature depicted.

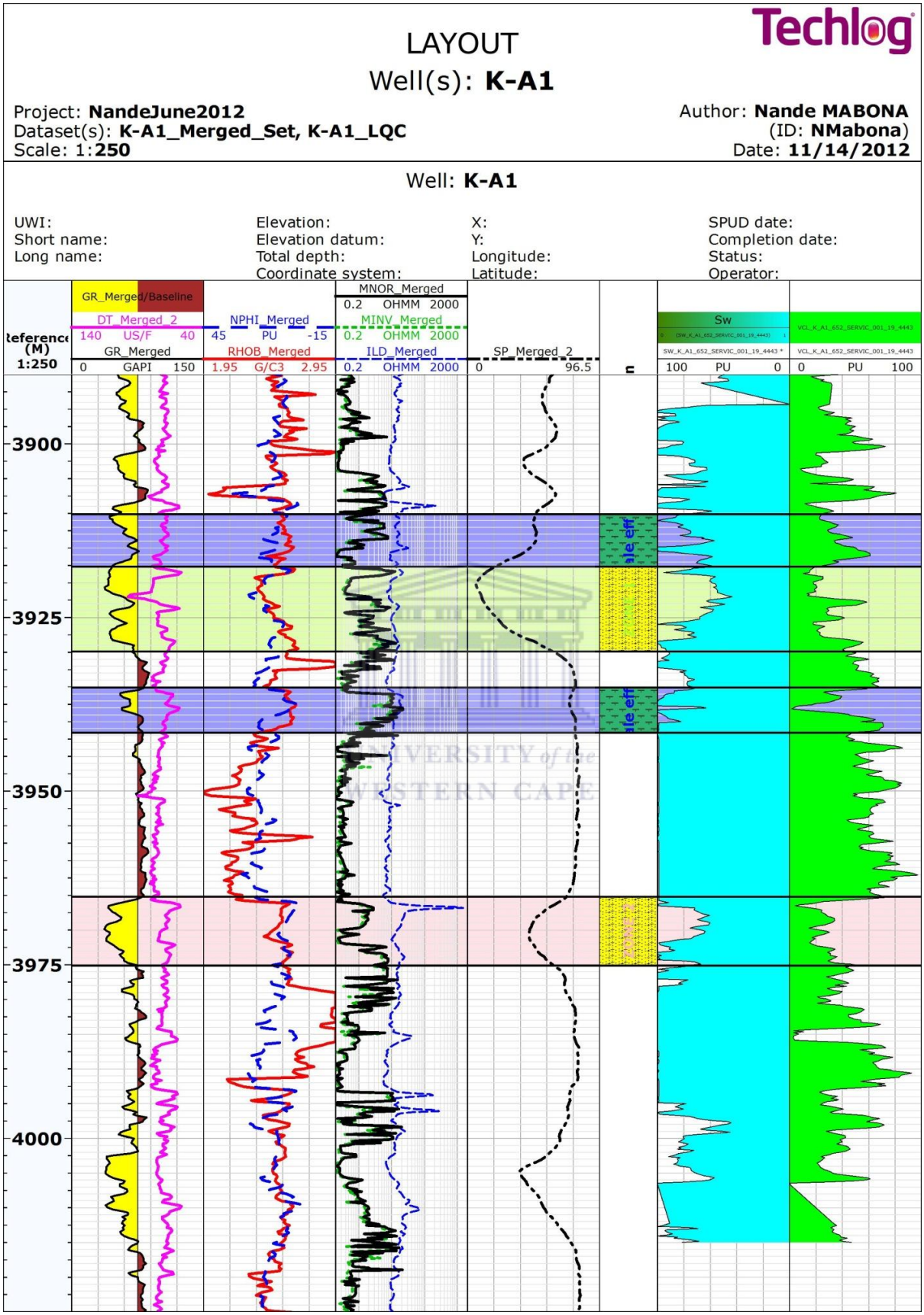

Figure 49: Log template of well K-A1 depicting zones of interest and petrophysical paramenters

K-A2

The gamma ray signatures for this well consisted of many sand and shale laminated beds. This meant that the possible reservoir zones were thin. This corresponds to the interpretation made on the well logging section. The neutron porosity values here are very low which means that the reservoirs are very poor.

Three potential reservoir zones are delineated at intervals: 3673.5m -3676m; 3753.5m -3775m, 3776m – 3779m and 3801m -3803.5m (Figure 50).

The shallow depth sandstone unit appears clean and has good porosity values and very low gamma ray values. Deep resistivity shows a spike and there is no deflection apparent on the SP log. Water saturation and Volume of clay values are not visible at this depth.

The interval 3776m – 3779m, shows very high water saturation values and low Vsh with a slight SP deflection visible. This is then a poor reservoir because of the large amounts of water present. This interval could possibly be a water contact. The water saturation values decrease with increase in depth and volume of shale values remain low. (Figure 51)

This continues to the deeper zones of the well where at 5350m -5750m, there are more developed sandstones with good porosity values. The volume of shale is low and so is the water saturation (Figure 51). Possibly if drilling at deeper levels could be done then gas could be spotted. This suggests that focus should be at the older sandstone units, ones that are older than the lower cretaceous sandstones.

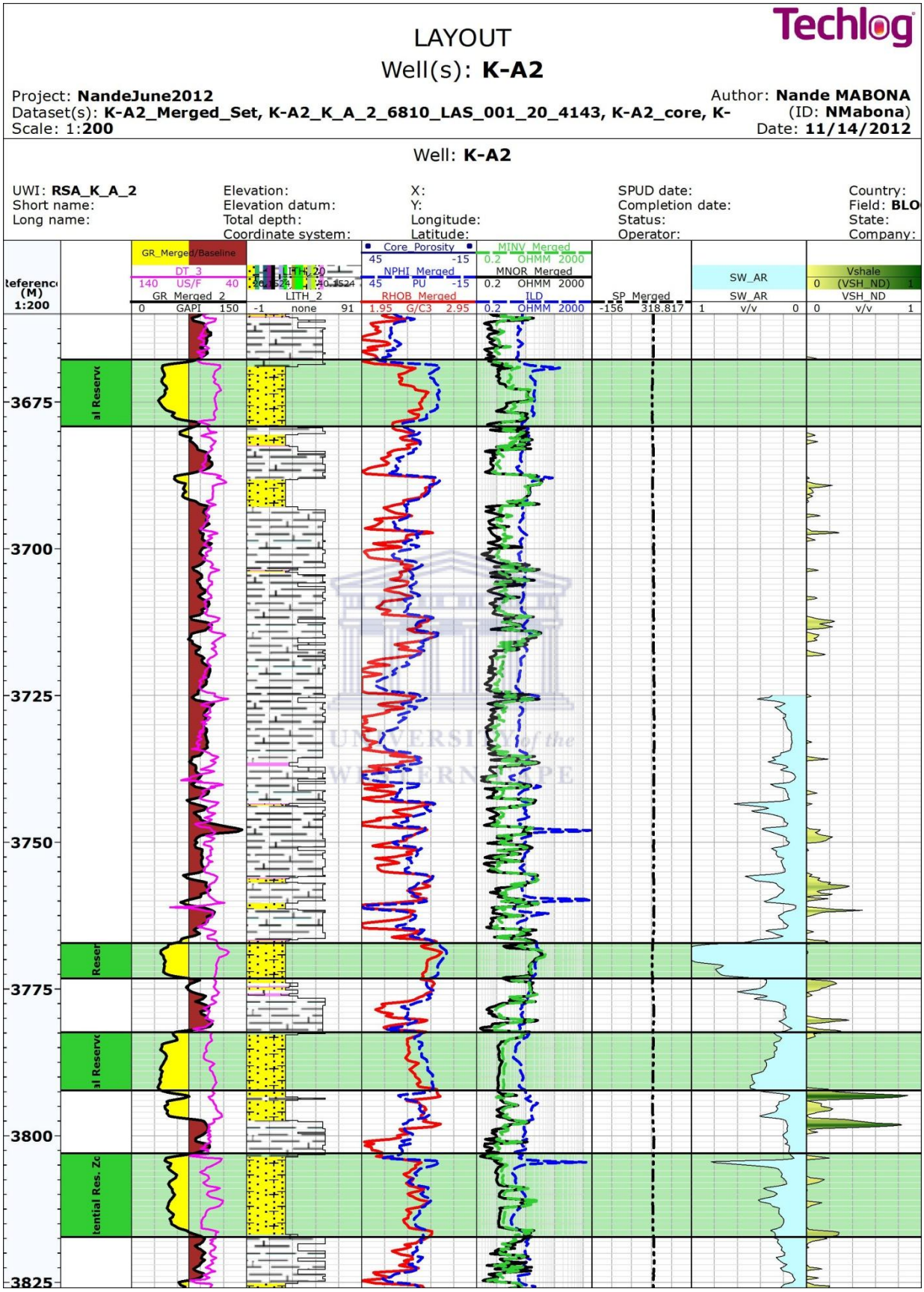

Figure 50: Log template of well K-A 2 depicting zones of interest and petrophysical parameters.

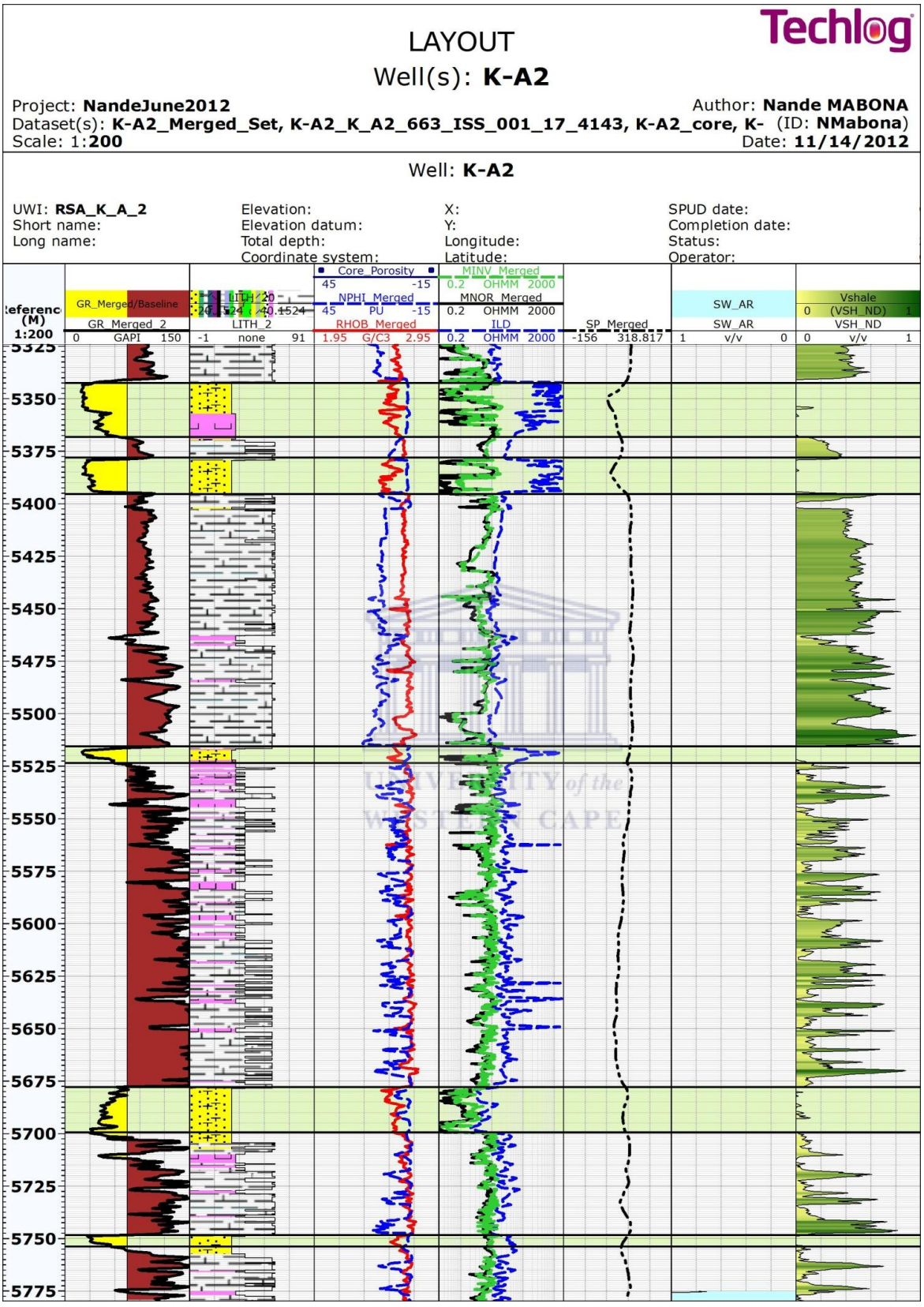

Figure 51: K-A2 logs at a deeper zone

K-A3

This well K-A3 consists mainly of sandstone's but the sandstone porosity values are low. The signature exhibited by the density log suggests that the sandstones are silty and there is a lot of interlamination in the beds. There is a cleaning upward trend visible. Three possible reservoir zones are picked out in this well but only the zone below 3700m holds much potential as the porosity values are higher and the sandstone seems cleaner.

This log track consists of a great deal of sandstones which hold potential of being reservoir zones. The porosity values are average throughout the zones of selection but there is an improvement in the porosity values at a deeper zone (3700m -3725m). This zone serves as the main zone of interest in this well. There is also an increase in resistivity values in this interval (Figure 52).

The SP log shows continuous negative deflection and the water saturation values are low. There are high shale volume values which decrease with an increase in water saturation.

K-H1

There is one reservoir zone in this area and it is potential very good and massive. The gamma ray shows very low values and porosity values are good. Shale effect is present above and below the sandstone layer. This layer is at an interval 3065 and 3077m. There is no SP log modeled in this area to assist in the confirmation of this reservoir zone (Figure 53).

All the signatures studied correlate with the core analysis that was run previously and the lithology signatures match. Porosity values are low and the wells are highly saturated in water.

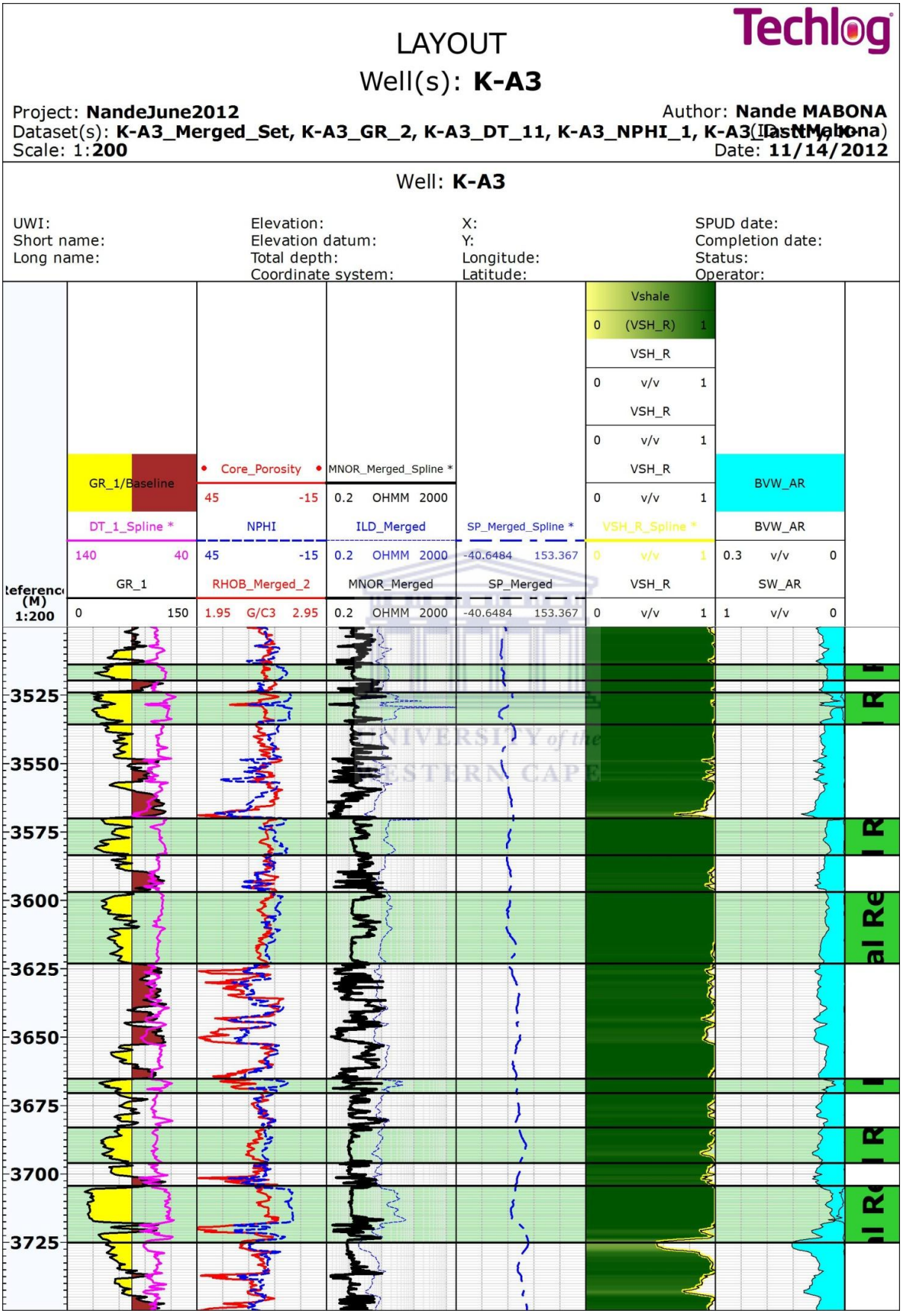

Figure 52: Log template of well K-A 3 depicting zones of interest and petrophysical paramenters

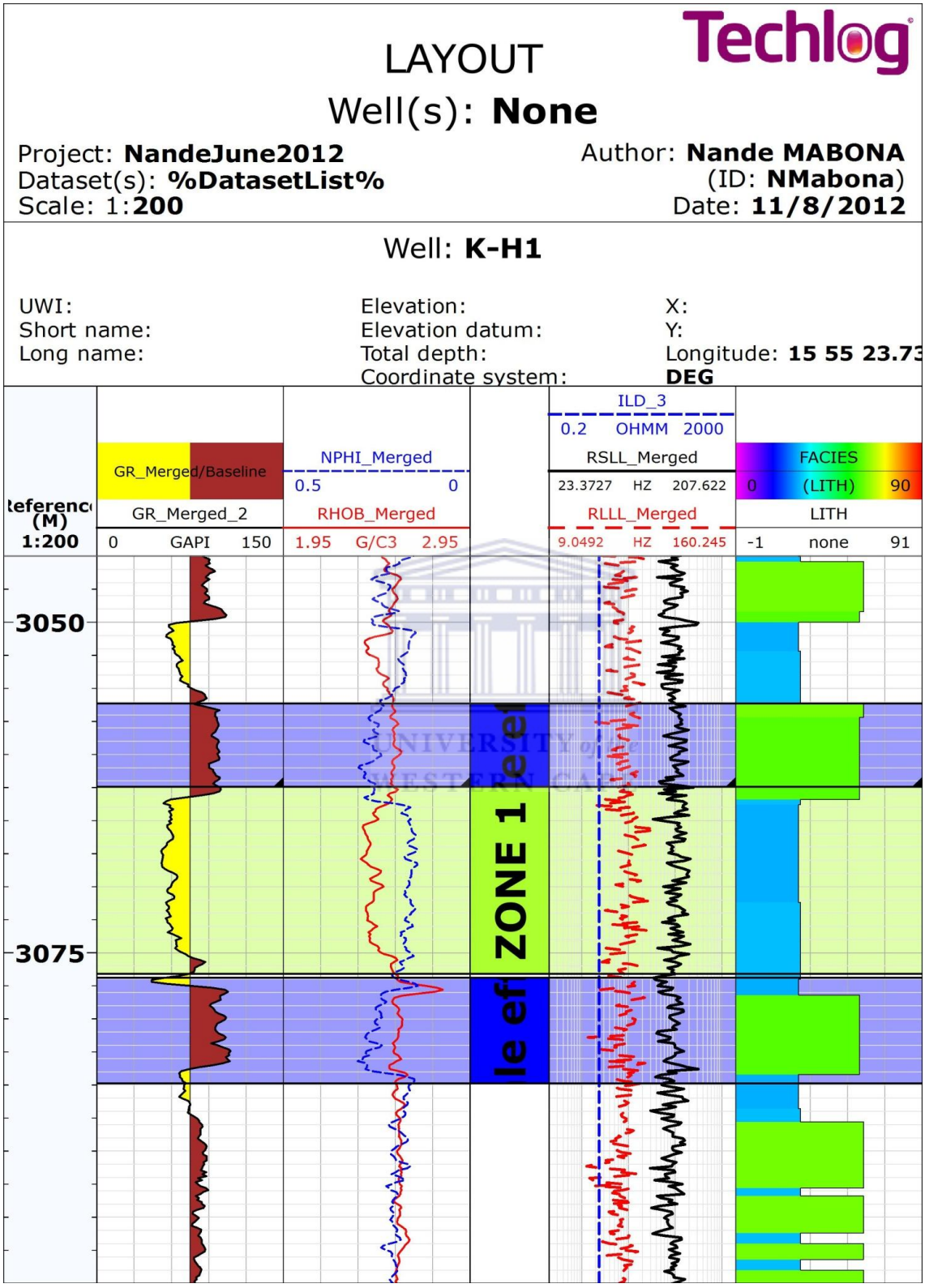

Figure 53: Log template of well K-H1 depicting zones of interest

5.3.4 Density Porosity Cross Plots

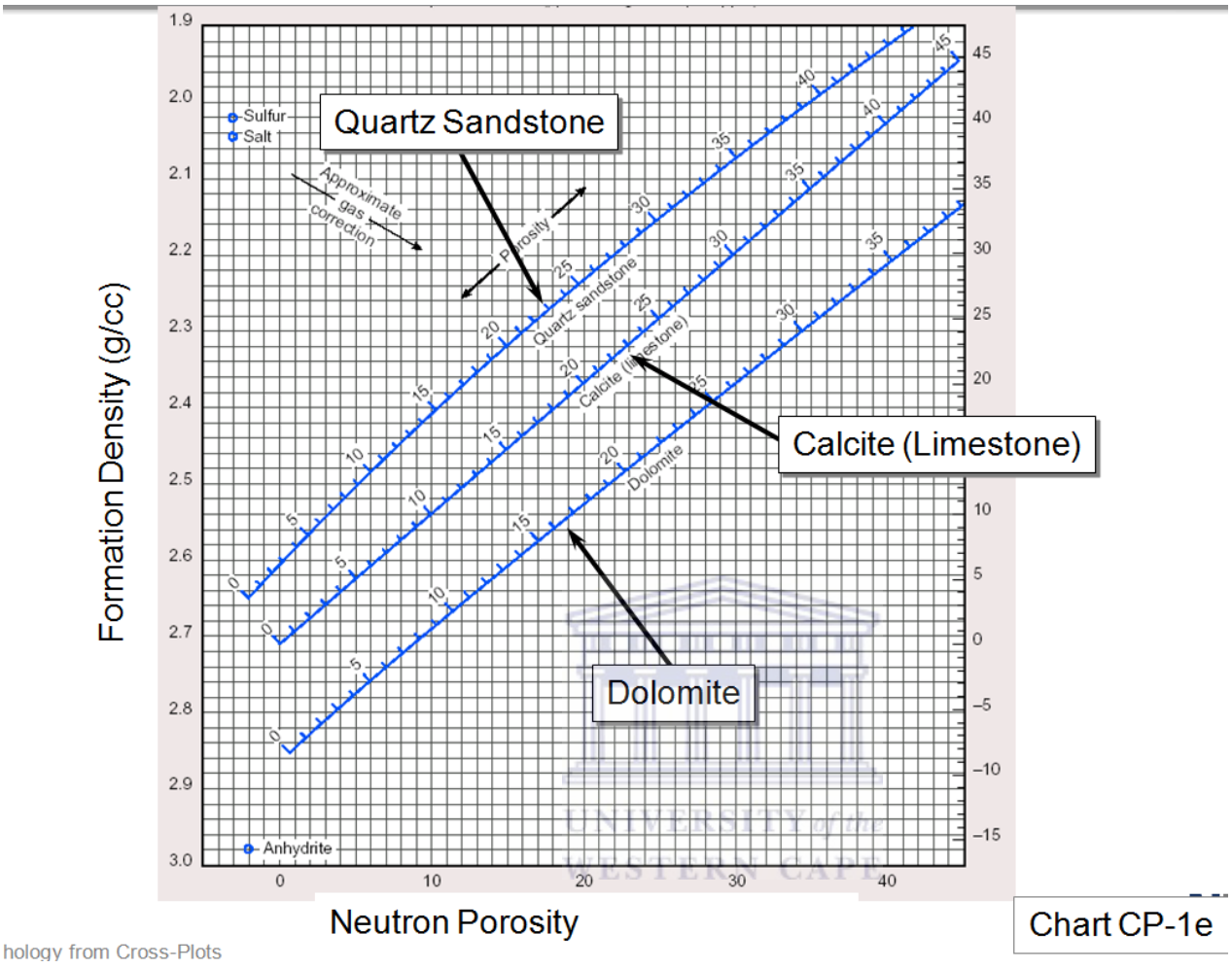

Figure 54: Environmental correction chart for neutron porosity (NPHI) log to compensated neutron Log (CNL).Density cross plots modified after Schlumberger 1972.

Density against porosity crossplots is useful in determining the mineralization in lithologies. No extensive petrographic studies were employed in this study but is good to determine the possible causes of the poor porosities and permeabilities that were exhibited in the lithologies.

The crossplot chat used is a Schlumberger crossplot and it depicts whether the lithology has quartz,calcite,dolomite or calcite in it. The plots below are a representation of these parameters in the wells studied.

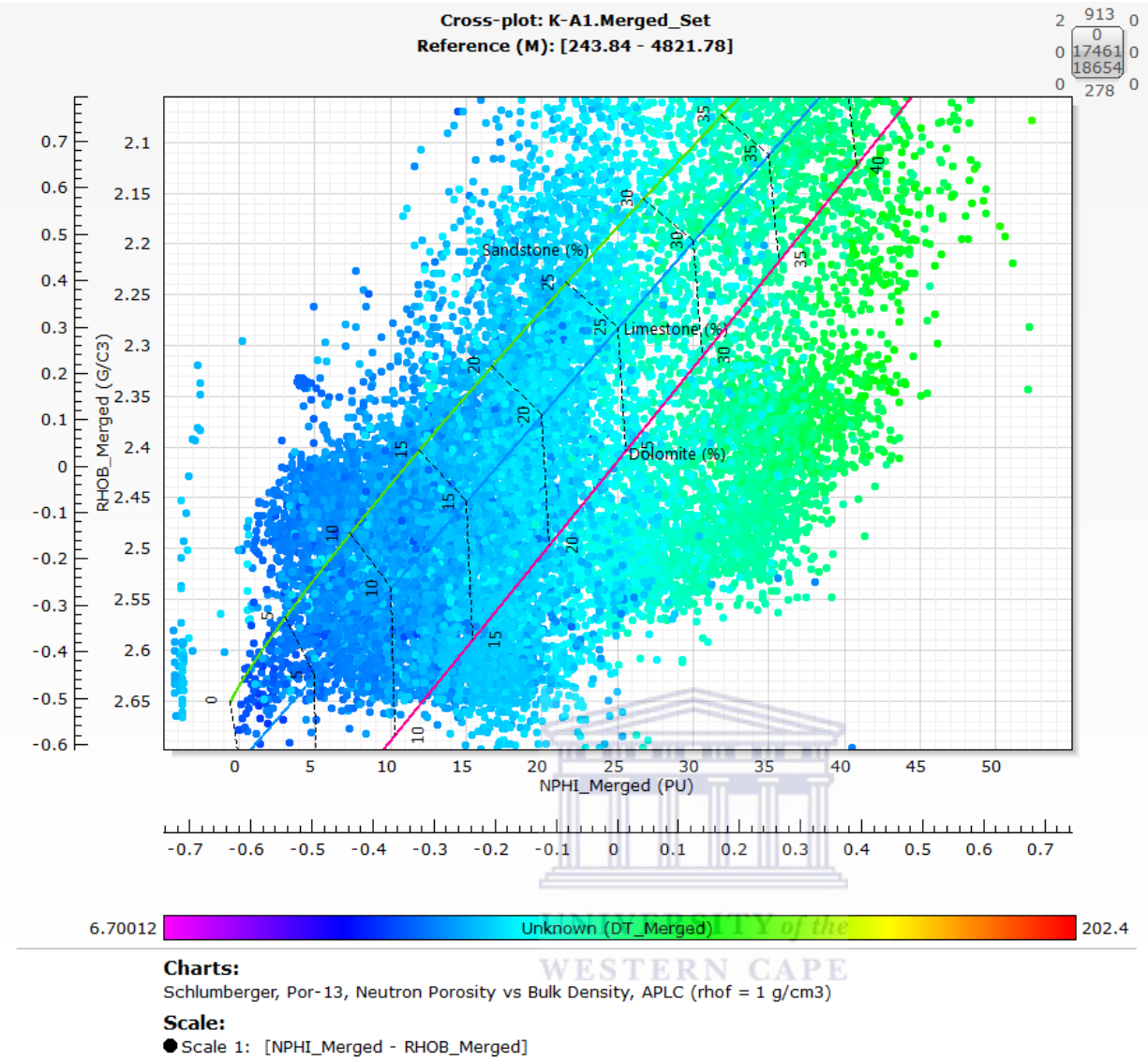

Figure 55: Crossplots of Density (RHOB) against Neutron (NPHI) for mineralogical for mineralogical prediction in well K-A1.

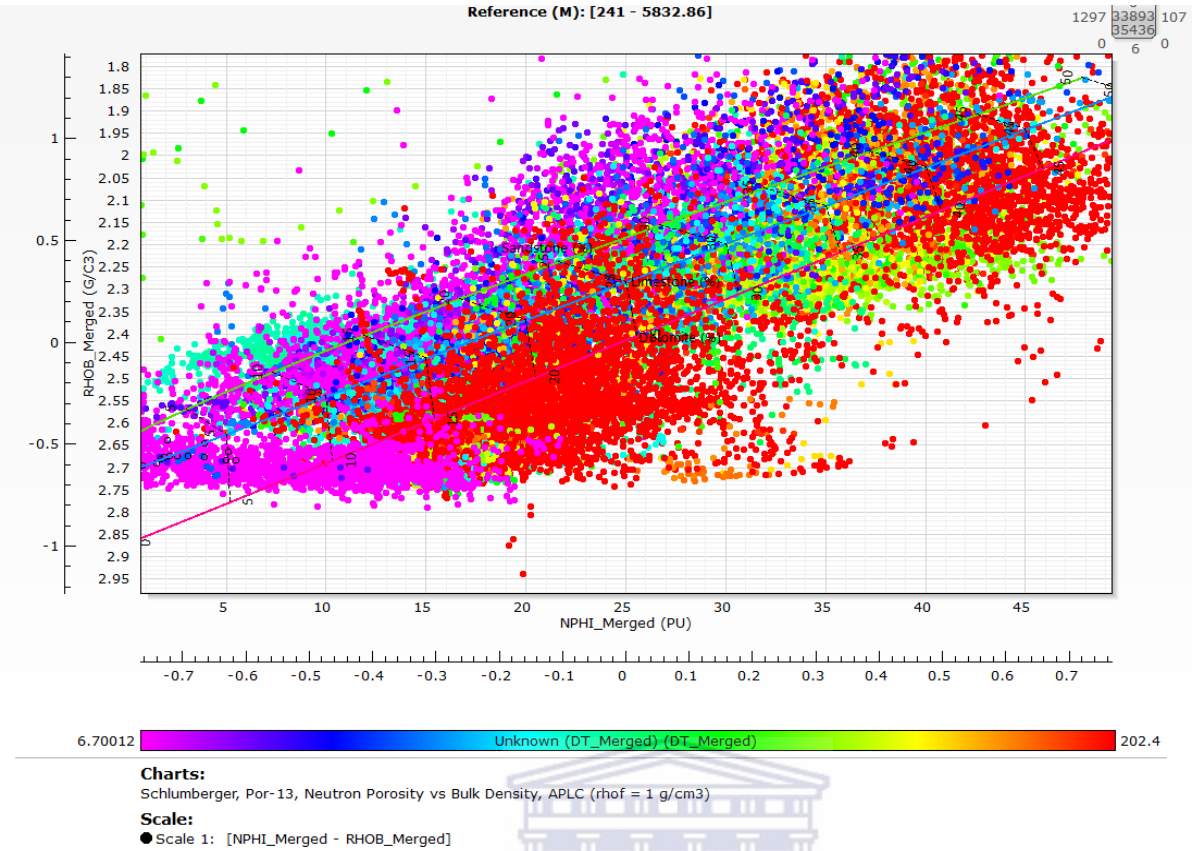

Figure 56: Crossplots of Density (RHOB) against Neutron (NPHI) for mineralogical for mineralogical prediction in well K-A2.

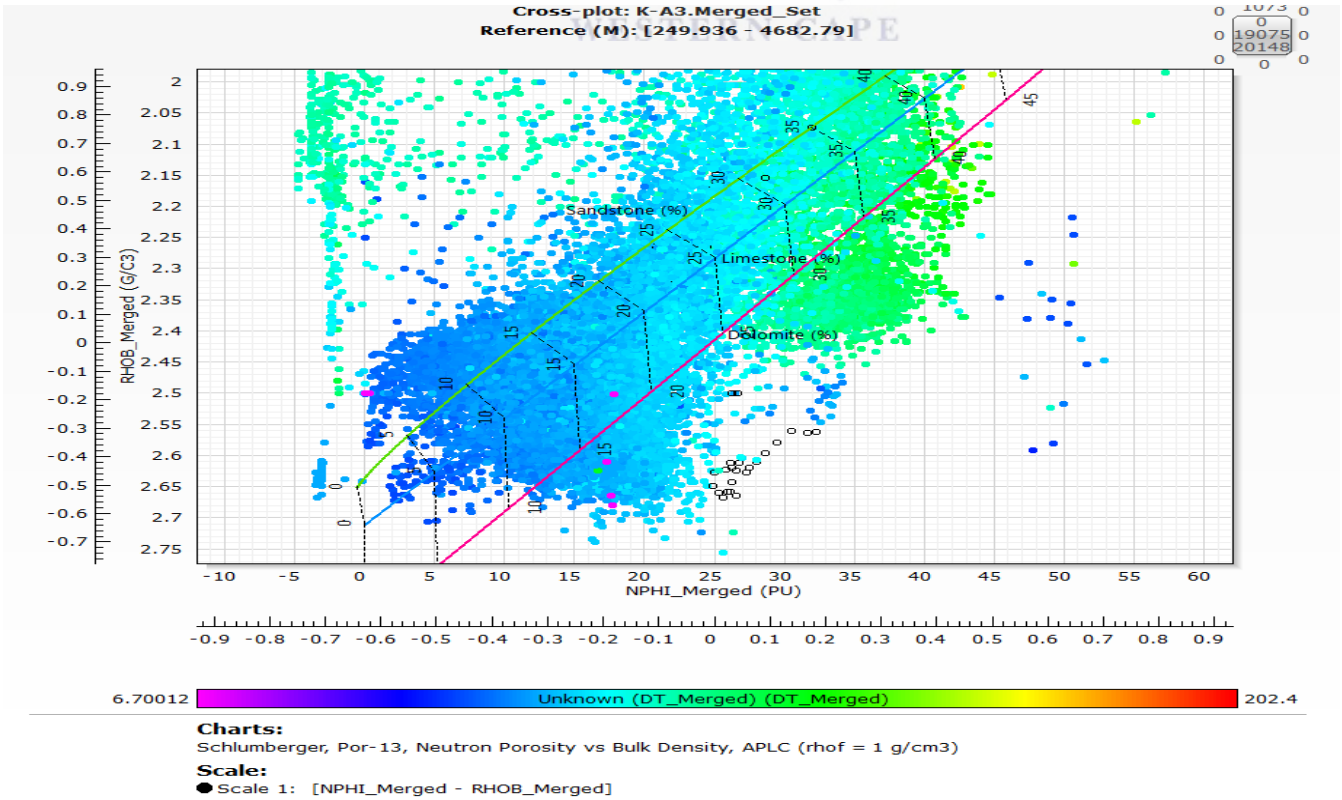

Figure 57: Crossplots of Density (RHOB) against Neutron (NPHI) for mineralogical for mineralogical prediction In K-A3.

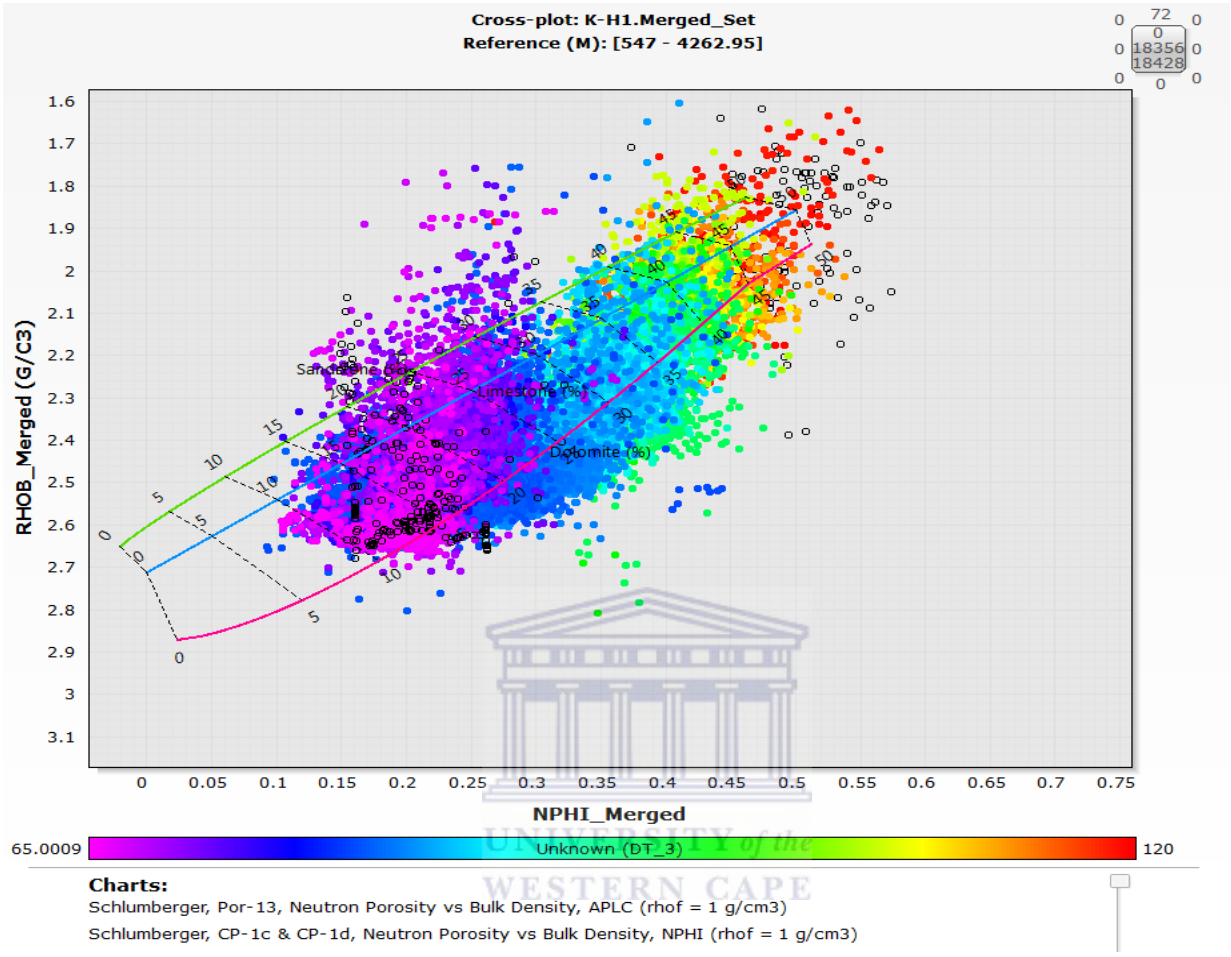

Figure 58: Crossplots of Density (RHOB) against Neutron (NPHI) for mineralogical prediction in well K-H1.

The cross plots are soley based on wireline logs. (Density- Neutron crossplots) Techlog was used to generate these logs.

From the plot above it is visible that K-A1 contains very low quarts sandstone and more dolomite. It contains higher porosity values by the dolomite mineralization. Sonic log is used to colour these plots. Sonic logs are dependent on lithology type, compaction and porosity. They can be used to determine porosity too. In this case the porosity is depicted and so is the lithology hence good interpretations are made based on mineral content.

An increase in sonic (Dt) values is visible where there is higher porosities and this owes to the high cluster depicting dolomite existence. The sandstones contain lower porosities in k-A1 and are very tight which is given by the low sonic.

K-A2 exhibits a wide variation of minerals present. The apparent cluster lies by dolomite which suggests that the well has a lot of dolomite mineralization's in some areas. These plots show that there is a majority of dolomite and calcite in the logs.

K-A3, consist of a cluster by quartzitic sandstone, meaning there is a large amount of sandstone present. There are apparent high porosity values around the sandstone. What is apparent from this plot is that there are many clusters that are scattered outside the chart. This could suggest some gas expulsions in K-A3. These could be around the limestone's as the density is also low and porosity values are highest.

K-H1 has porosity values above 0.15 and the dolomite contains the higher porosity values. Limestone (calcite is also visible at the high porosity values. The chart within this well shows that there is a variation of mineralization and the lithologies have average porosities. The sandstones here are calcitic and possibly contain dolomite too.

From these plots it can be depicted which minerals to e more aware of when conducting our interpretation and some also give confirmation to what was pointed out when the core log description was being performed.

5.4 Seismic well Tie and Seismic Interpretation and surface Models

It is recommended that well logs always be run in conjunction with another correlation technique because the results tend to be ambiguous at times and comparison with other methods is necessary to eliminate the ambiguity. The well logs also tend to fail at times and data would then be lost. Another reason why well logs should always because used in conjunction with another technique would be the fact that it is not possible to determine lithology accurately.

Seismic interpretation and subsurface mapping are key skills that are used commonly in the oil industry and hold vital information about the regional distribution of parameters in an area.

Primary seismic reflections are generated in response to significant impedance changes along stratal surfaces or unconformities. The fundamental principle that seismic reflection follows is gross bedding and therefore approximate time lines are the basis for seismic sequence stratigraphy.

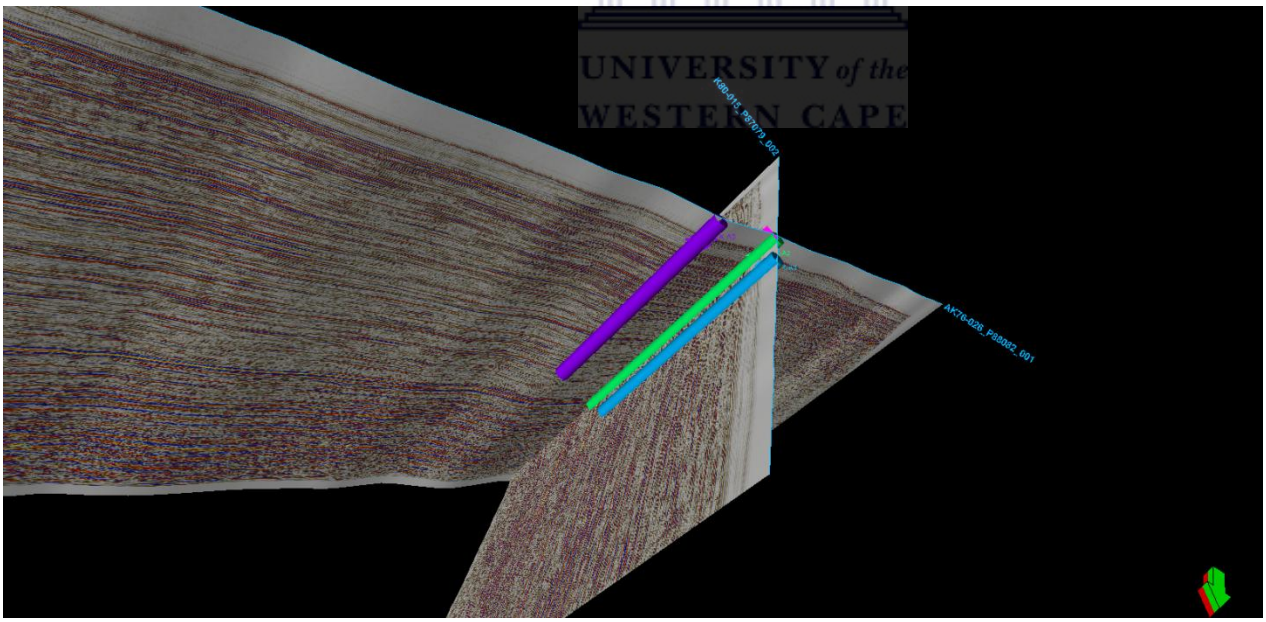

Figure 59: Seismic and well section prior to application of seismic well tie.

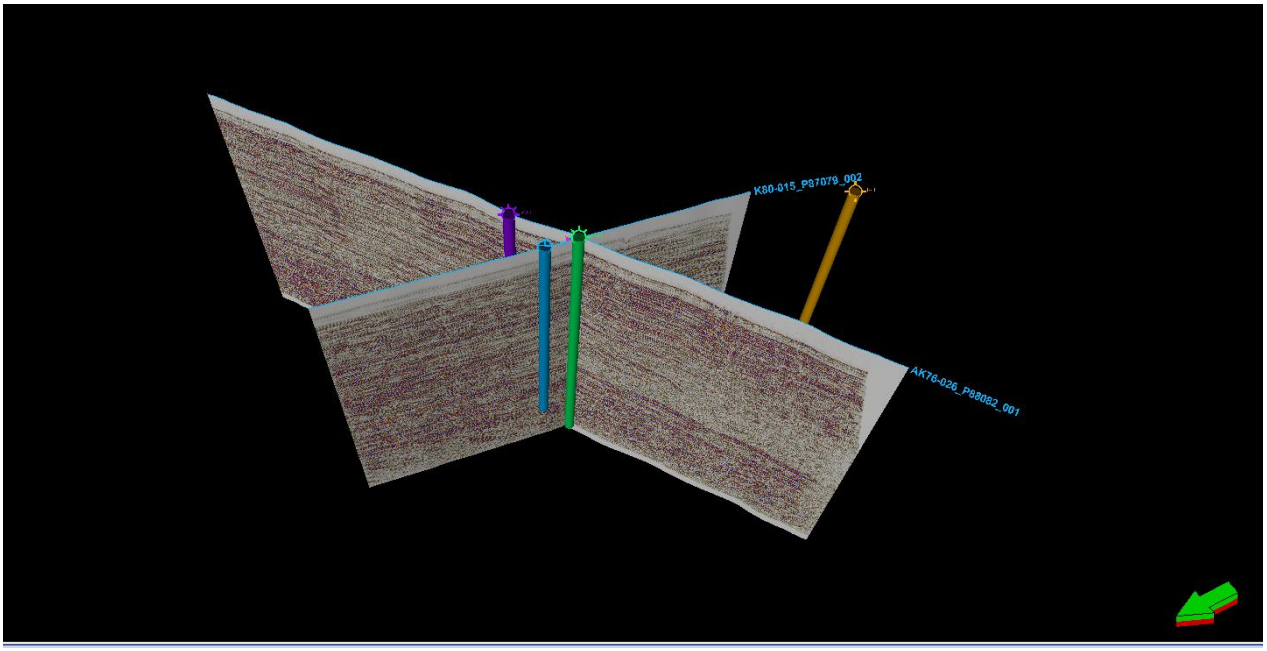

Figure 60: Well controlled seismic sections, seismic well tie applied.

Seismic well tie (Figure 62) is applied in order to make the interpretation process more accurate. The well log data is overlain on the seismic and a depth match is applied (Figure 59). Seismic data is measured in time and logs are taken in depth, therefore in order to work with both these data types at the same type it is needed to make sure they are in the same domain (figure 60).

The extracted wavelet statistics (Figure 61) and graphs below exhibit the distribution of the seismic and the shifting applied on the seismic to match the well data.

The example below is the process applied to K-A3 which controls the seismic line K 80-015

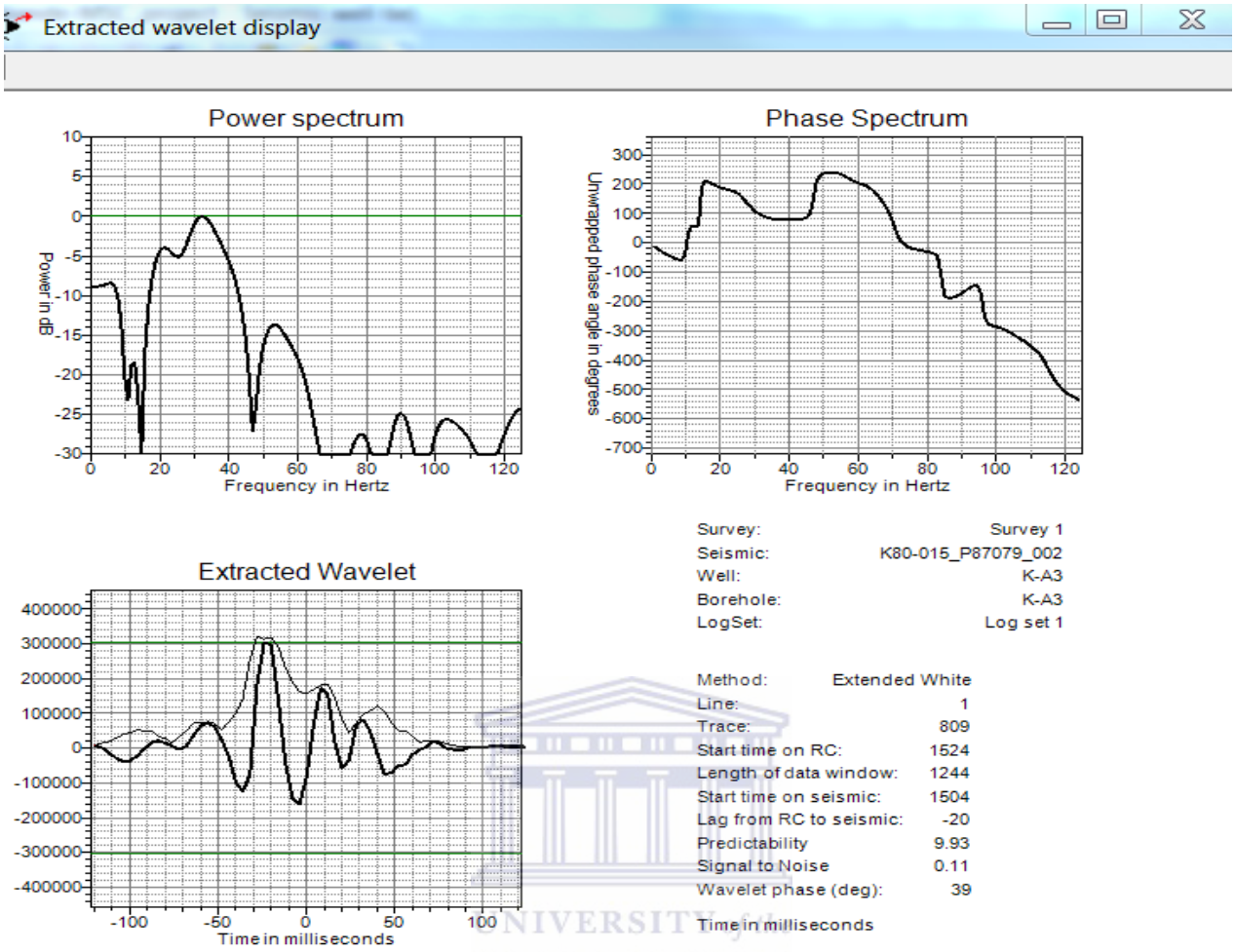

Figure 61: Extracted wavelet from the seismic tie process.

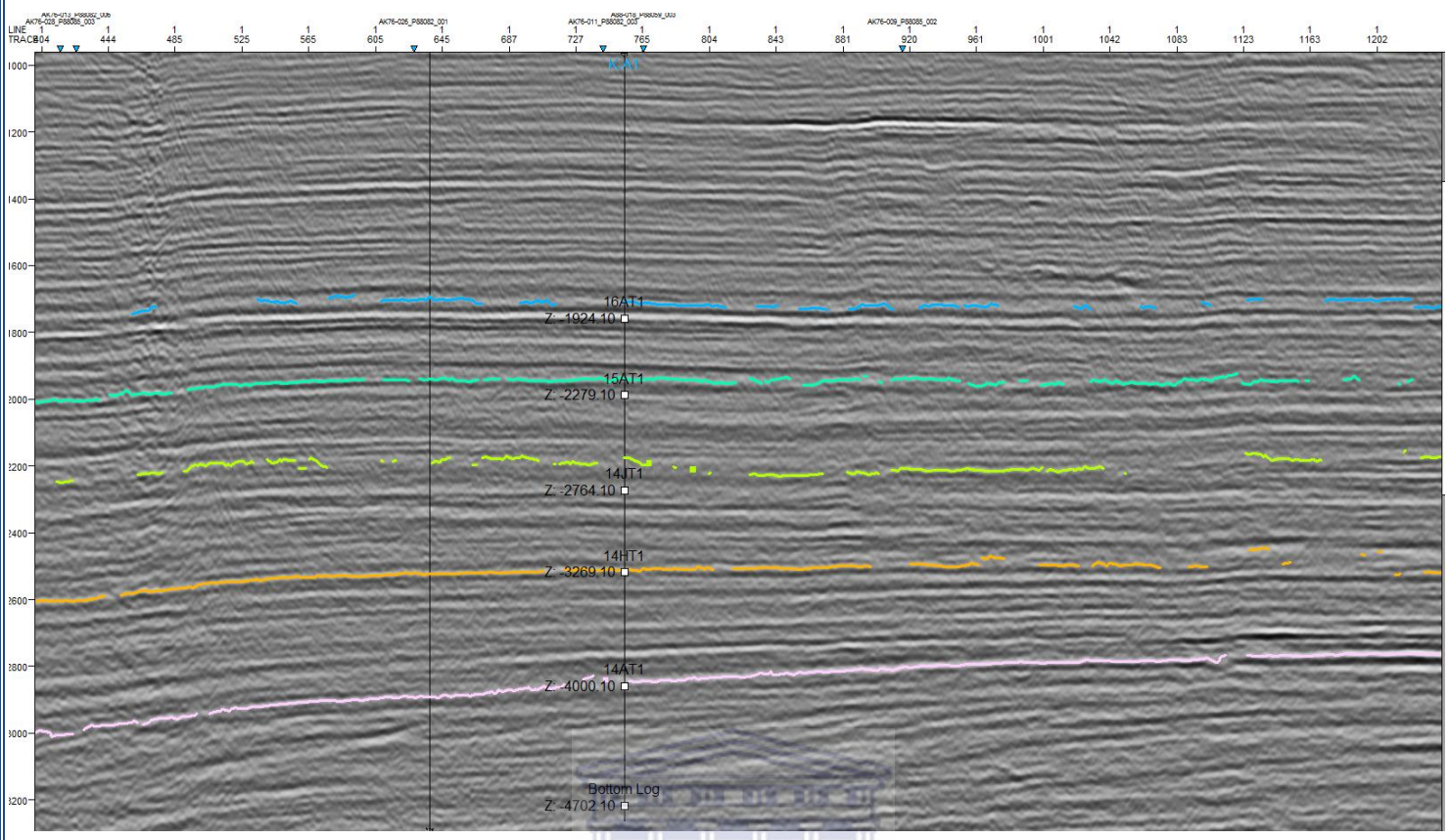

Figure 62: Seismic well tie with interpreted horizons which match. The intervals interpreted on the seismic have a direct match to those that are visible on the wireline logs.

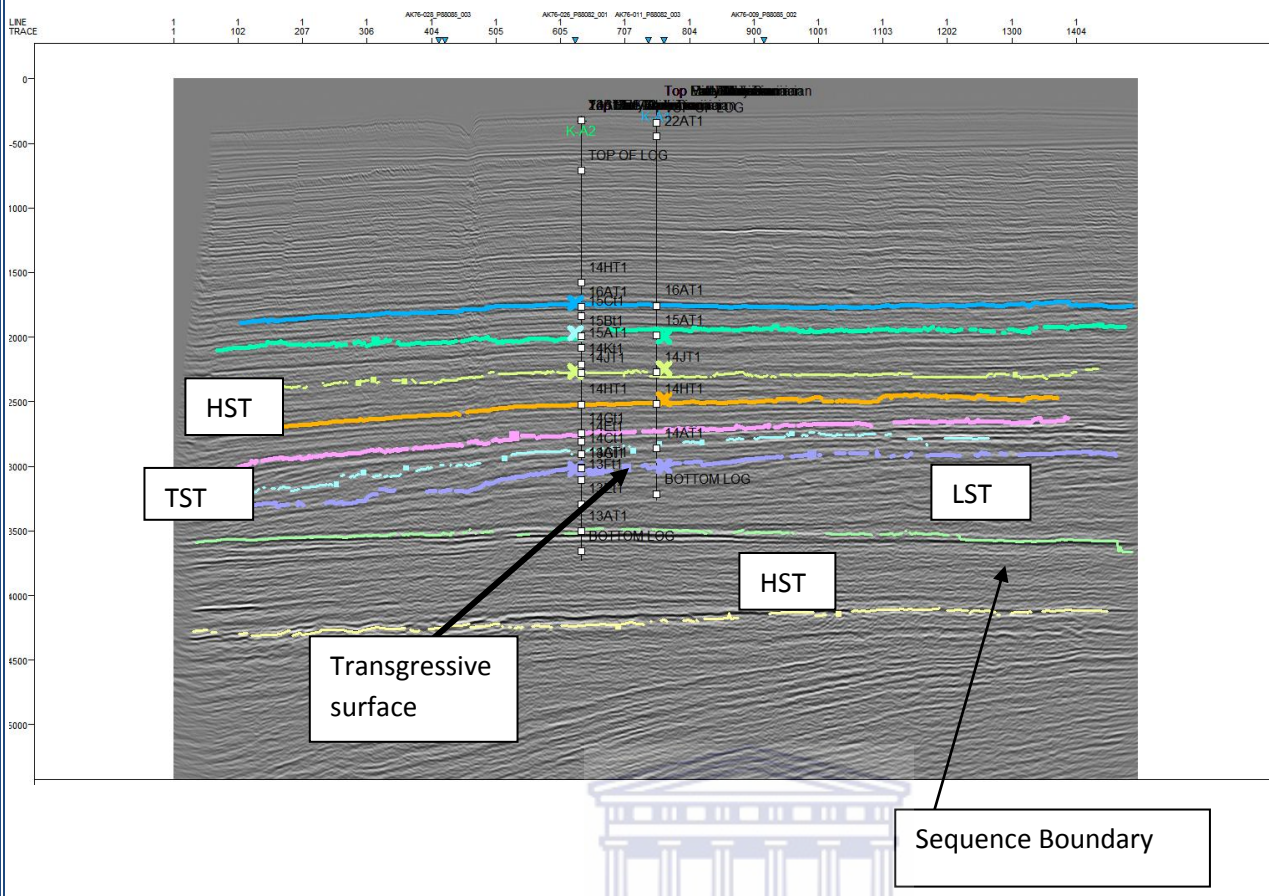

Figure 63: Illustration of modeled sequence system tracts on a seismic section.

The sequence stratigraphic cycles interpreted above exhibit that the reservoirs area. They show interest at shallow depths near the 14At1 interval and 14B2t1 (2714m). If possible, Drilling should occur at deeper depths below the shallower HST as prospect could be held there (Figure 63). The structural and elevation models below also suggest that prospect is possibly within the higher elevated areas. Wells in a North Easterly direction can be added to the study for correlation purposes and for better understanding of the facies as movement a bit inland occurs.

Sandstones within the 14B2t1 to 14At1 interval (Figure 64) are less developed in the vicinity covered by well K-A2 than at the K-A1 well location. The main targeted sandstones belong to the lower Cretaceous age and lie just below 13At1.

This horizon is not reached at well K-A1 but is clearly intersected by K-A2.

14At1 to 14B2t1 represents the secondary target sandstones which are similar to the sandstones in Well K-A1.

Potential source rocks are found below 13At1 but also there is presence of some argillaceous material below 15At1 and directly below it are some clearly visible sandstone units. Additionally at 14B2t1 – 14At1 is a potential source rock/seal and directly below it is a sandstone layer at 14At1 (Figure 64).

If possibly there could be movement into a more easterly direction, to follow the thinning of the seismic reflections then perhaps, more developed sandstones that are gas bearing could be located.

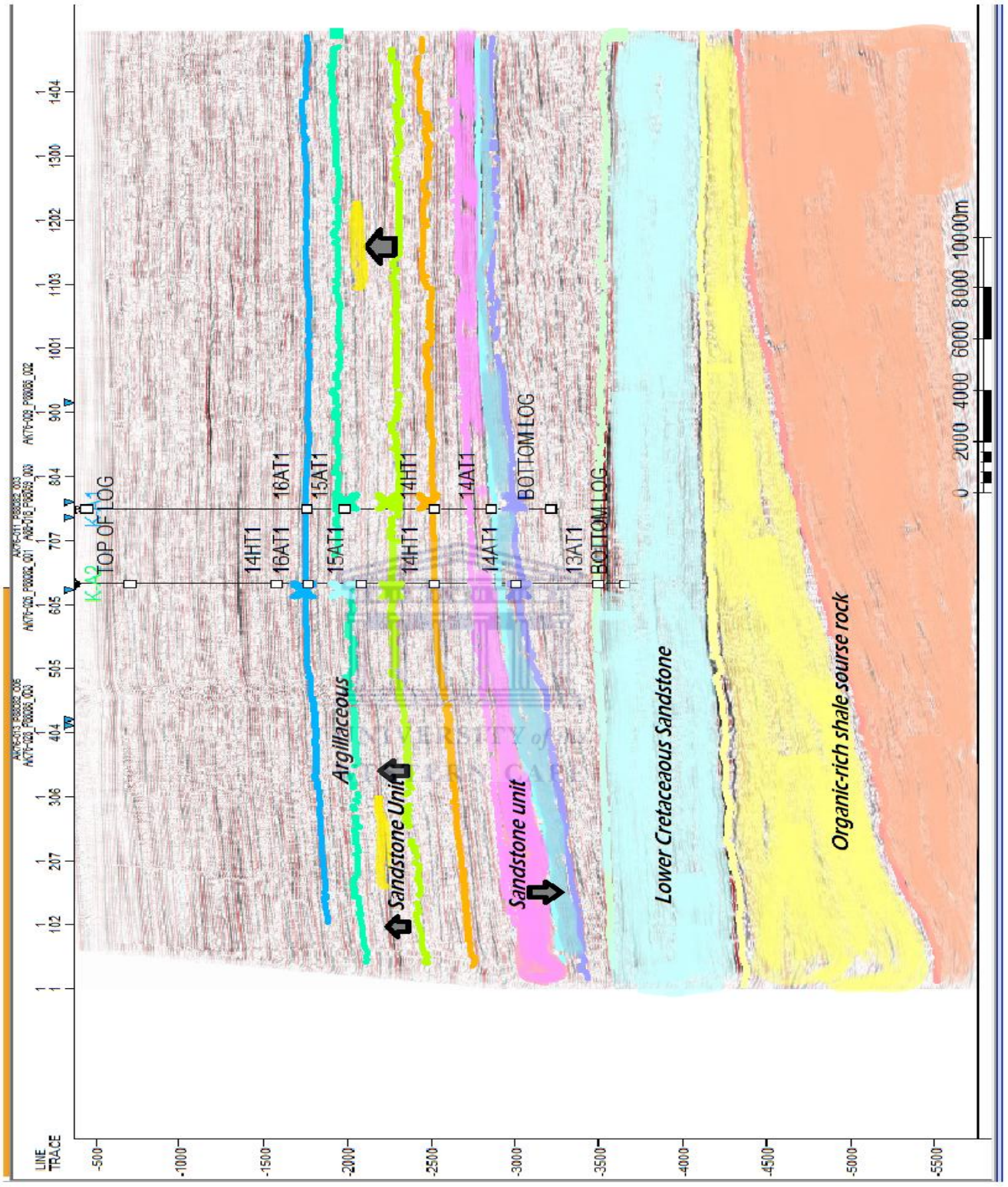

Figure 64: Fully interpreted seismic section controlled by well K-A1 and K-A2. (Interpreted in Petrel)

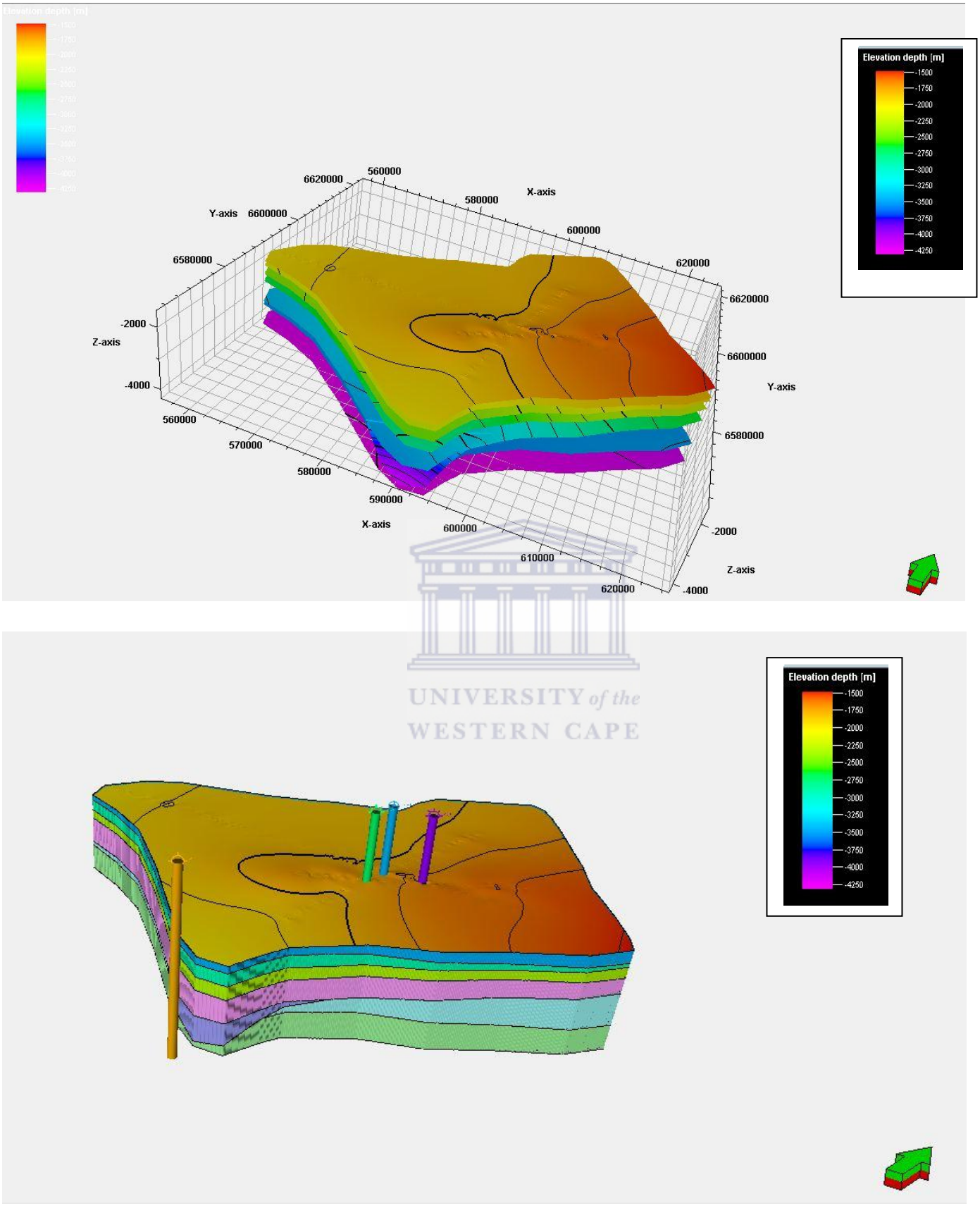

Figure 65: Depth model of surfaces generated with the interpreted horizons and a 3D depth grid with reference to well position.

The Depth model was created through the Make a Simple Grid process in Petrel. This process involves converting the seismic horizons into depth and generating 3D from them. The grid (Figure 65) provides a less rigorous structural framework of the study area as the faults are not interpreted. The grid is also has the wells displayed on it and from the edges an interpretation of the horizon interpretation can be made out. K-H1 does not fall with the grid as in the study it a reference well and does not control the same seismic lines as wells K-A1, K-A2 and K-A3.

From the 3D it can then be continued with constructing a petrophysical model. Below (Figure 66)

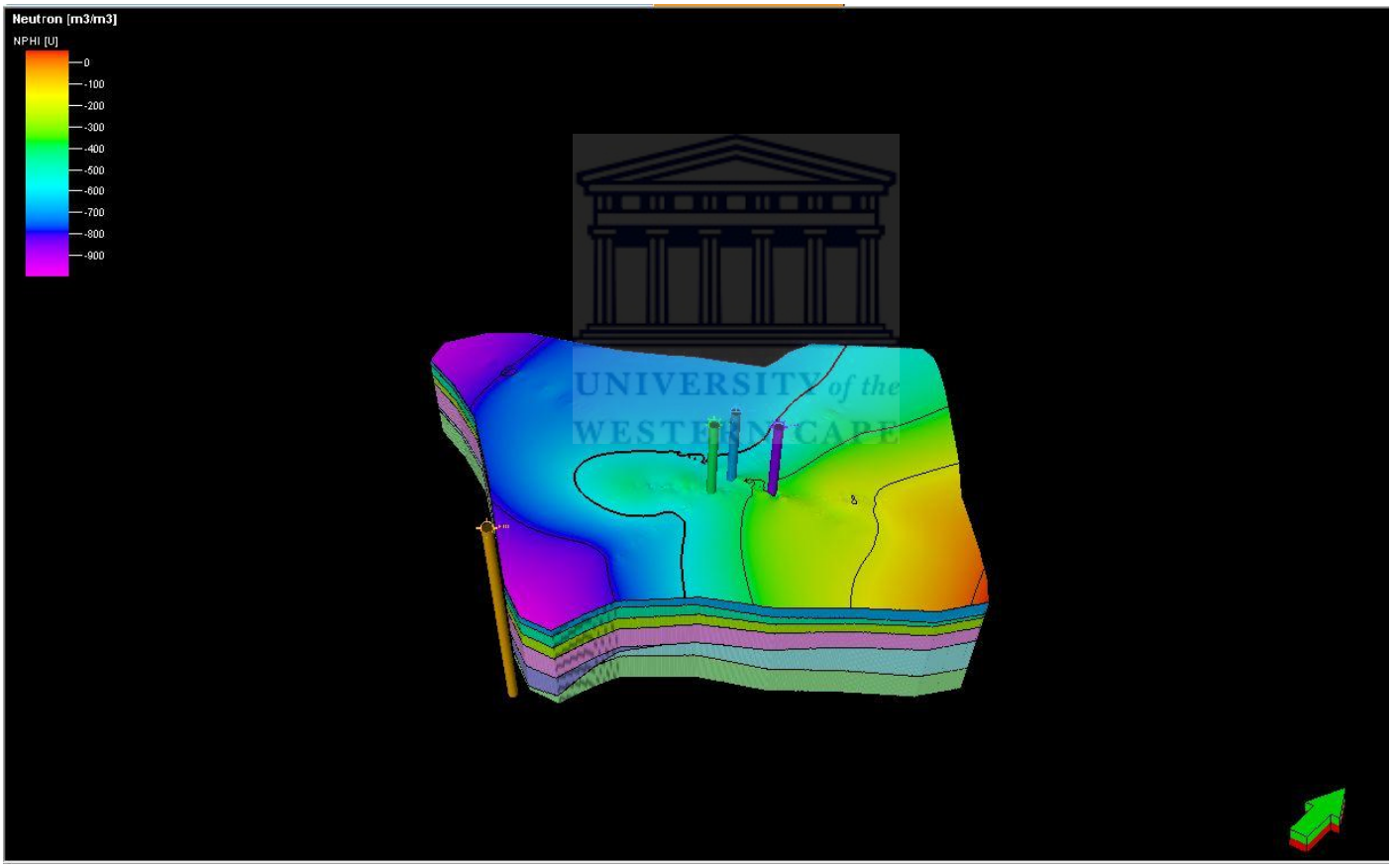

Figure 66: General distribution of an Upscaled Neutron log, with reference to well position

The grid was then populated with upscaled well logs; namely Neutron log was used. The grid then calculates an average value according to the distance from the wells. The average porosity distribution can be delineated

through the trend which is followed by the wells. From the trend it can be made out that low porosity values are trending north easterly and towards the North West the porosity is increasing.

Property modeling is required using algorithms to decrease the uncertainty and make certain that the trend is correct.

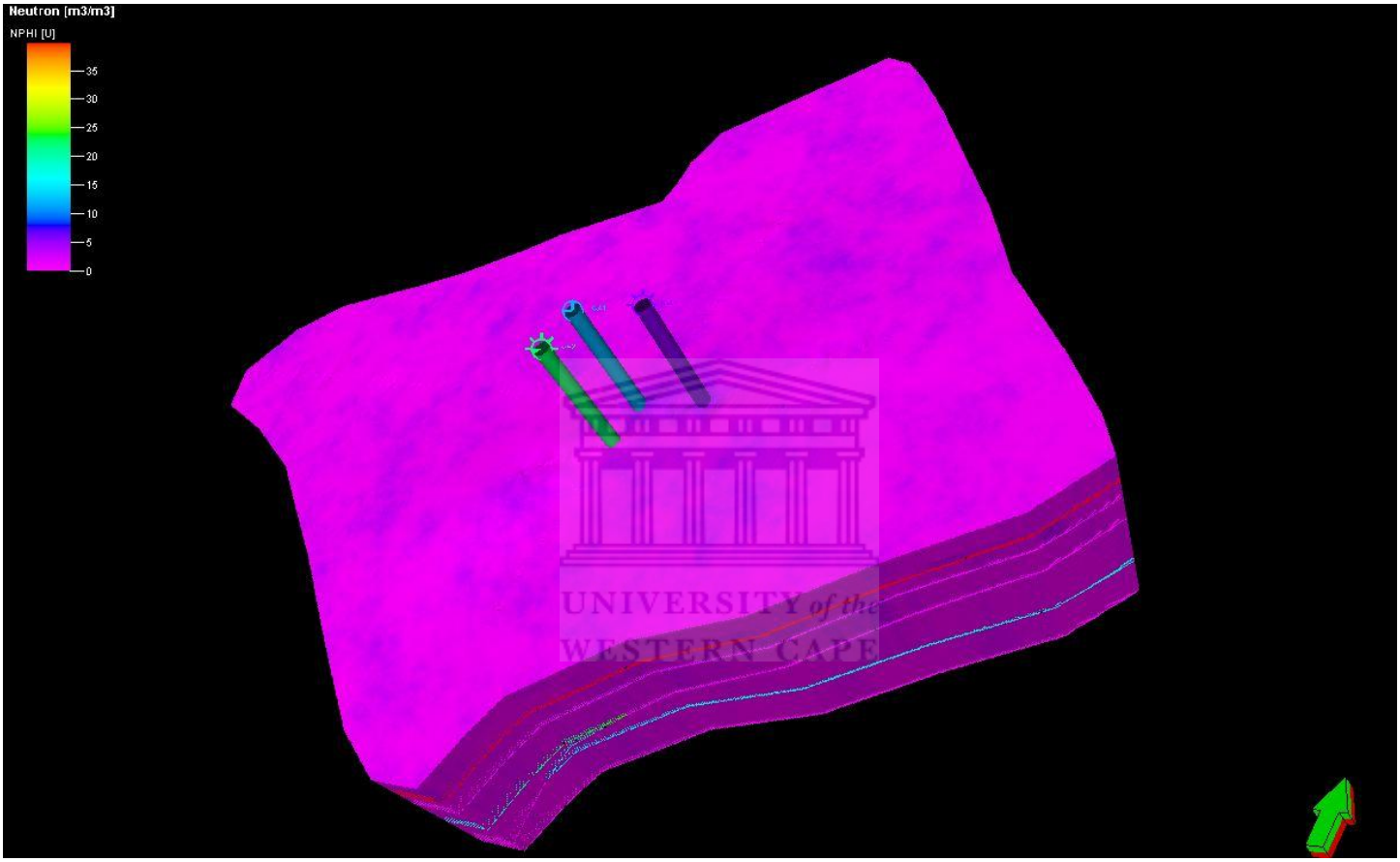

Figure 67: Property modeled grid using the Gaussian random function Simulation algorithm (GRFS).

The property modeling for the above figure 67 was run using GRFS. This method is stochastic and gives good variogram reproduction. A simple population was run from the upscaled neutron logs. No zones where delineated. It can now be seen that on average the study area has porosity values ranging at 1 – 10m3/m3. The limited data does not allow for a full model generation to be run but in the future it could be done.

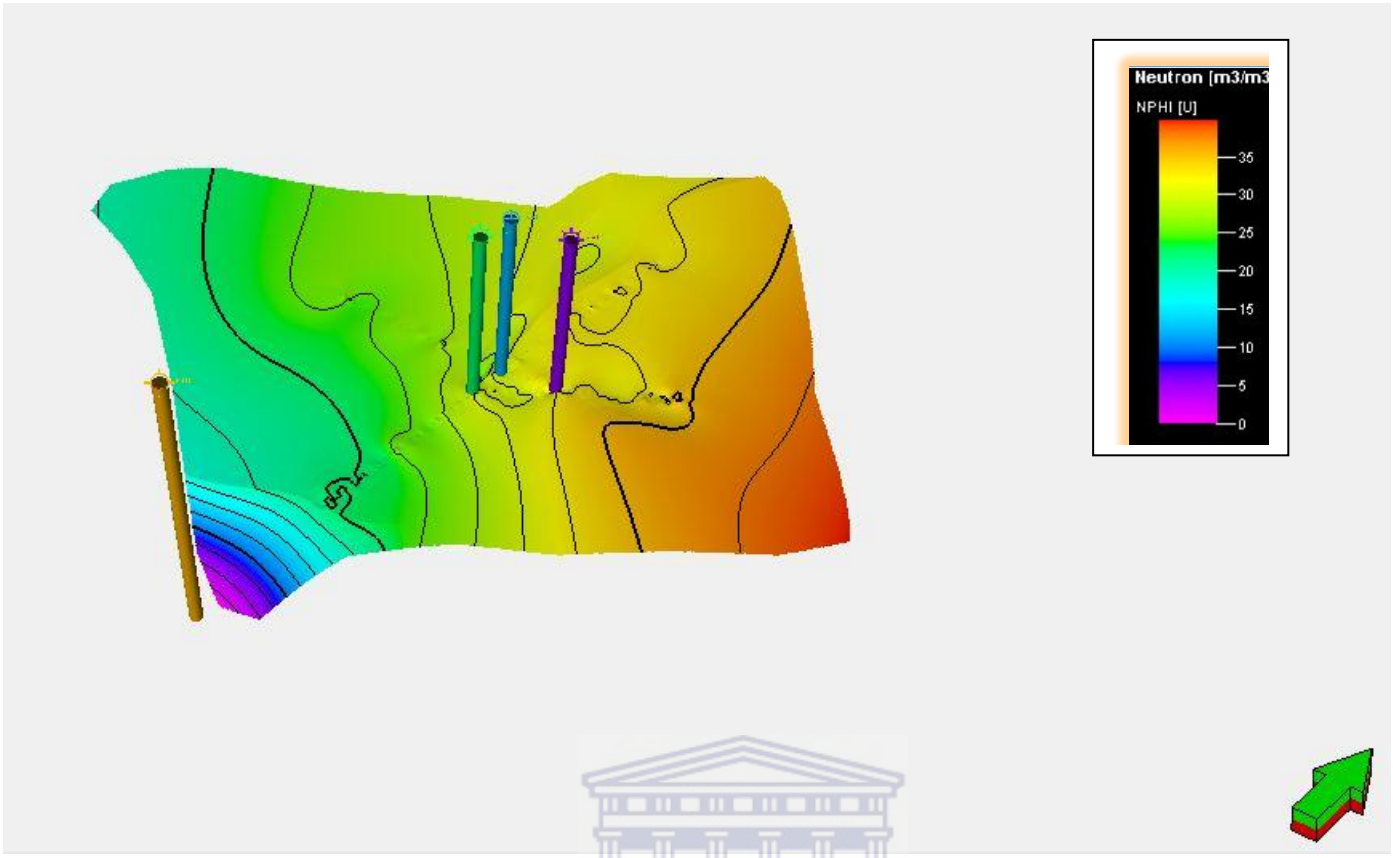

Figure 68: Property modeled 13At1 surface using the Gaussian random function Simulation algorithm.

The main target sandstones in the study area are the Lower Cretaceous sandstones which are at an interval 13At1. These sandstones are not well developed but from the property model of the target surface it can be seen that the porosity values are much more improved than the average values applied on all the zones on the 3D grid (Figure 68).

This surface can confirm that better porosity values could possibly exist if movement in a north easterly direction occurs. Within the area where the wells are positioned, the porosity values are average between 25 and 30 m/m3.

CHAPTER 6: Conclusions and Recommendations

6.1 Conclusions

The techniques used to characterize reservoirs are usually use independently of others. This study shows the impact of integrating different disciplines and techniques to characterize a reservoir. Core analysis and description form is a fundamental starting point for reservoir characterization.

More accurate information was provided which reduced the uncertainty. If there were promising saturations and porosities in the area, it would be suggested for a play study to be run. The study has showed that there is potential prospect in horizons older than the Cretaceous age.

The Orange Basin, offshore South Africa, is a relatively under explored basin with huge petroleum potential. To best understand the basin it is recommended that a basin-wide Chemostratigraphic study is undertaken. This will enhance the knowledge of the lithologies within the basin and also the provenance of the basin. Understanding these topics will better help to understand the petroleum elements within the basin.

Core Interpretation results show that the there is poor poroperm parameters in the area. The lithologies consist of silty sandstones that are water saturated. The wireline logs confirm this and show minor amounts of gas saturation. From the reservoir characterization study it is understood that the wells studied are dry wells and that is presence of dolomites and glauconite. Well KA3 contained some gas shows but not enough to run volumetrics. An empirical relationship was established from conventional core porosity and permeability plots to predict an absolute permeability in non-cored wells and intervals.

Four wells were evaluated in this study, namely, Wells K-A2, K-A3 and K-H1. The study presented a detailed description of the core of three wells K-A2, K-A3 and K-H1. Well K-A1 is a wild cat and no cores were cut here.

The poroperm plot for K-A2 was sampled at a depth of 3981.90m – 4081, 14m. The trend shows that the lithology is clay cemented sandstone. Looking at the Log interpretation this trend can be confirmed. The permeability values are very low and range between 0 and 0.01mD. The porosity values are higher at lower depths averaging at 14% whereas at the deeper levels they range between 3.4 – 5.3%.

The poroperm plot for K-A3 was sampled at a depth of 3876.74 m– 3882.72m. Within this zone the range in permeability values is very drastic. Above 3876.74m depth there are very high permeability values ranging between 31md – 58mD, whereas below that depth the permeability values are average of 0.1mD

Well K-H1 shows figures and data predominantly poor porosity and permeability (poroperm) qualities. The porosity and permeability decrease with depth. And from the core description it can be understood that this is a result of the claystones and interbedded and interlaminated sandstones present in the core.

Only K-A2 and K-A3 contain full sampled core data and hence there are some plots generated. The main target sandstones in the study area are the Lower Cretaceous sandstones which are at an interval 13At1. These sandstones are not well developed but from the property model of the target surface it can be seen that the porosity values are much more improved than the average values applied on all the zones on the 3D grid.

Sandstones within the 14B2t1 to 14At1 interval are less developed in the vicinity covered by well K-A2 than at the K-A1 well location. The main targeted sandstones belong to the lower cretaceous and lie just below 13At1.

Within deeper zones of the Wells, at approximately 5350m -5750m, there are more developed sandstones with good porosity values. The volume of shale is low and so is the water saturation. Possibly if drilling at deeper levels could be done then gas could be spotted. This suggests that focus should be at the older sandstone units, ones that are older than the lower cretaceous sandstones.

6.2. Recommendations

It is recommended that the next phase of this study be conducted where seismic attributes are used to understand structure and the structural grid be populated with petrophysical data to show distribution.

Possibly run a study with additional well that lie at a greater depth than K-A3 so that better correlation can be run.

3D seismic should be run in the area in order to assist with improved modeling of the study area.

Make use of seismic attributes and structural modeling to delineate the facie from the structural model created.

It is recommended that well logs always be run in conjunction with another correlation technique in order to be able to determine lithology and facie more accurately.

It is also recommended to edit old logs and perform porosity calibrations with density logs.

It is also recommended to look into sandstones that are older than the Cretaceous and run petrology studies and evaluate the sandstones.

References

- Archie GE (1942): The Electrical resistivity log as an aid in determining some reservoir characteristics. Transaction of AIME 146; 54.
- Adekola, S.A., Akinlua, A., & Fadipe.O.A. (2009). Sequence stratigraphic and diagenetic alterations within the Silisiclastic Reservoir Deposits of Orange Basin, Southwestern Africa Margin. 11th SAGA Biennial Technical Meeting and Exhibition Swaziland. 552-557pp
- Bailey.C, (2009). Comparative Study of the Chemostratigraphic and Petrophysical characteristics of Wells A-A1, A-L1, A-U1 and A-I1 in the Orange Basin, South Atlantic Margin, Offshore South Africa. Unpublished M.Sc thesis, University of the Western Cape, Cape Town. South Africa.
- Broad, D.S., Jungslager, E.H.A., McLachlan, I.R., & Roux, J., (2006). Offshore Mesozoic Basins. In: Johnson, M.R., Anhaeusser, C.R., Thomas, R.J. (Eds.). The Geology of South Africa. Geological Society of South Africa, Johannesburg/Council for Geosciences, Pretoria, p. 553–571.
- Broad, D., (2004). South Africa Activities and Opportunities, an unpublished PowerPoint Presentation to PetroChina.
- Brown, L.F., Brown, L.F, Jr., Benson, J.M., Brink, G.J., Doherty, S., Jollands, A., Jungslager, E.H.A., Keenan, J.H.G., Muntingh, A., Van Wyk, N.J.S., 1995. Sequence stratigraphy in offshore South Africa divergent basins. An Atlas on exploration for cretaceous lowstand traps by SQEKOR (Pty) Ltd. Am. Ass. Petro. Geol. Stud. In Geology. 41, 184pp.
- Campher.C.J., Primio., R., Kuhlumann., G., van der Spuy.,D. and Domoney.R.(2009) Geological modeling of the offshore Orange Basin, West Coast South Africa
- Crain E. R. (2000)The New Role of Petrophysics in Geophysical Interpretation P.Eng., Spectrum 2000 Mindware Ltd., Calgary .CSEG RECORDER
- De Vera J., Granadoa, P., & McClaya, K. (2010). Structural evolution of the Orange Basin gravity-driven system, offshore Namibia. Marine and Petroleum, vol. 27, Issue 1, 223-237 pp.

- Derder, O. M. A (2002). Intergration of core data and well log response over thin pay zones in the upper Cretaceous, Orange Basin, South Africa.
- Dingle, R.V., Siesser, W.G. and Newton, A.R.,1983, Mesozoic and Tertiary Geology of Southern Africa. A.A. Balkema, Rotterdam, 375 pp.
- Emery, E., Myers, K.J., 1996. Sequence Stratigraphy, Blackwell Science Ltd; London.
- Gerrard, I., & Smith, G. C.(1982). Post-Paleozoic Succession and Structure of the Southwestern Africa Continental margin.In: American Association of Petroleum Geologist, p. 49-74
- Gladczenko T. P., Hinz K., Eldholm O., Meyer H., Neben S. & Skogsied J. (1997) South Atlantic volcanic margins. Germany journal of the Geological Society, LondonPrinted in Great Britain Vol. 154.
- Harvey, M., Beck, B., & Haynes, M. (1994). Hydrocarbon Prospectivity of the Orange Basin, Western South Africa, pp 9-13.
- Haq, B.U., Hardenbol, J. and Vail, P.R., (1988). Mesozoic and Cenozoic chronostratigraphy and eustatic cycles of sea-level change. In: The geology of South Africa edited by M.R Johnson, C.R Anhaesser and R.J Thomas. 2006.
- Hirsch K.K., Scheck-Wenderoth M., Paton D.A, di Primo R., Horsfield B.,Cloetingh S.A.P.L F. Beekman F. (2007). 3D Gravity Modeling and Subsidence Analysis in the Orange Basin, Southwest African Continental Margin Geophysical Research Abstract, Vol. 9, 06275.
- Hirsch, K. K., Scheck-Wenderoth, M., van Wees, J., Kuhlmann, G., & Paton, D. A. (2010). Tectonic subsidence history and thermal evolution of the Orange Basin, Marine and Petroleum Geology, vol. 27, Issue 3, 565-584 pp.
- Jungslager, E.H.A. (1999a). Petroleum habitats of the South Atlantic margin. In: The Oil and Gas Habitats of the South Atlantic N.R. Cameron, R.H. Bate and V.S. Clure (eds), Spec. Publ. geol. Soc. Lond., 153-168.

- Ketzer, J.M., 2002. Diagenesis and sequence stratigraphy: An integrated Approach to constrain Evolution of Reservoir Quality in Sandstone. Dissertation for the Degree of Doctor of Philisophy in Mineral Chemistry, Petrology and Tectonics at the Department of Earth Science, Uppsala University. Sweden.
- Kuhlmann,G.,Adams,S.,Campher,C.,van der Spuy,D.,di Primio,.Horsefield,B. (2010) Passive margin evolution and its controls on natural gas leakage in the southern Orange Basin, blocks 3/4, offshore South Africa. Marine Geology 27, 973 -992
- Lofts, J., Harvey, P., Lovell, M. (1994). Reservoir characterization from downhole mineralogy. Marine and Petroleum Geology.
- Lombard.D.,Akinlua.A.(2009)Reservoir Characterization of wells KD1,KE1,KF1,KH1, in block 3, Orange basin, offshore South Africa. 11th SAGA Biennieal Technical meeting and Exhibition Swaziland,16 – 18 September 2009, page 574. (Abstract)
- Macdonald D., Gomez-Pereza I., Franzeseb J., Dalzielc I., Thomas C., Trewind ,N., Holed M., and Patona D. (2003). Mesozoic break-up of SW Gondwana: implications for regional hydrocarbon potential of the southern South Atlantic Marine and Petroleum Geology 20: 287–308.
- Mitchum Jr., R. M., (1977). Seismic Stratigraphy and Global Changes of Sea Level: Part 11. Glossary of Terms used in Seismic Stratigraphy: Section 2. Application of Seismic Reflection Configuration to Stratigraphic Interpretation, Memoir 26 pp. 205 -212.
- Muntingh A., (1993). Geology, prospects in Orange Basin offshore western South Africa. Oil and Gas Publication,25, 106-108
- Olajide, O., (2005). The Petrophysical Analysis and Evaluation of Hydrocarbon Potential of Sandstone Units in the Bredasdorp Central Basin. Unpublished M.Sc thesis, University of the Western Cape, Cape Town. South Africa.
- Paton, D.A., Di Primio, R., Kuhlmann, G., Van der Spuy, D. and Horsfield, B.(2007). Insights into the Petroleum System Evolution of the southern Orange Basin, South Africa. South African Journal of Geology, Geological Society of South Africa,Volume 110, pp 261-274.

- Petroleum Agency South Africa (2003), South African exploration Opportunities for promotion of petroleum exploration and exploitation, Cape Town
- Petroleum Agency South Africa (2005), Exploration Opportunities in the Deep water Orange Basin, off the West Coast of South Africa.
- Rider, M. (1996). The Geological Interpretation of Well Logs. 2nd Edition. Whittles Publishing
- Rider, M. (2000). The geological interpretation of well log . Scotland : Whittles publishing
- Schoen, J.H., Yu,G., & Strack, K.M. (2002)Properties of Rocks - Fundamentals,lecture notes, Baker Atlas.
- Schön, J.H., (1996). Physical Properties of Rocks Fundamentals and Principles of Petrophysics Handbook of geophysical exploration - seismic exploration (ed. K. Helbig, S. Treitel) 18, Pergamon Press JS96 Western Atlas, 1992, Introduction to Wireline Log Analysis, WA92
- Schalkwyk J.H.,(2005).Assessment controls on reservoir performance and the affects of granulation seam mechanics in the Bredasdorp Basin, South Africa. Thesis Msc.
- Schlumberger Ltd (1972). Log Interpretations Principles.Volume 1.
- Stewart,J.,Watts,A.B.,& Bagguley,J.G.(2000). Three-dimentional subsidence analysis and gravity modeling of the continental margin offshore Namibia. Geophysics Journal Int. 141, 724 – 746.
- Strack, K.M (2002) KMS Technologies – KJT Enterprises Inc. Reservoir Characterization with Borehole Geophysics
- Van Vuuren, C.J., Broad, D.S., Roux, J., McLachlan, I.R. (1998). The mineral resources of South Africa, 6th Ed., 483 - 494.
- Van der Spuy, D. (2003). Aptian source rocks in some South African Cretaceous basins. Geol. Soc. London, Spec Pub, 181-198.
- Van der Spuy D. (2005) Republic of South Africa 2007 Licence Round: Area A Northern Orange Basin
- Van Wagoner., Mitchum, R.M., Rahaman, V.D., 1990. Siliciclastic sequence stratigraphy in well logs core and outcrops; American Association of Petroleum Geologist, methods in exploration series, No 7.

- Walls J., Dvorkin J., Carr M. Well Logs and Rock Physics in Seismic Reservoir Characterization; Walls, Dvorkin, and Carr; Rock Solid Images www.rocksolidimages.com

Other Consulted Publications:

- NeXT (Network in Excellence Training) 1.Petroleum Exploration and Production training course slides, Basic Logging course slides.
- Western Atlas, 1992, Introduction to Wireline Log Analysis, WA92

Related Websites:

www.cseg.ca

www.META.EDU.TR

Appendice

Appendix A

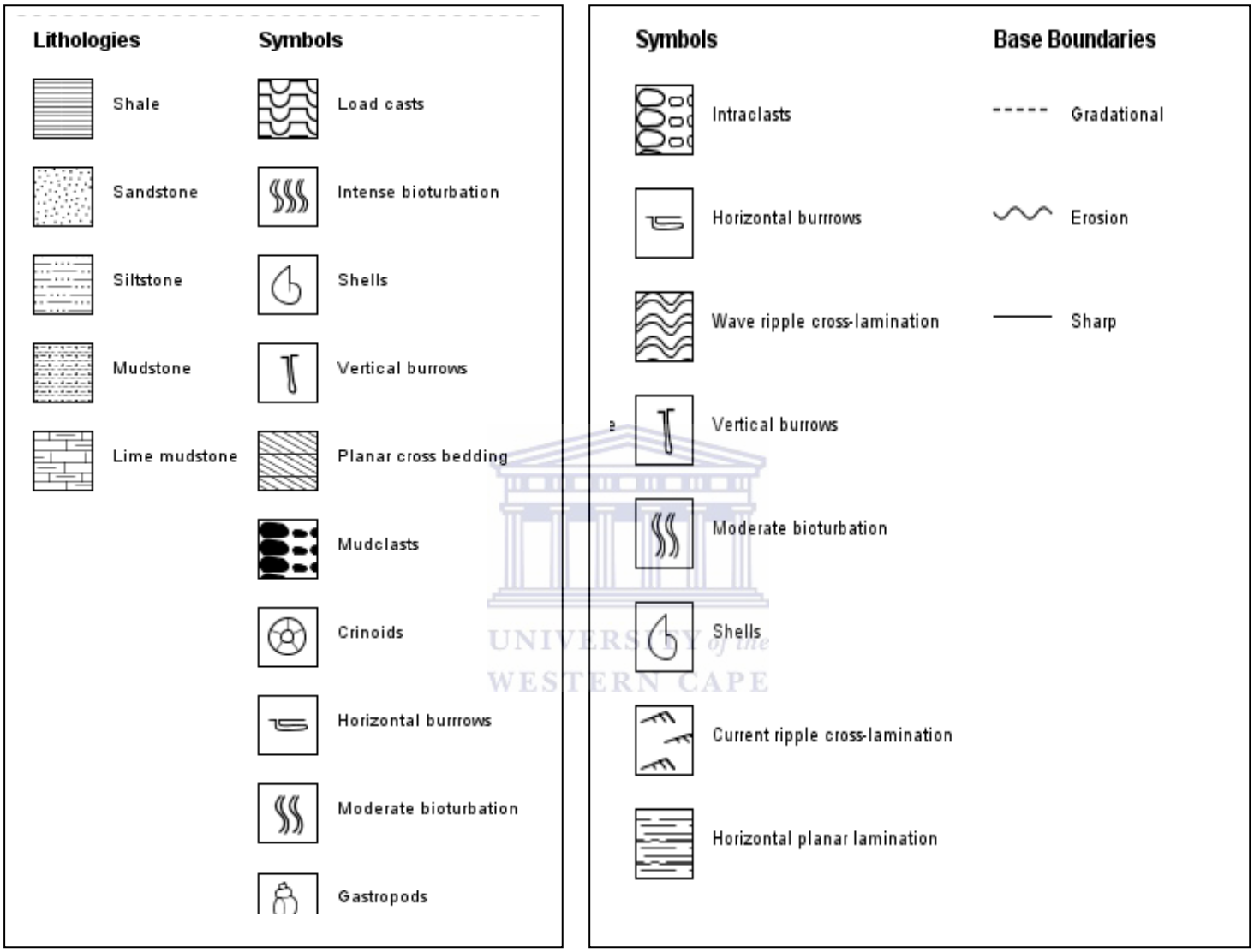

Figure A1: Legend for the logs of Wells K-A2, KA-2, K-A3 and K-H1.

Appendix B

Sample	Depth	PERMEABILITY				Porosity %		R. S % P.S	
		Horizontal		Vertical		Gas Exp	S. O Fluids	oil	Water
		Air	Liq	Air	Liq				
1	3876,735								
	3876,81	0.1	0	0.1	0	8.2	6.4	0	73
2	3877,455								
	3877,545	0.4	0.2	0.2	0.1	14	15.5	0	70
3	3878,44								
	3878,53	0.3	0.1	0.1	0	11.3	10.1	0	95
4	3879,65								
	3879,74	0.2	0.1	0.1	0	9	8.7	0	46.2
5	3880,73								
	8808,81	0.3	0.1	0.2	0.1	12.4	10	0	79
6	3881,75								
	3880,80	0.2	0.1	0.1	12.6	12.6	3.3	0	60
7	3882,72								
	3882,82	0.4	0.2	0.2	0.1	14.6	14.1	0	93

Figure B1: Core parameters Table for K-A3 core 2

Sample	Depth	PERMEABILITY				Porosity %		R. S % P.S	
		Horizontal		Vertical		Gas Exp	S. O Fluids	oil	Water
		Air	Liq	Air	Liq				
1	3981,90								
	3982,06	0,1	0	0,1	0	11,0	13,8	0	63,8
2	3982,61								
	3982,74	0,1	0	0,1	0	12,7	13,7	0	64,2
3	3983,71								
	3983,89	0,1	0	0,1	0	13,0	15,8	0	58,2

Figure B2: Core parameters table for K-A2 core 2

Name	Colour	Pattern	Description
Gas interval			possible reservoir
Shale effect			
water			
ZONE			Possible Reservoir Zone
ZONE 2			
ZONE 3			
Potential Res. Zone			
Sampled Zone			

Figure B3: Legend of geophysical logs

Appendix C

Nomenclature

F = formation resistivity factor

Ir = resistivity index

k = permeability

m = porosity exponent

n = saturation exponent

Q*v* = cation-exchange capacity per unit pore volume

Ro = resistivity of fully water saturated rock

Rw = resistivity of saturating water

Rt = resistivity of partially saturated rock

Rts = resistivity of sand

Sh = hydrocarbon saturation

Sw = water saturation

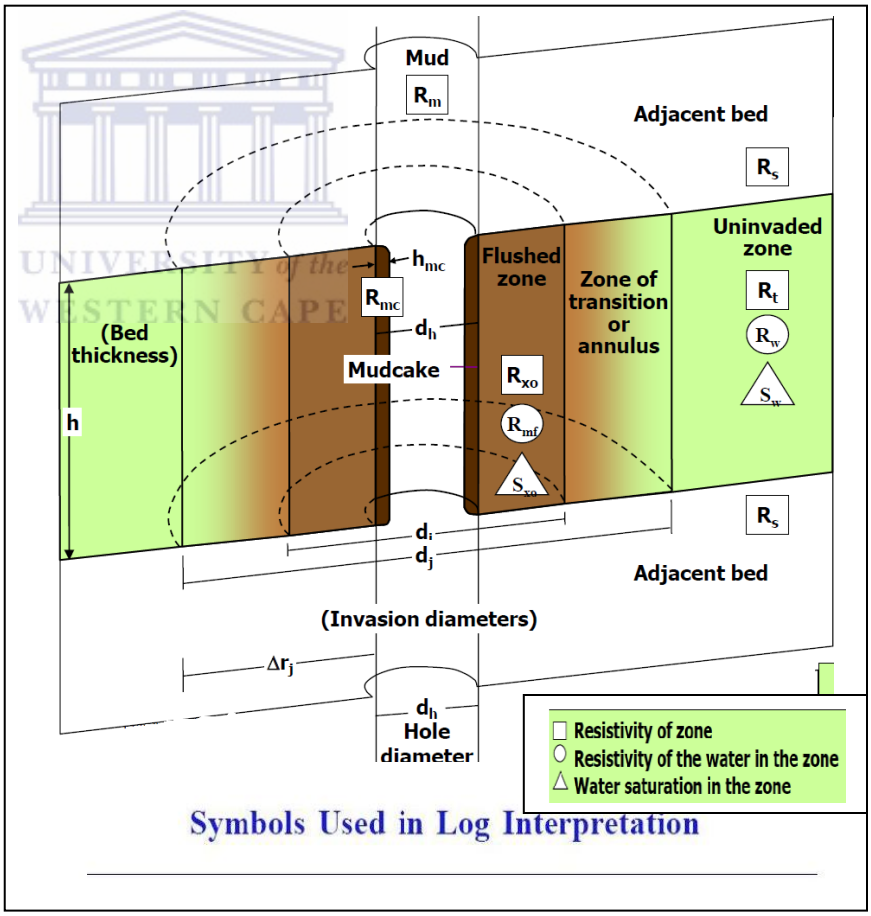

Figure C1: Symbols Used in log interpretation. Modified (Rider, 1996)

Vlam = laminated-shale-volume

fraction

Vsh = shale-volume fraction

X = extra conductivity term

ϕ = porosity

φ*t* = total porosity

φ*tsh* = shale total porosity

ϕ*tsd* = sand total porosity

Appendix D

API gravity

1. n . [Enhanced Oil Recovery, Heavy Oil]

A specific gravity scale developed by the American Petroleum Institute (API) for measuring the relative density of various petroleum liquids, expressed in degrees. API gravity is gradated in degrees on a hydrometer instrument and was designed so that most values would fall between 10° and 70° API gravity. The arbitrary formula used to obtain this effect is: API gravity = (141.5/SG at 60°F) - 131.5, where SG is the specific gravity of the fluid.

SPECIFIC GRAVITY CONVERSION TABLES

NOTE: To convert degrees API to specific gravity (liquids lighter than water)

$$\text{Sp. Gr.} = \frac{141.5}{131.5 + \text{Degrees API}}$$

To convert degrees Baumé to specific gravity (liquids heavier than water)

$$\text{Sp. Gr.} = \frac{145}{145 - \text{Degrees Baumé}}$$

CONVERSION TABLE BAUME

Specific Gravity — Weight per Gallon for liquids HEAVIER than water

Baumé	Specific Gravity	Wght. per Gal.	Baumé	Specific Gravity	Wght. per Gal.	Baumé	Specific Gravity	Wght. per Gal.	Baumé	Specific Gravity	Wght. per Gal.	Baumé	Specific Gravity	Wght. per Gall
0	1.000	8.33	10	1.074	8.95	20	1.160	9.67	30	1.260	10.50	40	1.381	11.51
1	1.006	8.38	11	1.082	9.02	21	1.169	9.74	31	1.271	10.59	45	1.450	12.08
2	1.014	8.45	12	1.090	9.08	22	1.178	9.82	32	1.283	10.69	50	1.526	12.72
3	1.021	8.51	13	1.098	9.15	23	1.188	9.90	33	1.294	10.78	55	1.611	13.42
4	1.028	8.57	14	1.106	9.22	24	1.198	9.98	34	1.306	10.88	60	1.705	14.21
5	1.035	8.62	15	1.115	9.29	25	1.208	10.07	35	1.318	10.98	65	1.812	15.10.
6	1.043	8.69	16	1.125	9.37	26	1.218	10.15	36	1.330	11.08	70	1.933	16.11
7	1.050	8.75	17	1.132	9.43	27	1.228	10.23	37	1.342	11.18	-----	-----	-----
8	1.058	8.82	18	1.141	9.51	28	1.239	10.32	38	1.355	11.29	-----	-----	-----
9	1.066	8.88	19	1.150	9.58	29	1.250	10.42	39	1.367	11.39	-----	-----	-----

CONVERSION TABLE API

Specific Gravity — Weight per Gallon for liquids LIGHTER than water

A.P.I.	Specific Gravity	Wght. per Gal.	A.P.I.	Specific Gravity	Wght. per Gal.	A.P.I.	Specific Gravity	Wght. per Gal.	A.P.I.	Specific Gravity	Wght. per Gal.	A.P.I.	Specific Gravity	Wght. per Gall
10	1.000	8.33	31	0.871	7.25	52	0.7712	6.42	73	0.6926	5.76	91	.636	5.29
11	0.993	8.27	32	0.865	7.21	53	0.7670	6.39	74	0.6893	5.73	92	.633	5.27
12	0.986	8.21	33	0.860	7.16	54	0.7637	6.35	75	0.6859	5.70	93	.630	5.25
13	0.979	8.16	34	0.855	7.12	55	0.7597	6.32	76	0.6826	5.68	94	.628	5.22
14	0.973	8.10	35	0.850	7.08	56	0.7556	6.28	77	0.6793	5.65	95	.625	5.20
15	0.966	8.04	36	0.845	7.03	57	0.7516	6.28	78	0.6750	5.62	96	.622	5.18
16	0.959	7.99	37	0.840	6.99	58	0.7476	6.22	79	0.6728	5.60	97	.619	5.15
17	0.953	7.94	38	0.835	6.95	59	0.7437	6.18	80	0.6696	5.57	98	.617	5.13
18	0.946	7.88	39	0.830	6.91	60	0.7398	6.15	81	0.6665	5.54	99	.614	5.11
19	0.940	7.83	40	0.825	6.87	61	0.7359	6.12	82	0.6634	5.52	100	.611	5.09
20	0.934	7.78	41	0.820	6.83	62	0.7310	6.09	83	0.6603	5.49	-----	-----	-----
21	0.928	7.73	42	0.816	6.79	63	0.7283	6.06	84	0.6572	5.47	-----	-----	-----
22	0.921	7.68	43	0.811	6.75	64	0.7246	6.03	85	0.6541	5.44	-----	-----	-----
23	0.916	7.63	44	0.806	6.71	65	0.7209	5.99	86	0.6511	5.42	-----	-----	-----
24	0.910	7.58	45	0.802	6.68	66	0.7172	5.96	87	0.6481	5.39	-----	-----	-----
25	0.904	7.53	46	0.797	6.64	67	0.7136	5.93	88	0.6452	5.37	-----	-----	-----
26	0.898	7.48	47	0.793	6.60	68	0.7090	5.90	89	0.6422	5.34	-----	-----	-----
27	0.893	7.43	48	0.788	6.56	69	0.7065	5.87	90	0.6393	5.32	-----	-----	-----
28	0.887	7.39	49	0.784	6.53	70	0.7020	5.85	-----	-----	-----	-----	-----	-----
29	0.882	7.34	50	0.780	6.49	71	0.6995	5.82	-----	-----	-----	-----	-----	-----
30	0.876	7.30	51	0.775	6.46	72	0.6950	5.79	-----	-----	-----	-----	-----	-----

ATMOSPHERIC PRESSURE CONDITIONS —

ELEVATIONS ABOVE SEA LEVEL

Altitude Above Sea Level	Atmospheric Pressure Pounds/sq. in.	Barometer Reading Inches of Mercury	Equivalent Head or Water Feet	Reduction to Max. Practical Dyn. Suction Lift
0	14.7	29.929	33.95	0 Ft.
1000	14.2	28.8	32.7	1.2 "
2000	13.6	27.7	31.6	2.3 "
3000	13.1	26.7	30.2	3.7 "
4000	12.6	25.7	29.1	4.8 "
5000	12.1	24.7	27.9	6 "
6000	11.7	23.8	27.	6.9 "
7000	11.2	22.9	25.9	8 "
8000	10.8	22.1	24.9	9 "

Figure D: i) Definition of A.P.I gravity. ii) Conversion factors used in the Oil Industry